

ClassNK

**Investigation Report
on Structural Safety of Large
Container Ships**

September 2014

**The Investigative Panel
on Large Container Ship Safety**

This report is the product of an investigation into possibility of the occurrence of the MOL COMFORT accident and the structural safety of large container ships, and has been prepared to assist the technical development of the relevant maritime industry including safety measures for large container ships following the accident.

Matters other than the above purpose are therefore outside the scope of this report, and nor should any content or description of this report be construed in any manner whatsoever as an admission of liability in any respect by ClassNK and parties concerned.

The copyright for this report is the property of ClassNK and the same or any part thereof may not be used in any manner whatsoever without the express permission of ClassNK in writing.

Copyright © 2014 ClassNK

All rights reserved

Contents

Chapter 1 The Committee on Large Container Ship Safety..... 1

Chapter 2 The Investigative Panel on Large Container Ship Safety..... 3

Chapter 3 Investigation on Possibility of Occurrence of the Fracture..... 3

3.1 Introduction..... 3

3.2 Uncertainty Factors in Strength and Loads 4

3.3 Estimation of Strength and Load in Consideration of Deviation of Uncertainty Factors 5

3.3.1 Estimation of strength in consideration of deviation of uncertainty factors 5

3.3.2 Estimation of wave-induced vertical bending moment in consideration of deviation of uncertainty factors 7

3.3.3 Estimation of still water vertical bending moment in consideration of deviation of uncertainty factors 8

3.3.4 Lower limit of strength and upper limit of load 8

3.4 Possibility of Occurrence of Fracture 8

Chapter 4 Investigation of Structural Safety..... 11

4.1 Introduction..... 11

4.2 Margin of Hull Girder Strength 12

4.2.1 Margin against the requirements of IACS UR S11 relating to the vertical bending strength 12

4.2.2 Margin of the hull girder ultimate strength calculated by the method specified in IACS CSR based on Smith’s method 14

4.2.3 Margin of the hull girder ultimate strength calculated by 3-hold model elasto-plastic analysis 15

4.3 Mechanism of Hull Girder Fracture..... 18

4.3.1 Buckling collapse strength of bottom shell plates..... 19

4.3.2 Mechanism of the process from buckling collapse of bottom shell plates to hull girder fracture..... 23

4.3.3 Assessment of the structural safety of large container ships 26

4.4 Characteristics of Container Ships, and Changes in Structure and Operation due to Increased Ship Size 28

4.5 ClassNK Rules for Container Ships..... 29

4.6 Analysis of On-board Full Scale Measurement Results of Large Container Ships..... 30

Chapter 5	Summary of the Investigation	30
Chapter 6	Future Action Plan	32
Appendix 1	The Investigative Panel on Large Container Ship Safety Member List (related to Chapter 2 of this Report)	34
Appendix 2	Estimation of Hull Girder Ultimate Strength of the Ship in 3-Hold Model Elasto-Plastic Analysis (related to 3.3.1 of this Report).....	35
Appendix 3	Effect of Local Deformation of Bottom Shell Plates and Welding Residual Stress of Bottom Longitudinals on Hull Girder Ultimate Strength (related to 3.3.1 of this Report)	51
Appendix 4	Simulation of Wave Vertical Bending Moment at the Time of Accident with Consideration of the Deviation of Sea States (related to 3.3.2 of this Report).....	56
Appendix 5	Investigation based on Draught Measurements at Ship's Departure (related to 3.3.3 of this Report).....	59
Appendix 6	Estimation of Probability Distribution of Strength and Loads (related to 3.4 of this Report)	76
Appendix 7	Stresses of Transverse Strength Occurring in Double Bottom Structure of Post-Panamax Container Ships (related to 4.2.3 of this Report)	85
Appendix 8	3-Hold Model Elasto-Plastic Analysis (Investigation of the Hull Girder Ultimate Strength for Target Ships including the Ship) (related to 4.2.3 of this Report)	88
Appendix 9	Loads acting on the Double Bottom Structure of Container Ships (related to 4.3.1 of this Report).....	99
Appendix 10	Relationship between Buckling Collapse Strength of Stiffened Bottom Panel and Stresses generated in the Panel (related to 4.3.1 of this Report)	101
Appendix 11	Double Bottom Local Stress generated in Bottom Shell Plate (related to 4.3.1 of this Report)	111
Appendix 12	Characteristics of Post-Panamax Container Ships (related to 4.4 of this Report)	114
Appendix 13	Analysis of Data of Past On-board Full Scale Measurements of Large Container Ships (related to 4.6 of this Report)	116

Chapter 1 The Committee on Large Container Ship Safety

In response to the hull girder fracture accident of the MOL COMFORT (hereinafter referred to as “the Ship”), the 8,000 TEU class large container ship flagged in The Bahamas, on June 17, 2013, the Committee on Large Container Ship Safety (hereinafter referred to as “JG Committee”), established on the initiative of the Japanese Ministry of Land, Infrastructure, Transport and Tourism, held four meetings as mentioned below, and published an interim report (hereinafter referred to as “JG Interim Report”) on December 17, 2013.

- The first JG Committee meeting: August 29, 2013
- The second JG Committee meeting: September 27, 2013
- The third JG Committee meeting: October 28, 2013
- The fourth JG Committee meeting: December 12, 2013

In Chapter 2 of JG Interim Report, it was confirmed that the Ship’s drawings and hull structure conformed to the relevant requirements of ClassNK rules through drawing approval, and that the classification surveys during construction and in service were carried out satisfactorily.

In Chapters 3 and 4, JG Interim Report concluded that the hull fracture originated from buckling collapse of the bottom shell plates in way of a butt joint in the double bottom structure underneath No. 6 Cargo Hold in the midship part (See **Fig. 1-1**).

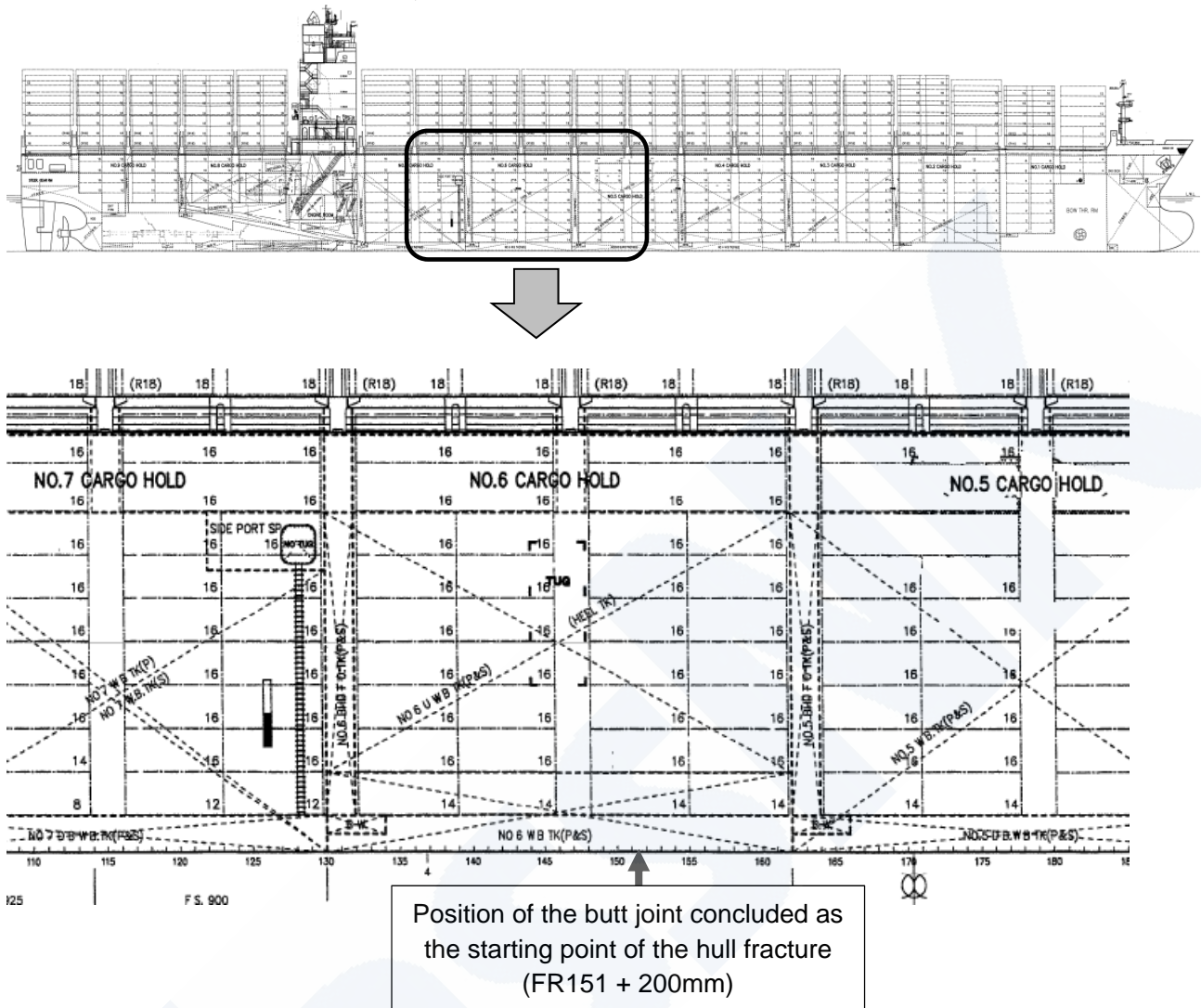


Fig. 1-1 Layout of midship part of the Ship

JG Committee carried out the following investigations in order to reproduce the accident as stated from Chapter 5 to 7 of JG Interim Report.

Firstly, JG Committee estimated the sea state at the time of the accident to be the significant wave height of 5.5 meters, the mean wave period of 10.3 seconds and the encountered wave direction of 114 degrees (oblique sea from bow and Port side) based on the weather and sea states data at that time. Secondly, the wave loads acting on the Ship such as vertical bending moment, external sea pressure on side and bottom shell, cargo and ballast weight at the time of the accident were evaluated in the estimated sea state and then numerical simulations of the hull structural strength of the Ship under the evaluated acting loads, i.e. lateral loads and vertical bending moment, were conducted.

The result of the simulation showed that the hull girder ultimate strength was around 150% of the estimated vertical bending moment and the simulation could not reproduce the fracture.

Chapter 8 of JG Interim Report suggested future tasks related to the simulation of acting loads and the strength considering uncertainty factors, margins of the structural strength, on-board full scale measurement and so on.

Chapter 2 The Investigative Panel on Large Container Ship Safety

In light of the findings from the investigation at JG Committee, Nippon Kaiji Kyokai (ClassNK) set up a new Investigative Panel on Large Container Ship Safety (hereinafter “NK Panel”) in February 2014. It comprised Japanese shipyards building large container ships, shipping companies operating such ships and academic experts. It also invited the Japanese Ministry of Land, Infrastructure, Transport and Tourism and the Japanese National Maritime Research Institute as observers. **Appendix 1** presents the list of members of NK Panel.

NK Panel investigated the two issues described below and delivered the Investigation Report on Structural Safety of Large Container Ships (hereinafter “this Report”) containing the findings, the conclusions and the action plan to be implemented by ClassNK.

(i) Investigation on possibility of occurrence of the fracture

JG Committee obtained a result that the hull girder ultimate strength of the Ship was around 150% of the vertical bending moment estimated to act on the Ship at the time of the accident, and could not reproduce the fracture. Taking such result into account, NK Panel investigated the possibility of occurrence of the fracture considering uncertainty factors on the strength and the loads with reasonable ranges of the deviations.

(ii) Investigation on structural safety

NK Panel conducted 3-hold model elasto-plastic analyses for a number of large container ships including the Ship and investigated the margin of hull girder ultimate strength. NK Panel also investigated the relationship between the collapse strength of the bottom shell plates and the hull girder ultimate strength in order to figure out the mechanism of occurrence of the fracture.

Chapter 3 Investigation on Possibility of Occurrence of the Fracture

3.1 Introduction

JG Interim Report published in December 2013 estimated that the hull girder ultimate strength of the Ship had been around 150% of the estimated vertical bending moment at the time of the accident and could not show the possibility of the occurrence of the fracture.

JG Interim Report suggested the need to consider the effects of uncertainty factors involved in the strength and loads.

With consideration of the suggestion of JG Interim Report, the possibility of the occurrence of the fracture accident was investigated by probabilistic approach in this Chapter taking into

account uncertainty factors affecting the hull girder ultimate strength and the vertical bending moments.

3.2 Uncertainty Factors in Strength and Loads

A key point in the investigation on the possibility of the occurrence of the fracture is the margin of the hull girder ultimate strength against the loads.

The factors related to the margin of the hull girder ultimate strength are listed below in the case of the fracture accident.

The followings are definite factors on the strength which are clearly specified in the hull structural drawings.

- Scantling of the structural members of the double bottom structure and structural arrangement of the double bottom structure such as spacing of bottom longitudinals, arrangement of girders and floors. (It was concluded that the fracture had originated from the bottom shell plates in the double bottom structure of the midship part.)
- Scantlings and structural arrangement of surrounding structural members which affect the strength of the double bottom structure such as the partial bulkheads.
- Structural details around the starting point of the fracture such as butt joint, scallop, opening and discontinuity in scantling of structural members.

Meanwhile the followings are considered as uncertainty factors on hull girder ultimate strength in general referring to JG Interim Report.

- Yield stress of steel (hereinafter "yield stress")
- Effect of welding residual stress
- Lateral loads, such as sea pressure and container loads
- Sea states
- Effect on still water bending moment due to deviations of container weight

Among these factors affecting the structural strength, definite factors such as scantling, arrangements and structural details were taken into consideration on the 3-hold model elasto-plastic analyses carried out in JG Interim Report to estimate the hull girder ultimate strength of the Ship.

On the other hand, uncertainty factors such as the yield stress and the effects of local deformations of the bottom shell plates found in the sister ships of the Ship were not taken into consideration in JG Interim Report.

With respect to the loads, JG Interim Report estimated the sea state at the time of the accident as the significant wave height of 5.5 meters, the mean wave period of 10.3 seconds and the encountered wave direction of 114 degrees (oblique sea from bow and Port side) from the weather and sea states data at that time and information on her heading and ahead speed. Based on the above estimated sea state, the wave-induced vertical bending moment

including whipping response was estimated through the simulations by a non-linear strip method. However as commented in JG Interim Report, the estimation of the sea state at the time of the accident may have some deviations due to the measurement errors of the weather and sea states data used in the estimation.

In addition, the uncertainty of the still water vertical bending moment caused by deviations in container weights, i.e. the differences between declared weights and actual weights, was also not taken into account in JG Interim Report.

In view of the above, the possibility of the occurrence of the fracture was investigated by NK Panel with consideration of uncertainty factors in strength and loads which had not been considered in JG Interim Report.

3.3 Estimation of Strength and Load in Consideration of Deviation of Uncertainty Factors

The five factors listed below were considered as the uncertainty factors in this investigation. Strength and loads were estimated in the consideration of their deviations within reasonable ranges instead of giving uniquely defined values.

【Uncertainty factors related to the strength】

- Yield stress
- Effect of local deformations of the bottom shell plates
- Effect of residual stress of the fillet welding part of bottom longitudinals

【Uncertainty factors related to the loads】

- Sea state in connection with wave-induced vertical bending moment
- Actual container weight in connection with still water vertical bending moment

The strength, i.e. hull girder ultimate strength of the Ship was estimated by 3-hold model elasto-plastic analyses in this Chapter, and they were carried out with the full draught (14.5m), the same as in JG Interim Report, instead of the actual draught at the time of the accident. It was expected that the effect of the deviations of the lateral loads acting on the double bottom structure, which was mainly caused due to the deviation of wave-induced pressure, could be taken into account by the difference between the full draught used in the analyses and the actual draught. Therefore, the uncertainty of the lateral loads was not taken into account in the investigation of this Report, although this had been pointed as an uncertainty factor in JG Interim Report.

3.3.1 Estimation of strength in consideration of deviation of uncertainty factors

Yield stress, effect of local deformation and effect of welding residual stress were considered as the uncertainty factors in the strength.

In consideration of the deviation of the yield stress, the average value of the yield stress

was calculated based on the values on the mill sheets of the bottom shell plates in the area where the fracture of the Ship was concluded to have originated. Using the average value of the yield stress based on the mill sheet values, the hull girder ultimate strength was calculated and defined as *the mean value of the hull girder ultimate strength*.

For the minimum value of the hull girder ultimate strength corresponding to the minimum value of the yield stress, the following two cases were considered. The investigation of Case 1 estimated smaller deviation of the yield stress than that of Case 2.

Case 1	<ul style="list-style-type: none"> • The standard deviation (σ) of the yield stress was calculated based on the mill sheet values of the bottom shell plates. The minimum yield stress was defined to be the value lower by three times the standard deviation (3σ) than the average value of the yield stress obtained through the mill sheets values. • The hull girder ultimate strength was calculated in consideration where the yield stress of all bottom shell plates in the calculation was equal to the above minimum yield stress, and the calculated value was defined to be <i>the minimum hull girder ultimate strength</i>.
Case 2	<ul style="list-style-type: none"> • The hull girder ultimate strength was calculated in consideration where the yield stress of all bottom shell plates in the calculation was equal to the specified minimum yield stress, and the calculated value was defined to be <i>the minimum hull girder ultimate strength</i>.

The hull girder ultimate strength was calculated by 3-hold model elasto-plastic analyses. Details of the analysis conditions are shown in **Appendix 2**.

The effects on the hull girder ultimate strength caused by the local deformations of bottom shell plates and the residual stress at the fillet welding part of bottom longitudinals were treated as follows. **Appendix 3** shows further details.

- The possibility was considered that deformations might have existed in the bottom shell plates of the Ship which had the similar mode to the local deformations found in the sister ships through the inspections after the accident. The effect of the local deformations in the bottom shell plates was considered to reduce the hull girder ultimate strength and estimated at maximum 4%.
- It was estimated that the reduction of the hull girder ultimate strength due to the effect of the welding residual stress in the longitudinal direction caused by the fillet welding of bottom longitudinals was maximum 5%.

The minimum hull girder ultimate strength corresponding to the minimum yield stress shown in the above table was multiplied by the two effects values of the strength reduction, that is to say one is due to the effect of the local deformations in the bottom shell plates and

the other is due to the effect of the welding residual stress. The resulting value of the hull girder ultimate strength was defined as *the lower limit of the hull girder ultimate strength*.

Table 3-1 shows the values of the hull girder ultimate strength of the Ship thus calculated.

Table 3-1 Hull girder ultimate strength of the Ship considering the deviation of uncertainty factors

(Unit : kN-m)

<p><i>Mean value of the hull girder ultimate strength</i> (Value corresponding to average yield stress of bottom shell plates of the Ship based on the mill sheet values)</p>	<p>14.8 × 10⁶</p>	
<p><i>Minimum hull girder ultimate strength</i> corresponding to the minimum yield stress</p>	<p>Case 1 Minimum yield stress was estimated based on the deviation of the mill sheets values of the Ship</p>	<p>Case 2 Minimum yield stress was defined as the specified minimum yield stress</p>
	<p>14.2 × 10⁶</p>	<p>13.2 × 10⁶</p>
<p><i>Lower limit of the hull girder ultimate strength</i> (Value calculated by multiplying <i>Minimum hull girder ultimate strength</i> by 0.96 and 0.95 considering the effects of local deformation and welding residual stress, respectively)</p>	<p>13.0 × 10⁶</p>	<p>12.0 × 10⁶</p>

3.3.2 Estimation of wave-induced vertical bending moment in consideration of deviation of uncertainty factors

JG Interim Report estimated that the sea state at the time of the accident had a significant wave height of 5.5 meters, the mean wave period of 10.3 seconds and the encountered wave direction of 114 degrees (oblique sea from bow and Port side). It also pointed out that the significant wave height might have variation from 0.5 meters to 2 meters due to the measurement errors in the weather and sea states data used for the estimation.

In the investigation of this Chapter, wave-induced load simulations in a total of 27 different cases of sea states at the time of the accident were carried out combining significant wave

heights of 5.5 m, 6.5 m and 7.5 m, mean wave periods of 10.3 seconds, 12.5 seconds and 15 seconds and encountered wave directions of 120 degrees, 150 degrees and 180 degrees (head sea) to estimate the deviation of the wave-induced vertical bending moment at the time of the accident under different conditions. **Appendix 4** describes the details. The simulations showed the result that the upper limit of the wave-induced vertical bending moment at the time of the accident was 7.23×10^6 kN-m including whipping response component of 3.05×10^6 kN-m corresponding to the significant wave height of 7.5 meters, mean wave period of 15 seconds and encountered wave direction of 180 degrees (head sea).

3.3.3 Estimation of still water vertical bending moment in consideration of deviation of uncertainty factors

JG Interim Report concluded the still water vertical bending moment at the time of the accident to be 6.0×10^6 kN-m. This value was calculated from the container weights declared by the shippers. In reality, there could have been gaps between the declared weight and the actual weight of the containers. This means that the actual still water vertical bending moment might have deviated from that which was calculated based on the declared weight. The investigation in this Chapter took into consideration 10% deviation at maximum from the calculated still water vertical bending moment in accordance with the investigation result of draught measurement data of the sister ships of the Ship at the time of their departure as shown in **Appendix 5**.

3.3.4 Lower limit of strength and upper limit of load

As stated in 3.3.1 of this Report, it is estimated that the lower limit of strength was 13.0×10^6 kN-m in Case 1 and 12.0×10^6 kN-m in Case 2 respectively as shown in **Table 3-1**.

As stated in 3.3.2 and 3.3.3, the total vertical bending moment at the time of the accident, the sum of the wave-induced vertical bending moment and the still water vertical bending moment, was estimated to be 13.8×10^6 kN-m ($=7.23 \times 10^6$ kN-m + 6.0×10^6 kN-m $\times 1.1$) as the upper limit.

The results of the investigation on strength and loads considering the deviations of the five uncertainty factors listed in the beginning of this section indicate a possibility that the upper limit of the load (the vertical bending moment) may have exceeded the lower limit of the strength (the hull girder ultimate strength).

3.4 Possibility of Occurrence of Fracture

As concluded in 3.3 of this Report, there was a possibility that the upper limit of the load exceeded the lower limit of strength at the time of the fracture. The possibility of the occurrence of the fracture was estimated in the probabilistic way by estimating the probability distributions of the strength and the load in the investigation of this section.

Given the limitation of data on both the strength and the loads used for the estimation of the probability distribution, at first the types of the probability distribution of the strength and the loads were assumed and then the parameters which figured the deviations of the probability distributions were estimated based on the values of the strength and the loads as evaluated in 3.3 of this Report considering the deviations. While there are many different methods of estimating the probability distributions for the strength and for the loads with the various assumptions, the probability distributions were estimated by the following methods in the investigation of this Report.

The probability distribution of the hull girder ultimate strength was presumed to follow the normal distribution. The degree of the deviation of the strength was calculated using the two methods, one is according to Case 1 in 3.3.1, where the minimum yield stress was estimated from the deviation of the mill sheet values of the bottom shell plates of the Ship and the other method is according to Case 2 in 3.3.1, where the minimum yield stress was defined as the specified minimum yield stress.

The probability distribution of the wave-induced vertical bending moment resulting from the simulations of the 27 cases was presumed to follow the Gumbel distribution, which is one of extreme value distributions. On the other hand, the probability distribution of the still water vertical bending moment was presumed to follow the normal distribution according to the investigation results shown in **Appendix 5**.

The details of the estimation of probability distributions for the strength and the loads are shown in **Appendix 6**. **Appendix 6** also shows the result in case where the probability distribution of the wave-induced vertical bending moment was presumed to be the normal distribution for reference.

Fig. 3-1 shows relationship between the strength and the load at the time of the accident based on the probability distribution, which was estimated by the above method. In **Fig. 3-1**, the deviation of the strength was used as calculated by the method of Case 1 in 3.3.1 where the minimum yield stress was estimated from the deviation of the mill sheet values of the bottom shell plate of the Ship, which was considered more realistic than the other cases. Results of the other cases are shown in **Appendix 6**.

Fig. 3-1 shows that it is actually possible where the load of the vertical bending moment exceeded the hull girder ultimate strength at the time of the accident when the effects of the deviations of the uncertainty factors were considered although the overlap between the strength and the load is very narrow.

In **Fig. 3-1**, the size of the overlapping part between the blue curve which shows the probability of the strength and the red curve which shows the probability of the load indicates the qualitative level of occurrence probability of the fracture. Therefore it can be said that the following two factors are important to investigate the possibility of occurrence of the fracture:

- the margin of strength against the load represented by the gap between the respective peaks; and
- the degree of the deviation, i.e. the ranges of the probability distribution curves of the strength and the load.

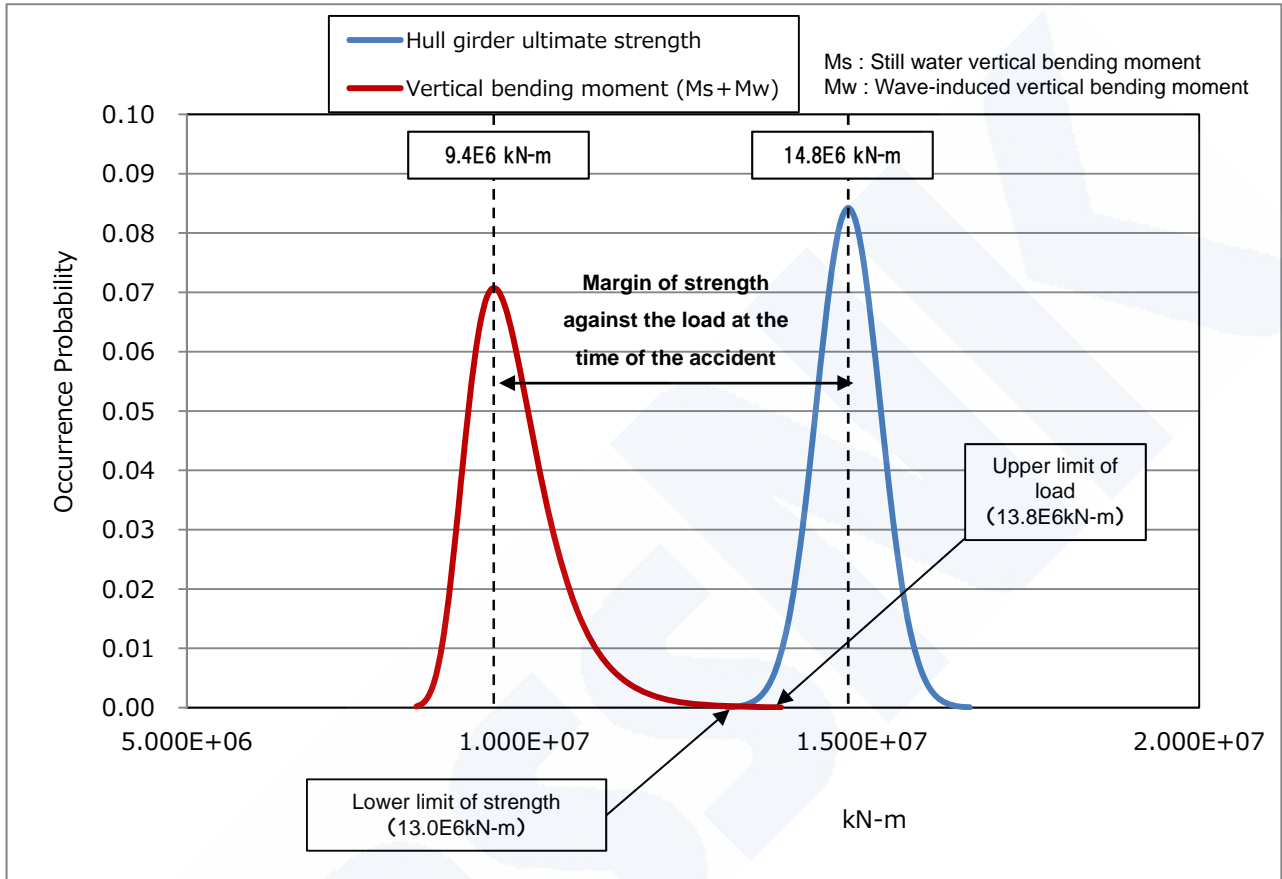


Fig. 3-1 Relationship between strength and load at the time of the accident
(Probability distribution curve of strength and load)

Probability distribution of strength : Normal distribution
(The deviation to be estimated from the deviation of the mill sheets values of the Ship)
Wave-induced vertical bending moment : Gumbel distribution
Still water vertical bending moment : Normal distribution

Note : The vertical axis shows the occurrence probability corresponding to the band of strength and load of 1.0×10^5 kN-m.

The margin of the strength becomes very important for large container ships in the same category, where the degrees of the deviations of the strength and the loads represented by the range of the blue and the red curves in **Fig. 3-1** respectively are almost the same among large container ships.

Chapter 4 Investigation of Structural Safety

4.1 Introduction

As stated in JG Report, it is inferred that in the fracture accident, the bottom shell plates were buckled and collapsed in the midship part of the Ship first and the hull girder was fractured subsequently in a short time. As far as investigated, there have been no cases in the past where collapse of bottom shell plates was the origin of hull girder fracture

It is essential to find out the mechanism of the hull girder fracture and to establish adequate assessment procedures for the hull structural strength in order to prevent similar fracture accidents.

In this investigation, 3-hold model elasto-plastic analyses were carried out on a number of large container ships including the Ship and the margin against the expected loads was investigated. The relationship between the buckling collapse strength of bottom shell plates and the hull girder ultimate strength was also investigated in order to find out the mechanism of the fracture accident this time, namely the process from the buckling collapse of bottom shell plates to the hull girder fracture.

Furthermore the analysis was conducted on the on-board full scale measurement results of large container ships carried out in the past with cooperation of the owners and the shipyards in order to grasp the wave-induced loads including whipping responses in actual navigating conditions.

The following knowledge was obtained concerning the hull structural strength of large container ships through these investigations.

- The local strength of the double bottom structure, i.e. the transverse strength, against lateral loads such as bottom sea pressure and container loads is closely related to the hull girder ultimate strength through the buckling collapse of bottom shell plates.
- Double bottom structure of a container ship is always subjected to upward loads of the bottom sea pressure. Under this condition there is a possibility that local buckling collapse of bottom shell plates causes reduction in the strength of double bottom structure and it leads to the hull girder fracture due to superimposition of the vertical bending moment.
- Hull structural strength can be adequately assessed relating to the hull girder fracture accident when the hull girder ultimate strength is evaluated in consideration of the effects of lateral loads.

The overview of these inspections is given below.

The investigations were carried out on seventeen Post-Panamax container ships of 6,000TEU class and 8,000TEU class including the Ship (hereinafter "all ships in investigation") constructed by the major shipyards both inside and outside of Japan including

some container ships designed based on the rules of other classification societies than ClassNK. The results of the investigations therefore represent the general features and trends of typical large container ships.

The investigations were carried out by 3-hold model elasto-plastic analyses on seven ships including the Ship among the above seventeen Post-Panamax container ships as stated in 4.2.3, and hereinafter these seven ships are called as the “target ships”.

4.2 Margin of Hull Girder Strength

As noted in Chapter 3 of this Report, it is important to evaluate strength margins against loads adequately in order to assess the possibility of similar fracture accidents.

Investigation was carried out with respect to the following three strength margins.

- (1) Margin against the requirements of IACS UR S11 relating to the vertical bending strength on the all ships in investigation
- (2) Margin of the hull girder ultimate strength calculated by the method specified in IACS CSR, i.e. Smith’s method on the all ships in investigation
- (3) Margin of the hull girder ultimate strength calculated by 3-hold model elasto-plastic analysis on the target ships

The specified minimum yield stress required by the rules as shown in the table below was used for the above investigations in order to get normalized results for the comparison.

Steel Strength	Specified minimum yield stresses required by the Rules
Mild Steel	235 N/mm ²
HT32	315 N/mm ²
HT36	355 N/mm ²
HT40	390 N/mm ²
HT47	460 N/mm ²

4.2.1 Margin against the requirements of IACS UR S11 relating to the vertical bending strength

IACS specifies the Unified Requirement of the hull section modulus (Z) in the midship (UR S11) relating to the vertical bending strength as follows.

$$Z = \frac{|M_S + M_W|}{\sigma} \text{ (cm}^3\text{)}$$

- σ : Permissible bending stress (175/k N/mm²)
- k : Factor on material strength (1.0 for Mild steel)
- M_S : Allowable still water vertical bending moment (kN-m)

M_W : Wave-induced vertical bending moment given by the following formulae:

$$M_W = +0.19C_1C_2L_1^2BC'_b \text{ (Hog) (kN-m)}$$

$$M_W = -0.11C_1C_2L_1^2B(C'_b + 0.7) \text{ (Sag) (kN-m)}$$

L_1 : Length of the ship specified in the rules (m)

B : Breadth of the ship (m)

C_1 : Coefficient determined by the length of the ship (L_1)

$$10.75 \text{ when } 300\text{m} < L_1 \leq 350\text{m}$$

C_2 : Coefficient determined by the position in the longitudinal direction of the ship

$$1.0 \text{ in the midship between } 0.4L \text{ and } 0.65L$$

C'_b : Block coefficient, but not to be taken less than 0.6

Furthermore IACS UR S11 also specifies the requirements of elastic buckling strength of bottom shell plates and bottom longitudinals against the vertical bending stress caused by the vertical bending moment of M_S and M_W stated in the above.

Fig. 4-1 shows the margins against the above requirements of IACS UR S11 concerning the all ships in investigation including the Ship (Ship A). No substantial differences are observed between the Ship and the other ships in the margins against the requirements of IACS UR S11. The requirements of IACS UR S11 on the vertical bending strength consider the vertical bending moment acting on a hull girder only and do not take into consideration the effect of the lateral loads acting on double bottom structure such as bottom sea pressure and container loads.

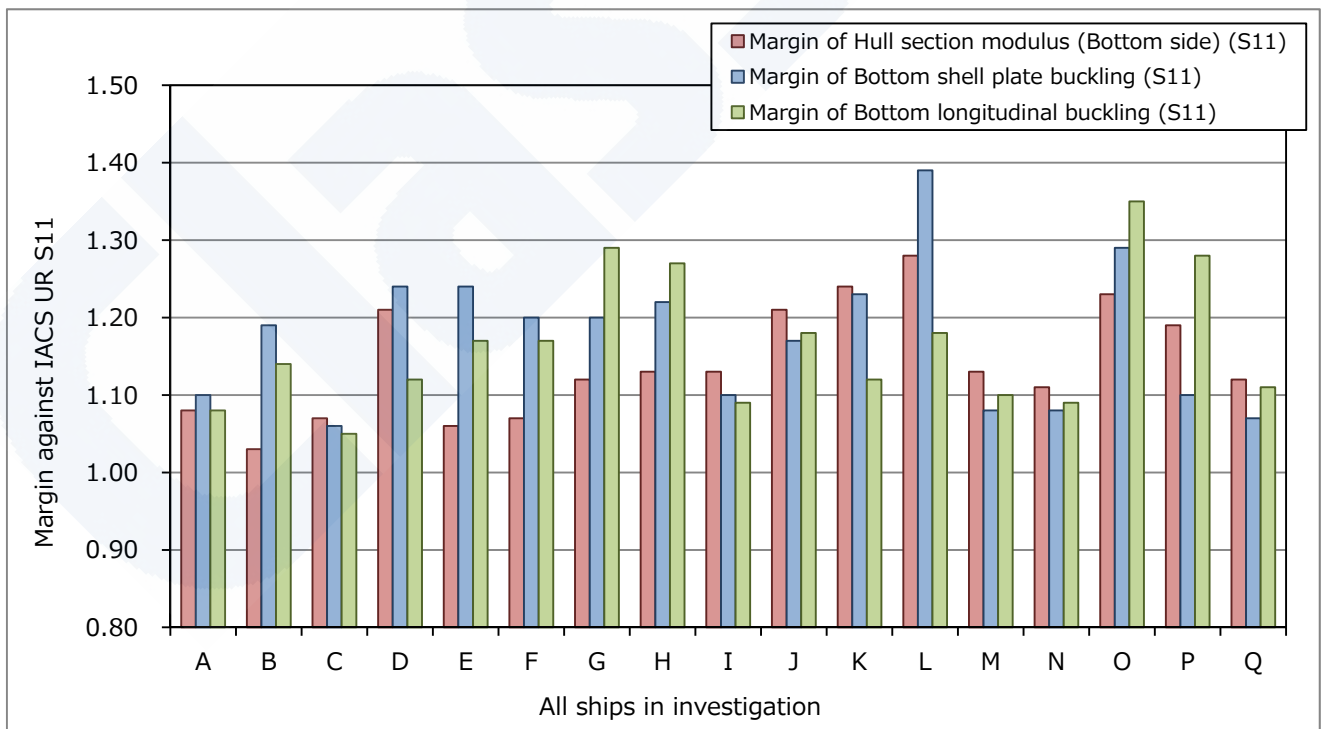


Fig. 4-1 Margin against the requirements of IACS UR S11 relating to vertical bending strength in consideration of no effect of the lateral loads

4.2.2 Margin of the hull girder ultimate strength calculated by the method specified in IACS CSR based on Smith's method

IACS CSR specify the method to calculate the hull girder ultimate strength, which is a relatively simple method based on Smith's method.

The hull girder ultimate strength was calculated according to the method specified in IACS CSR on the all ships in investigation and the margin against the wave-induced vertical bending moment of the rules was obtained.

Here, "margin against the wave-induced vertical bending moment of the rules" is defined by the following formula and it shows the limit of the wave-induced vertical bending moment, in other words, the ratio of the hull girder ultimate strength to the wave-induced vertical bending moment of the rules when a ship is in the condition of 100% of the allowable still water bending moment.

$$\text{Margin against the wave-induced vertical bending moment of the rules} = \frac{M_U - M_S}{M_W}$$

M_U : Hull girder ultimate strength calculated by IACS CSR method

M_S : Allowable still water vertical bending moment

M_W : Wave-induced vertical bending moment specified in IACS UR S11.

For the reference, the effect of whipping response is not taken into account in the wave-induced vertical bending moment specified in IACS UR S11. The hull girder ultimate strength calculated by the method of IACS CSR considers only the vertical bending moment and the effects of lateral loads are not taken into consideration as same as IACS UR S11 described in 4.2.1 above.

In the calculation of the hull girder ultimate strength calculated by the IACS CSR method, the yield stress was taken as the specified minimum yield stress.

Fig. 4-2 shows the result obtained from the above investigation. As same as the case of 4.2.1, no substantial difference is observed between the Ship (Ship A) and other ships in investigation with respect to the margin of the hull girder ultimate strength calculated by IACS CSR method, which does not consider the effect of the lateral loads.

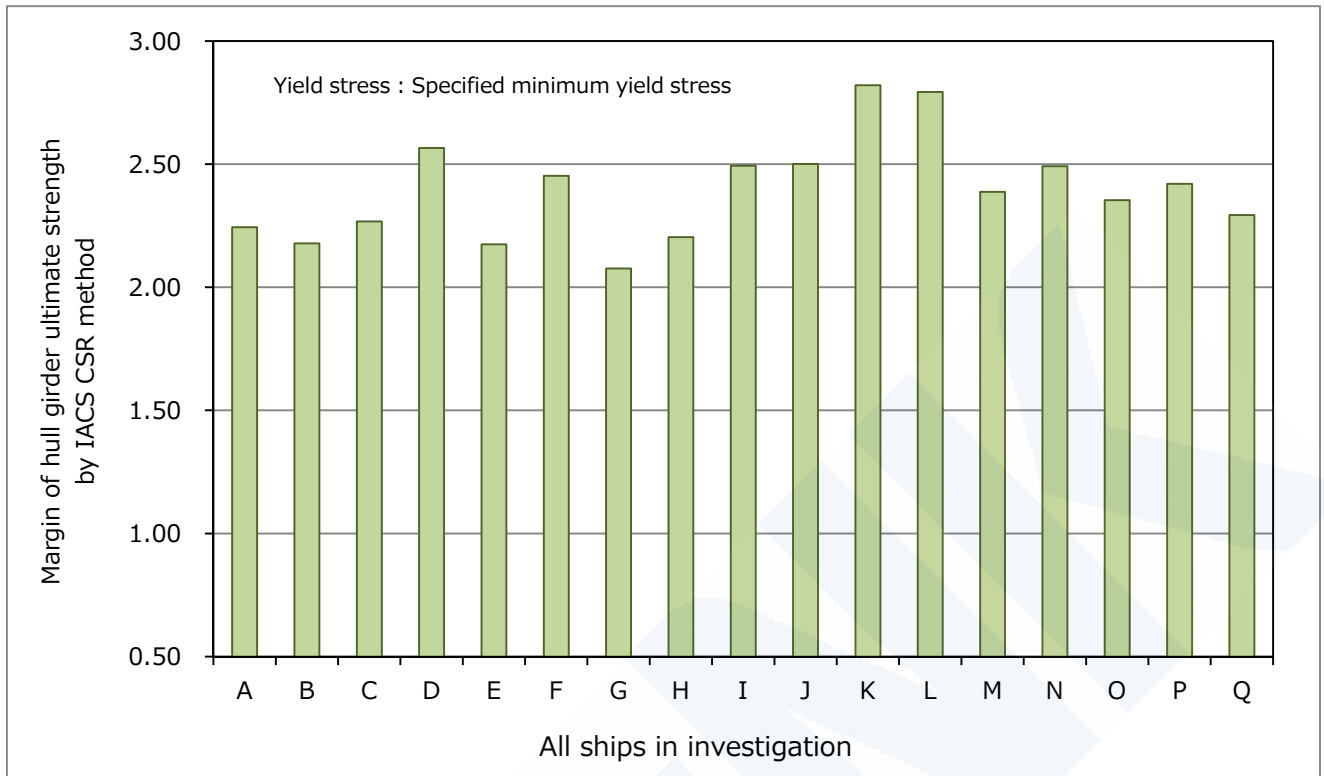


Fig. 4-2 Margin of hull girder ultimate strength calculated by IACS CSR method in consideration of no effect of lateral loads

(Margin against the wave-induced vertical bending moment specified in IACS UR S11)

4.2.3 Margin of the hull girder ultimate strength calculated by 3-hold model elasto-plastic analysis

The hull girder ultimate strength was calculated by 3-hold model elasto-plastic analysis considering the lateral loads on the target ships, and the margin of the hull girder ultimate strength was investigated. The specified minimum yield stress was used for the investigation as well as 4.2.2 of this Report.

One-bay empty condition without ballast in double bottom was applied as the loading condition for the analyses because of the following two reasons. Firstly, One-bay empty condition without ballast in double bottom is one of the most severe loading conditions for the strength of double bottom structure and it was expected to be effective to compare the strength margin of the target ships.

Secondly, it sometimes happens that the stress of the transverse strength of double bottom structure in the normal loading conditions becomes nearly equal to the stress corresponding to One-bay empty condition without ballast in double bottom in the case of Post-Panamax container ships, since various loading conditions are available for Post-Panamax container ships, as detailed in 4.4 of this Report and **Appendix 7**.

It is noted that direct strength calculation of the double bottom structure had been carried out in One-bay empty condition with ballast in double bottom for some of the target ships when they had been constructed.

Appendix 8 shows the details of the 3-hold model elasto-plastic analyses. Unlike the cases of 4.2.1 and 4.2.2, the hull girder ultimate strength can be evaluated with consideration of the effect of the lateral loads such as bottom sea pressure and container loads, by 3-hold model elasto-plastic analyses.

The margins against the requirements of IACS UR S11 shown in 4.2.1 and the margin of the hull girder ultimate strength calculated by the method of IACS CSR shown in 4.2.2 were compared in each other among the all ships in investigation. In addition the buckling collapse strength of bottom shell panels of the all ships in investigation was also compared to each other. The target ships for 3-hold model elasto-plastic analyses were selected among the all ships in investigation based on these comparison results. Accordingly, it can be said that the target ships represent the feature and trend of the margin of the hull girder ultimate strength. The ships represented by alphabets in the horizontal axes of **Fig. 4-3** and **Fig. 4-4** are the same ships as those in **Fig. 4-1** and **Fig. 4-2**.

The margin against the wave-induced vertical bending moment of the rules was calculated on the hull girder ultimate strength obtained by 3-hold model elasto-plastic analyses in the same way as shown in the following formula. The result was shown in **Fig. 4-3**.

$$\text{Margin against the wave-induced vertical bending moment of the rules} = \frac{M_U - M_S}{M_W}$$

M_U : Hull girder ultimate strength calculated by 3-hold model elasto-plastic analysis

M_S : Allowable still water vertical bending moment

M_W : Wave-induced vertical bending moment specified in IACS UR S11.

The difference between the Ship (Ship A) and other target ships is observed in **Fig. 4-3** unlike **Fig. 4-1** "Margin against the requirements of IACS UR S11" and **Fig. 4-2** "Margin of the hull girder ultimate strength calculated by IACS CSR method" both of which do not consider the effect of the lateral loads.



Fig. 4-3 Margin of hull girder ultimate strength calculated by 3-hold model elasto-plastic analysis in consideration of effect of the lateral loads (Margin against the wave-induced vertical bending moment specified in IACS UR S11)

Fig. 4-4 shows the ratio of the ultimate strength calculated by 3-hold model elasto-plastic analysis to the ultimate strength calculated by IACS CSR method (hereinafter “the ratio of the hull girder ultimate strength”), which indicates the degree of the decrease in the ultimate hull girder strength calculated by 3-hold model elasto-plastic analysis compared to the ultimate strength calculated by IACS CSR method.

According to Fig. 4-4, while the ratio of the hull girder ultimate strength of the Ship (Ship A) is around 70%, the ratios of the hull girder ultimate strength of the other target ships are from 80% to 85%. The difference between the Ship (Ship A) and the other target ships shows similar tendency as in Fig. 4-3.

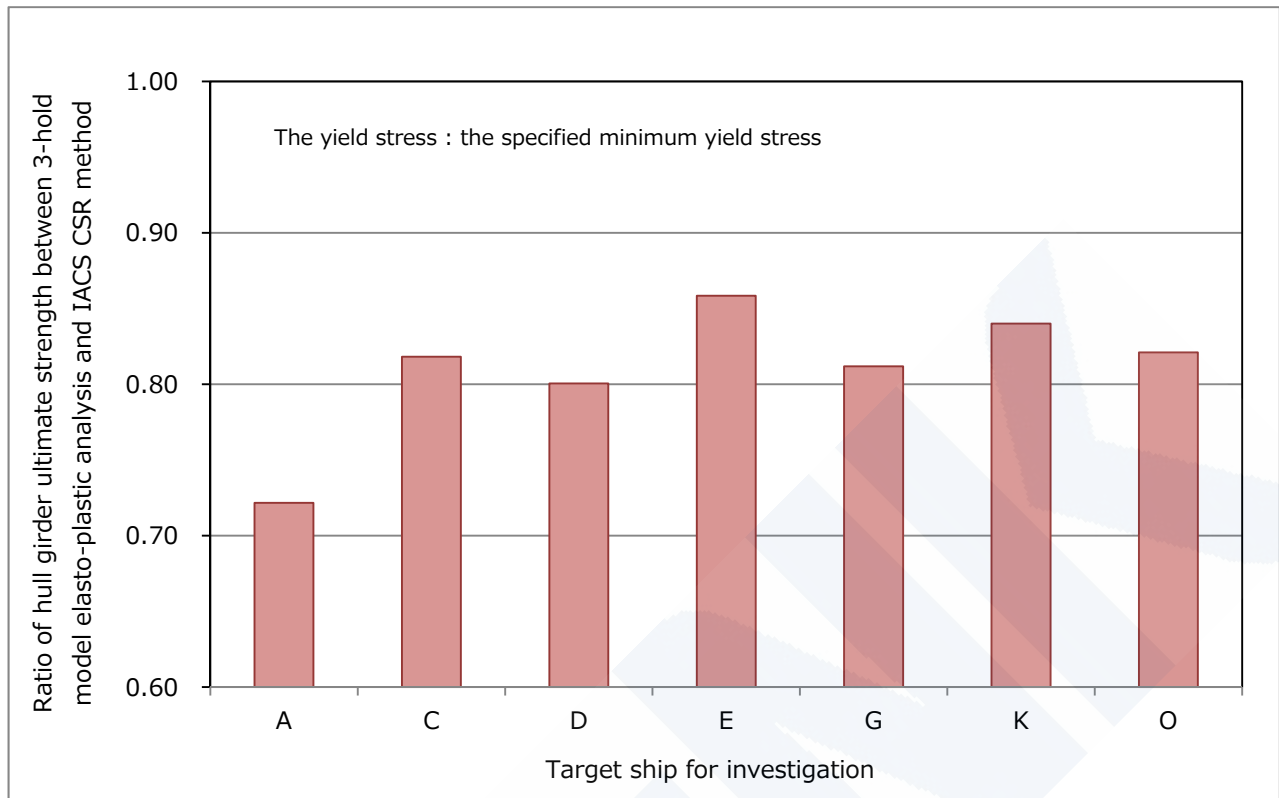


Fig. 4-4 Decrease in hull girder ultimate strength calculated by 3-hold model elasto-plastic analysis compared to the ultimate strength calculated by IACS CSR method

No difference is found between the Ship and the other target ships on the margin against the requirements of IACS UR S11 and the margin of the hull girder ultimate strength calculated by the method of IACS CSR, which do not consider the effect of the lateral loads acting on double bottom structure. On the other hand, the difference is found on the margin of the hull girder ultimate strength calculated by 3-hold model elasto-plastic analysis which considers the effect of the lateral loads acting on double bottom structure.

The 3-hold model elasto-plastic analysis considering the effect of the lateral loads reproduces the actual condition of the ships more precisely. Therefore it can be concluded that the strength of double bottom structure against the lateral loads such as bottom sea pressure and container loads has close relationship to the hull girder ultimate strength in the case of the fracture accident.

4.3 Mechanism of Hull Girder Fracture

The mechanism of hull girder fracture was investigated focusing on the following three points, which were considered to be especially important.

- Reasons why the difference is observed between the Ship and the other target ships having safe service records on the margin of hull girder ultimate strength calculated by 3-hold model elasto-plastic analysis which considers the effect of the lateral loads.

- How the buckling collapse of the bottom shell plates leads to the hull girder fracture in a short time
- Relationship between the transverse strength of the double bottom structure against the lateral loads and the hull girder ultimate strength

4.3.1 Buckling collapse strength of bottom shell plates

First, the investigation results on the buckling collapse strength of bottom shell plates are reported below, because it was inferred that the hull girder fracture had originated from the buckling collapse of the bottom shell plates.

As explained in **Appendix 9**, the followings are the main loads always acting on the double bottom structure of container ships. It is noted that container loads are relatively smaller than the bottom sea pressure in general as the lateral loads.

- Compressive loads in longitudinal direction due to vertical bending moment in hogging condition
- Lateral loads in upward direction due to bottom sea pressure
- Compressive loads in transverse direction due to side sea pressure

The compressive loads due to vertical bending moment causes longitudinal compressive stress and the compressive loads due to side sea pressure causes transverse compressive stress respectively on the bottom shell plates.

Furthermore the lateral loads cause upwards bending on the double bottom structure, and result in compressive stresses in the bottom shell plates in the middle part of the double bottom structure both in longitudinal and transverse directions respectively (hereinafter these compressive stresses are referred to as "double bottom local stress"). (Refer to **Appendix 9**.)

Due to the superimposition of the above stresses, the bottom shell plates of container ships are always in the compressive condition both in the longitudinal and transverse directions in the middle part of the double bottom structure.

Therefore in the investigation of the buckling collapse of the bottom shell plates in 4.3.1 of this Report, bottom shell plates were considered as panels which were stiffened by bottom longitudinals and surrounded by girders on side edges and by floors on fore and aft edges as shown in **Appendix 10** (hereinafter "stiffened bottom panel").

According to the explanation above, the stiffened bottom panels are subjected to bi-axial compressive stress composed of the following stresses:

- Compressive stress in longitudinal direction due to vertical bending moment
- Compressive stress in transverse direction due to side sea pressure
- Double bottom local stresses due to the lateral loads both in the longitudinal and transverse directions

Furthermore, the stiffened bottom panels are also subjected to lateral loads of bottom sea pressure.

Fig. 4-5 shows the buckling collapse strength of the stiffened bottom panel of the Ship between No.3 girder and No.9 girder which is the panel adjacent to the keel plate panel in way of the butt joint in the midship part from which it was concluded the fracture had originated. The buckling collapse strength of the panel was estimated by an elasto-plastic analysis using the FE model of the panel with the following analysis conditions. (Refer to **Appendix 10** for the details.)

Initial shape deformation	Deformation simulating "hungry horse" mode (Pattern A shown in Fig. A10-2 of Appendix 10)
Yield stress	General average values used in JG Interim Report (Value are shown in 2.3 of Appendix 10)
Stress condition	Bi-axial compressive condition in longitudinal direction and transverse direction
Load condition	Lateral loads of bottom sea pressure applied

The blue line of **Fig. 4-5** shows the buckling collapse strength of the stiffened bottom panel of the Ship. In the case where a stress in the panel which is a combination of the stresses in longitudinal direction (σ_x) and in transverse direction (σ_y) is located outside the blue line, it means the buckling collapse occurs in the panel.

However it should be noted that the hull girder ultimate strength is larger than the buckling collapse strength of one stiffened bottom panel and a collapse of one panel does not immediately lead to the hull girder fracture.

Fig. 4-5 shows the trend that the buckling collapse strength in the longitudinal direction, i.e. a critical stress of σ_x , becomes considerably reduced when the stress in transverse direction (σ_y) exceeds 100 N/mm². Other graphs of the buckling collapse strength of the target ships are shown in **Appendix 10** and the same trend is seen.

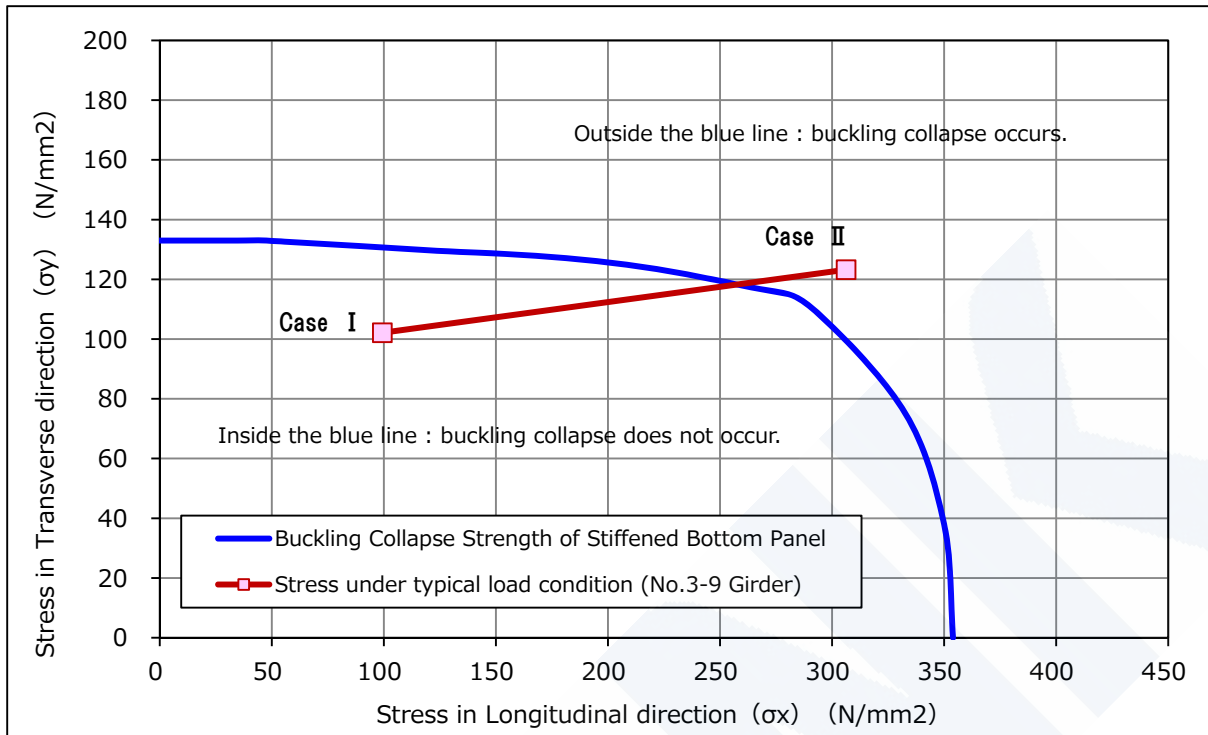


Fig. 4-5 Buckling collapse strength of stiffened bottom panel and stress in the panel under typical load conditions shown in **Table 4-1** (the Ship / No.3 Girder - No.9 Girder / in way of butt joint in midship part)

Note : Initial shape deformation of buckling collapse strength is deformation simulating "hungry horse" mode and yield stress is general average values. (Refer to **Appendix 10** for details.)

Fig. 4-5 also shows the stresses in longitudinal direction (σ_x) and in the transverse direction (σ_y) generated in the stiffened bottom panel under typical load conditions as stated in **Table 4-1**. In the calculation of the stresses in the panel, elastic analyses using 3-hold FE models were applied and the fore and aft ends of the models were simply supported, the same as the 3-hold model elasto-plastic analyses. One-bay empty condition without ballast in double bottom was applied in the calculation. The reason why One-bay empty condition without ballast in double bottom was applied in the calculation of the stresses of the panel is the same as explained in 4.2.3. Firstly, One-bay empty condition without ballast in double bottom is one of the most severe loading conditions for the strength of double bottom structure and it was expected to be effective to compare the buckling collapse strength of the target ships. Secondly, it sometimes happens that the stress of the transverse strength of double bottom structure in the normal loading conditions becomes nearly equal to the stress corresponding to One-bay empty condition without ballast in double bottom in the case of Post-Panamax container ships, since various loading conditions are available for Post-Panamax container ships, as detailed in 4.4 and **Appendix 7**.

Table 4-1 Load conditions for calculation of stresses in the stiffened bottom panel

Condition	Applied load
Case I	Lateral loads such as hydrostatic pressure corresponding to the full draught, wave-induced pressure specified in ClassNK Guidelines ^(note) , hull self-weight, container loads
Case II	Case I + Allowable still water vertical bending moment (Allowable Ms) + Wave-induced vertical bending moment specified in IACS UR S11

Note: Guidelines for Container Carrier Strength (Guidelines for Direct Strength Analysis) in 2012

In the case of the Ship as shown in **Fig. 4-5**, the stress in transverse direction of the stiffened bottom panel exceeds 100 N/mm² in Case I under One-bay empty condition without ballast in double bottom. When the vertical bending moments are applied, the stress in transverse direction of the panel further increases due to the Poisson's effect of the bottom shell plates and reaches around 120 N/mm² in Case II, and a combination of the stresses of the panel, i.e. the stress in longitudinal direction (σ_x) and the stress in transverse direction (σ_y), is located outside the curve of the buckling collapse strength of the panel, i.e. the zone where the buckling collapse occur.

Appendix 10 shows the relationships between the buckling collapse strength of the stiffened bottom panels and the stresses generated in the panels under typical load conditions for the target ships. In the case of the target ships other than the Ship, the stresses of the panels in Case II are located inside the curves of the buckling collapse strength of the panels, which is different from the Ship. **Fig. 4-6** shows an example of the relationship between the buckling collapse strength and the stresses generated in the panel related to one of the target ships (Ship E) other than the Ship.

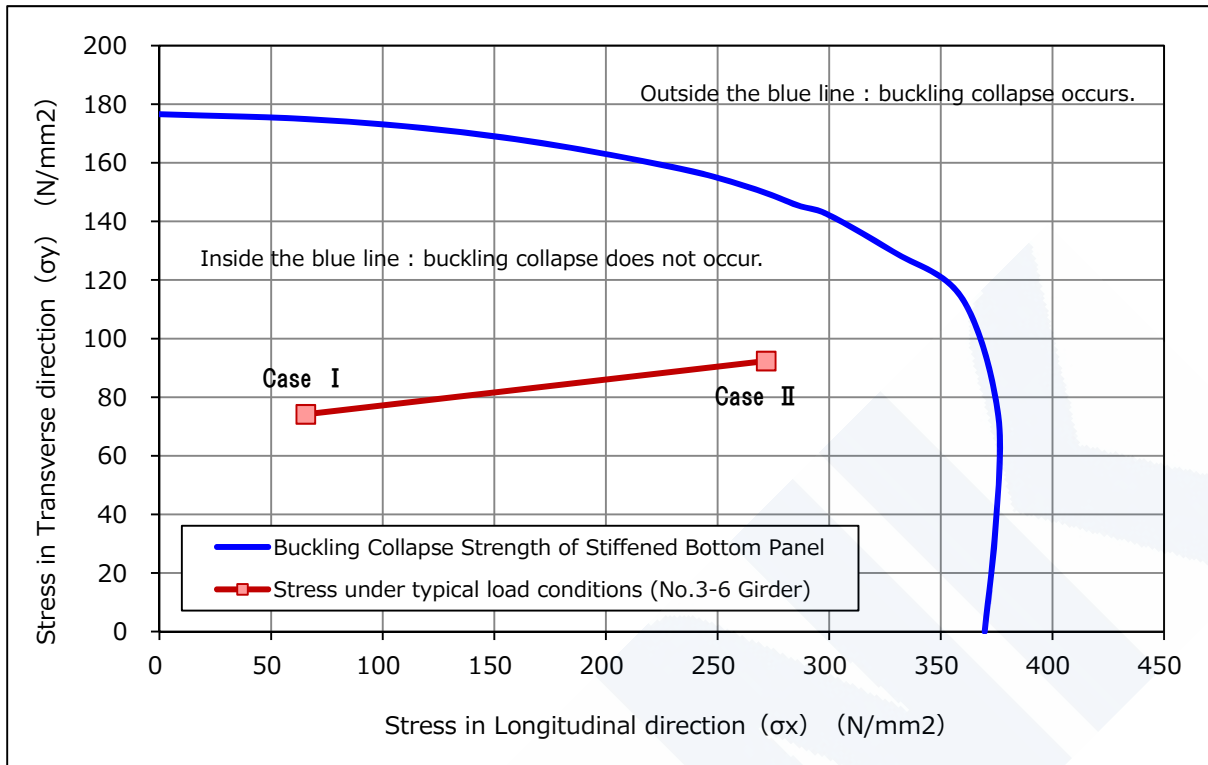


Fig. 4-6 Buckling collapse strength of stiffened bottom panel and stress in the panel under typical load conditions as shown in **Table 4-1** (Ship E / No.3 Girder - No.6 Girder / in way of butt joint in midship part)

Note : Initial shape deformation of buckling collapse strength is deformation simulating "hungry horse" mode and yield stress is general average values. (Refer to **Appendix 10** for details.)

Furthermore it is observed that the double bottom local stress in transverse direction in the bottom shell plates in the Ship is relatively higher than that of the other target ships as shown in **Appendix 11**.

It can be concluded that the possibility of the buckling collapse of the stiffened bottom panels of the Ship is relatively higher than that of the other target ships because the stress in transverse direction of the panel is relatively higher in the Ship and the stress of the panel is at the level of around 100 N/mm² or above in transverse direction (σ_y), resulting in rapid reduction of the buckling collapse strength of the panel in longitudinal direction.

4.3.2 Mechanism of the process from buckling collapse of bottom shell plates to hull girder fracture

From the results of the 3-hold model elasto-plastic analyses on the target ships it is observed in general that local buckling collapse first occurred in bottom shell plates that had plastic deformations in transverse direction just before the loading stage of the maximum load of the hull girder ultimate strength, and subsequently the girders adjacent to the collapsed bottom shell plates yielded partly, and finally the applied load reached the maximum load.

The above results lead to the conclusion of the mechanism from the buckling collapse of bottom shell plates to the hull girder fracture as follows.

- The upward loads of bottom sea pressure are dominant among the lateral loads acting on the double bottom structure of container ships. The lateral loads are mainly supported by I beams with flanges of bottom shell plates and inner bottom plates and with webs of girders and floors.
- Once bottom shell plates are locally buckled and collapsed with plastic deformations, the effective breadth of the flange of bottom shell plates attached to the girder is reduced. The reduction of the effective breadth of bottom shell plate flange increases the compressive bending stress of the girder caused by the lateral loads. As the result of the superimposing with vertical bending stress of compression, the lower half of the girder partly yields.
- Bending strength of double bottom structure against the lateral loads is reduced due to the local buckling collapse of bottom shell plates and due to the partial yielding of adjacent girders, which causes the subsequent propagation of the buckling collapse of bottom shell plates and the yielding of the girders leading to the hull girder fracture finally.

The buckling collapse of the bottom shell plates which might trigger the above phenomenon generally occurs in the middle part of the hold around one floor space before or after the partial bulkhead in the longitudinal direction of the ship and near the center line of the ship, mainly in the stiffened bottom panel adjacent to the keel plate in the transverse direction of the ship. In both the case, compressive local stress of the bottom shell plates is relatively high.

The extent of the buckling collapse of bottom shell plates until the adjacent girders partly yield depends on the followings:

- the size of the lateral loads acting on the double bottom structure;
- the condition of double bottom local stress distribution; and
- the relationship between the buckling collapse strength of bottom shell plates and the bending strength of the girders.

Fig. 4-7 and **Fig. 4-8** show a typical example of the result of the 3-hold model elasto-plastic analysis on one of the target ships other than the Ship showing the plastic strain condition of the bottom shell plates and the girders just before the hull girder ultimate strength condition.

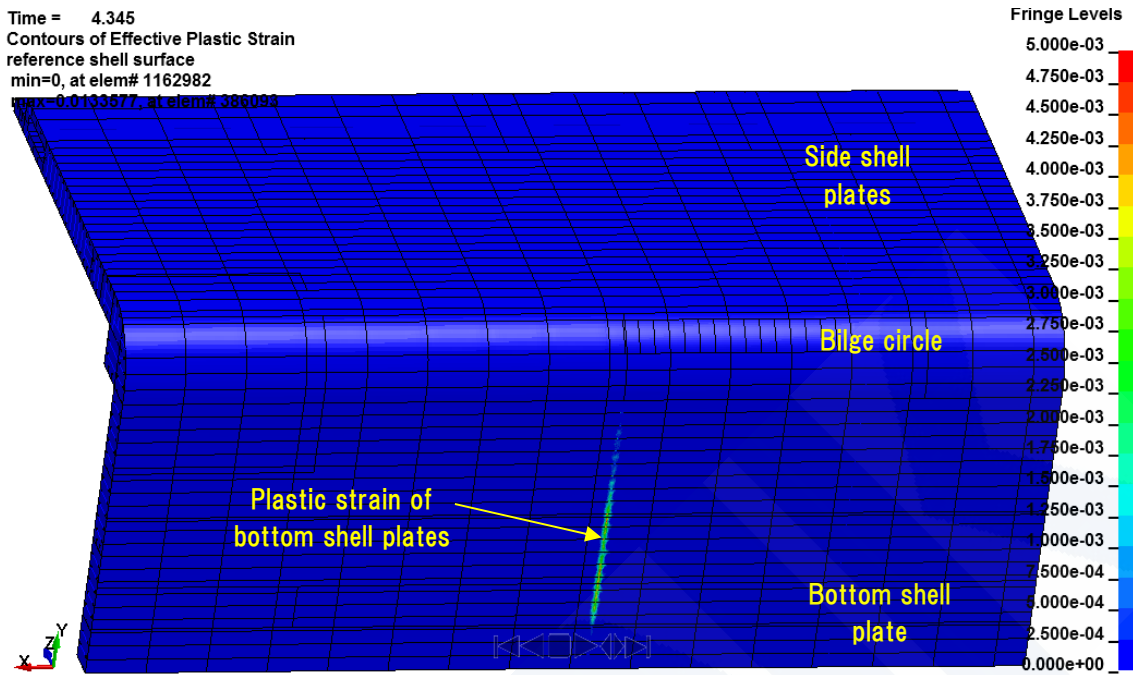


Fig. 4-7 Example of result of 3-hold model elasto-plastic analysis
 (Case of one of the target ships other than the Ship)
 (Equivalent plastic strain condition of the bottom shell plate
 just before the hull girder ultimate strength condition)

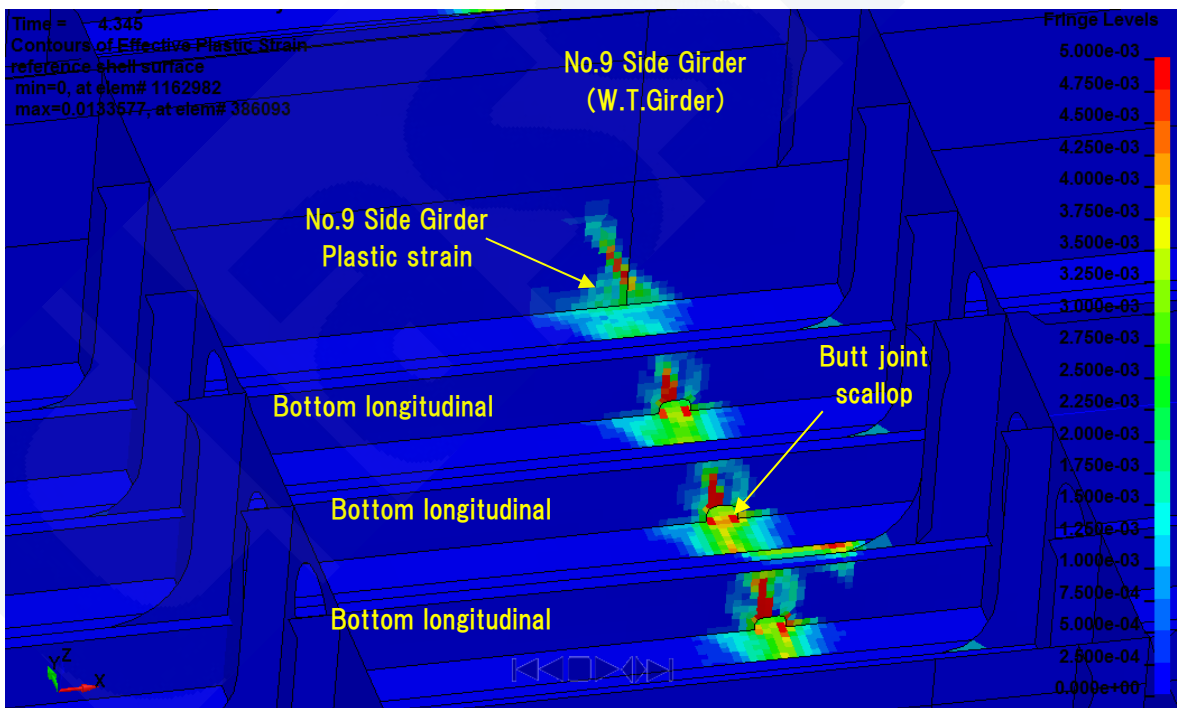


Fig. 4-8 Example of result of 3-hold model elasto-plastic analysis
 (Case of one of the target ships other than the Ship)
 (Equivalent plastic strain condition of No.9 Girder
 just before the hull girder ultimate strength condition)

As stated in 4.3.1 the double bottom local stress in transverse direction of the stiffened bottom panel adjacent to the keel plate panel is relatively higher in the case of the Ship and the stress of the panel is at the level of around 100 N/mm^2 or above in transverse direction (σ_y), at which the buckling collapse strength of the panel under bi-axial compressive condition considerably reduces in longitudinal direction. Therefore the possibility of the occurrence of the buckling collapse of the stiffened bottom panels is relatively higher than in other target ships, which might have accelerated the subsequent buckling collapse of the panels.

It is concluded in this Report that the difference between the Ship and other target ships in the margin of hull girder ultimate strength described in 4.2.3 arises from the result as explained the above.

4.3.3 Assessment of the structural safety of large container ships

The investigation results described in 4.2 and 4.3 of this Report can be summarized as follows.

- There is no difference between the Ship and other target ships of the investigation on the margin against the requirements of IACS UR S11 and on the margin of the hull girder ultimate strength calculated by IACS CSR method.

On the other hand differences are found between the Ship and the other target ships on the margin of the hull girder ultimate strength calculated by 3-hold model elasto-plastic analysis as shown in **Fig.4-3** and **Fig.4-4**.

The above two contrary results can be attributed to whether the effects of the lateral loads are taken into consideration or not. While the requirement of IACS UR S11 and the calculation method of the hull girder ultimate strength of IACS CSR do not consider the effect of the lateral loads, the calculation of the hull girder ultimate strength calculated by 3-hold model elasto-plastic analysis considers the effect of the lateral loads.

- The reasons for the difference between the Ship and the other target ships in the margin of the hull girder ultimate strength calculated by 3-hold model elasto-plastic analysis which takes into account the effect of the lateral loads can be as follows:

- (1) The difference of the possibility on the buckling collapse occurrence of stiffened bottom panels

The occurrence of the buckling collapse of stiffened bottom panels depends on the relationship between the buckling collapse strength of the panels and the stress generated in the panels.

The buckling collapse strength is given by scantling of the stiffened bottom panels such as thickness of bottom shell plates, size of bottom longitudinals, and spacing of bottom longitudinals. Meanwhile, the stress generated in the panel is determined by the lateral loads acting on the double bottom structure (difference between the

bottom sea pressure and the container loads) as well as by the scantling of the panels.

As stated in 4.3.1 not only the buckling collapse strength of the panel but also the stress generated in the panel of the Ship are different from the other target ships

- (2) The difference of the bending stress condition of the double bottom structure caused by lateral loads

The stress condition in bottom shell plates as the double bottom local stress is different between the Ship and the other target ships.

The double bottom local stress depends on various factors such as construction details of opening arrangement of girders and floors, arrangement of butt joints and arrangement of plate joints, etc., in addition to the scantling and the arrangement of the structural members of double bottom structure. Furthermore it also depends on the conditions of the lateral loads acting on the double bottom structure.

The difference in the stress condition of bottom shell plates is due to the complex relationship of these factors.

Taking into account of these results mentioned above, it is concluded that the structural safety of large container ships can be comprehensively assessed at this moment through the following investigations in order to prevent similar fracture accidents.

- (1) The hull girder ultimate strength is estimated by 3-hold model elasto-plastic analysis considering the effect of the lateral loads and assessed on the followings.
 - Margin of the hull girder ultimate strength calculated by 3-hold model elasto-plastic analysis against the wave-induced vertical bending moment specified in IACS UR S11 (Refer to **Fig. 4-3.**)
 - Decrease of the hull girder ultimate strength calculated by 3-hold model elasto-plastic analysis compared to the ultimate strength calculated by IACS CSR method (Refer to **Fig. 4-4.**)
 - Stress and strain conditions of structural members of double bottom structure in the process of 3-hold model elasto-plastic analysis. (Refer to **Fig. 4-7** and **Fig. 4-8.**)
- (2) The buckling collapse strength of stiffened bottom panels in the middle part of the holds is assessed. The stress generated in the panel used for the assessment is to be possible maximum values in actual cases. (Refer to **Fig. 4-5** and **Fig. 4-6.**)

The above assessments were made to the target ships through the investigation of this Report. As the results of the assessments, significant differences were confirmed between the Ship and the other target ships. In addition, as the results of the inspections carried out for the target ships other than the Ship after the accident, local deformations as observed in the sister ships of the Ship were not found in the bottom shell plates.

Therefore it can be concluded that the other target ships have the sufficient structural safety against the occurrence of similar fracture accidents.

4.4 Characteristics of Container Ships, and Changes in Structure and Operation due to Increased Ship Size

Container ships carry container cargoes which are light in weight compared to their volumetric capacity, and thus the still water vertical bending moment is always in hogging condition. Due to this characteristic, the ship's double bottom structure under wave-induced vertical bending moment is always subjected to compressive load. As for cargo holds, the upward load due to bottom sea pressure is dominant on the double bottom structure since container cargoes are relatively light.

Unlike tankers and bulk carriers, container ships are always operated with containers loaded onboard. Further, the number, weight and layout of containers differ in each voyage even in the same navigation route. For these reasons, operators need to make the cargo loading plan for each voyage while checking compliance with the requirements of stability and longitudinal strength.

Based on such characteristics of load and voyage, container ship design is generally carried out considering "One-bay empty condition" with the assumption that one of the bays is not loaded with containers, in addition to the standard loaded condition with homogenous container loading in each cargo hold. In this One-bay empty condition, the double bottom structure under the empty bay of a cargo hold is subjected to severe load condition from the structural viewpoint of the transverse strength, because of no container weights balanced with the upward load due to bottom sea pressure.

As stated in **Appendix 12**, Post-Panamax container ships have improved their stability in comparison with Panamax container ships and have gained more cargo loading flexibility in complying with the stability requirements, because the breadth of Post-Panamax container ships is relatively increased than the depth. As a result, the need to ballast in the double bottom tanks to improve stability is reduced. On the other hand, the upward lateral load due to bottom sea pressure acting on double bottom structure has increased because of the increased breadth of the hull. The container weight cannot be balanced sufficiently with this increased upward lateral load even in the case of normal loading conditions where containers are homogeneously loaded in every bay. Consequently the occasion increases where the load acting on double bottom structure becomes almost equal to the load in One-bay empty condition without ballast in double bottom, which is the severe condition for the transverse strength. This trend is especially obvious in Post-Panamax container ships of 8,000 TEU class or larger.

As a result, the minimization of ballast increases the frequency with which the still water vertical bending moment reaches close to the allowable value. Meanwhile, it sometimes

happens that the transverse stress of double bottom structure becomes almost equal to the transverse stress in One-bay empty condition without ballast in double bottom, even in the normal loading conditions, where the ship is in around the full draught.

It can be concluded that the possibility to use the strength margin is relatively increased for Post-Panamax container ships due to the flexibility in the stability restriction in contrast to Panamax container ships where it has been difficult to use the strength margin due to the stability restriction. Accordingly in the case of Post-Panamax container ships, it is important that design conditions can deal with various loading conditions in service adequately, and such design conditions are to be understandable to both operators and ships.

4.5 ClassNK Rules for Container Ships

Irrespective of the ship type, whether container ships or bulk carriers, it is difficult to assess the entire hull structure all at once because the hull structure is large and complicated, and also the hull is subjected to various types of loads such as wave and cargo loads. For the safety assessment of container ships, therefore, the strength of the hull structure has been evaluated based on the ClassNK rule requirements as shown in **Table 4-2**, with respect to the following three categories: longitudinal strength, transverse strength and local strength.

Table 4-2 Container ship rule requirements for each strength category in ClassNK rules

Strength category	Rule requirements
Longitudinal strength	Chapter 15, Part C of the Rules for the Survey and Construction of Steel Ships
Transverse strength	C1.1.22, Part C of the Guidance for the Survey and Construction of Steel Ships
Local strength	Chapter 13, 14 and 23, Part C of the Rules for the Survey and Construction of Steel Ships

For longitudinal strength, the strength of the hull structure, which is regarded as a beam, over the entire ship length is evaluated based on stresses due to the vertical bending moment and shear force caused by internal and external load differences.

For transverse strength, the primary supporting members such as girders and floors which support plates and stiffeners are assessed by the direct strength calculation taking into account local loads caused by cargoes, ballast water, sea water and so on. For the yield strength assessment in the direct strength calculation, the allowable stress of longitudinal structural members is reduced in order to take into account the effect of the vertical bending stress in the assessment. For the buckling strength assessment, it is performed by applying the elastic buckling check along with a certain safety factor instead of the ultimate strength check in order to consider the effect of the vertical bending moment. It has been understood that the elastic buckling check gives more strength margin to evaluated structural members

than the ultimate strength check because the former prohibits elastic buckling whereas the latter permits the evaluated structural member to be subjected to additional compressive loads after the elastic buckling.

For local strength, the strength against local loads is evaluated for the stiffeners supported by primary supporting members and the plates surrounded by the stiffeners. The evaluation also takes into account the effect of vertical bending moment through a reduction in allowable stress from the specified minimum yield stress.

For container ships, torsional strength is evaluated in addition to the aforementioned strength assessments because container ships have large openings in the deck. The evaluation involves yielding strength assessment which considers superposed warping stress caused by torsional moment and bending stress caused by vertical and horizontal bending moments.

On the other hand, regarding the effect of lateral loads on hull girder ultimate strength of container ships, which was recognized through this investigation as previously explained in 4.2 and 4.3 of this Report, the effect of lateral loads has been hitherto implicitly taken into consideration, along with other uncertainty factors, by the strength margin against loads in ClassNK rules.

4.6 Analysis of On-board Full Scale Measurement Results of Large Container Ships

The analysis was conducted on the results of on-board full scale measurements of large container ships carried out in the past with the cooperation of the owners and the shipyards focusing on the whipping response ratio which indicated how wave-induced vertical bending moment was increased by the effect of whipping responses. The outlines of the analysis are shown in **Appendix 13**.

Conclusive outcomes could not be drawn because of the limitation of the amount of the data and the periods of the measurements, and further on-board full scale measurements of large container ships are being carried out and in planning in order to get more measurement data.

Chapter 5 Summary of the Investigation

The findings of the investigations are summarized in this Chapter. The related chapter and section number of this Report are provided for reference at the end of each finding.

- ✓ The investigation was carried out relating to the possibility of the occurrence of the fracture in consideration of deviations of uncertainty factors, including the yield stress, the sea states at the time of the accident and the differences between declared weights and actual weights of the containers. The investigation concluded that it was actually possible that the

load of the vertical bending moment exceeded the hull girder ultimate strength at the time of the accident when the effects of the deviations of the uncertainty factors were taken into account although the overlap between the strength and the load was very narrow. (3.4)

- ✓ As evaluation of structural safety, 3-hold model elasto-plastic analyses were carried out on the target ships with consideration of lateral loads such as bottom sea pressure and container loads, and investigation was conducted on the hull girder ultimate strength obtained by the analyses. Significant differences were observed between the Ship and the other target ships on the margin of the hull girder ultimate strength calculated by 3-hold model elasto-plastic analysis against the wave-induced vertical bending moment specified in IACS UR S11. (4.2)

Meanwhile, no substantial difference was observed among the all ships in investigation including the Ship on the margin against the requirements of IACS UR S11 relating to the vertical bending strength and on the margin of the hull girder ultimate strength calculated by IACS CSR method (Smith's method), which do not consider the effect of the lateral loads. (4.2)

It is considered that the difference between the Ship and the other target ships observed in this investigation is mainly derived from the difference in possibility of buckling collapse of stiffened bottom panel adjacent to the keel plate panel under bi-axial compression with consideration of the superimposition of local stress in double bottom structure due to lateral loads and compressive stress by vertical bending. (4.3)

- ✓ To prevent similar fracture accidents, it is necessary to assess the hull girder ultimate strength in proper consideration of the effects of the lateral loads and to assess the buckling collapse strength of stiffened bottom panels in the middle part of the holds. (4.3)
- ✓ It was confirmed that the target ships other than the Ship investigated in this Report have the sufficient structural safety against the occurrence of similar fracture accidents. (4.3)
- ✓ Post-Panamax container ships have improved their stability in comparison with Panamax container ships and have gained more cargo loading flexibility in complying with the stability requirements. As a result, the need to ballast in the double bottom tanks to improve stability is reduced. On the other hand, from the strength view point, the occasion increases where the load acting on double bottom structure becomes almost equal to the load in One-bay empty condition without ballast in double bottom even in the case of normal loading conditions, which means the load acting on double bottom structure has become severe conditions in the transverse strength. This trend is especially obvious in Post-Panamax container ships of 8,000 TEU class or larger. (4.4)

As a result, the minimization of ballast increases the frequency with which the still water vertical bending moment reaches close to the allowable value. Meanwhile, it sometimes

happens that the transverse stress of double bottom structure becomes almost equal to the transverse stress in One-bay empty condition without ballast in double bottom even in the normal loading conditions where the ship is in around the full draught. (4.4)

- ✓ In order to manage the changes in structure and operation following the trend towards larger container ships, in the case of Post-Panamax container ships, it is important that design conditions can deal with various loading conditions in service adequately, and such design conditions are to be understandable to both operators and ships. (4.4)

Chapter 6 Future Action Plan

In light of the outcomes from the investigation mentioned above, actions to be taken by ClassNK are listed up as follows.

- ✓ To confirm the structural safety of the Post-Panamax container ships of 8,000 TEU class except the target ships investigated in this Report by assessing their strength margin through the followings:
 - Evaluation of the hull girder ultimate strength calculated by 3-hold model elasto-plastic analysis with consideration of the effect of the lateral loads.
 - Evaluation of the buckling collapse strength of stiffened bottom panels in the middle part of the holds.
- ✓ To review the relevant ClassNK rules such as the Rules, the Guidance and the Guidelines, in view of the outcomes from the investigations by NK Panel. The main points to be considered are as follows:
 - To develop practical methods to evaluate the hull girder ultimate strength with consideration of the effect of the lateral loads;
 - To review the procedures concerning the direct strength calculation on the transverse strength;
 - To investigate ways of evaluating the wave-induced load including the effects of whipping response;
 - To consider procedures and measures so that the design conditions can deal with various loading conditions in service adequately and so that such design conditions are understandable to operators and ships in order to manage the change in structure and operation for Post-Panamax container ships; and
 - To consider the utilization of hull monitoring systems to provide useful information for ships referring to the data obtained from the on-board full scale measurement.
- ✓ To submit this Report of NK Panel to JG Committee set up on the initiative of the Japanese Ministry of Land, Infrastructure, Transport and Tourism.

- ✓ To provide information from this Report of NK Panel to other classification societies as appropriate.
- ✓ To make necessary proposals and suggestions to IACS on the related IACS Unified Requirements.
- ✓ To utilize the collected data in on-board full scale measurements which are in planning and being carried out.

The Investigative Panel
on Large Container Ship Safety
September 2014

Appendix 1 The Investigative Panel on Large Container Ship Safety Member List (related to Chapter 2 of this Report)

Chairperson

Dr. Eng. Yoichi SUMI Professor Emeritus, Yokohama National University

Members (Alphabetical order)

Dr. Eng. Masahiko FUJIKUBO Professor, Osaka University
Mr. Hitoshi FUJITA Managing Director, General Manager
Ship Designing Group
Imabari Shipbuilding Co., Ltd.
Mr. Junichi IWANO General Manager, Technical Group
NYK Line
Mr. Yoshikazu KAWAGOE Executive Officer, General Manager
Technical Division
Mitsui O.S.K. Lines, Ltd.
Mr. Kazuya KOBAYASHI Associate Officer, General Manager
Engineering Division, Ship & Offshore Structure Company
Kawasaki Heavy Industries, Ltd.
Mr. Toyohisa NAKANO General Manager, Technical Group
Kawasaki Kisen Kaisha, Ltd.
Mr. Tomoaki TAKAHIRA General Manager
Planning & Development Department
Ship & Offshore Division
Japan Marine United Corporation
Mr. Naoki UEDA General Manager
Shipbuilding & Ocean Development Division
Commercial Aviation & Transportation Systems
Mitsubishi Heavy Industries, Ltd.

Observers (Alphabetical order)

Mr. Kazuhiro TABUCHI Director of Ship Safety Standards Office
Safety Policy Division
Maritime Bureau
Ministry of Land, Infrastructure, Transport and Tourism
Dr. Eng. Kenkichi TAMURA Senior Director for Research
National Maritime Research Institute

Secretariat

NIPPON KAIJI KYOKAI (ClassNK)

Appendix 2 Estimation of Hull Girder Ultimate Strength of the Ship in 3-Hold Model Elasto-Plastic Analysis (related to 3.3.1 of this Report)

In the investigation of the possibility of the occurrence of the accident described in 3.3.1 of this Report, 3-hold model elasto-plastic analyses were conducted taking into account the deviation of the yield stress of steel and the hull girder ultimate strength of the Ship was estimated. The outline of the elasto-plastic analyses using 3-hold models is explained in the followings.

1. Estimation of Hull Girder Ultimate Strength of the Ship

1.1 Analysis Conditions

Table A2-1 shows the analysis conditions of 3-hold model elasto-plastic analysis for the estimation of the hull girder ultimate strength. The purpose of 3-hold model elasto-plastic analysis is to investigate the possibility of the occurrence of the accident as stated in Chapter 3 of this Report. Accordingly the analysis conditions were given as same as those described in Chapter 5 of JG Interim Report.

Table A2-1 Analysis conditions of 3-hold model elasto-plastic analysis for estimation of hull girder ultimate strength of the Ship

Analysis program	LS-DYNA (explicit method)
Extent of model	Longitudinal direction : 1/2 + 1 + 1/2 holds Transvers direction : half breadth
Condition of initial shape deformation	Following initial shape deformations were given to bottom shell plates, inner bottom plates, longitudinal bulkhead, side shell plates and longitudinals attached to them. Deformations were given only below the neutral axis of the transvers section. <ul style="list-style-type: none"> • Plates : Buckling mode with 4 half-waves • Longitudinals : Euler buckling mode and lateral buckling mode given respectively
Thickness	Gross thickness
Boundary condition	<ul style="list-style-type: none"> • Cantilever condition, i.e. aft end was fixed and the other end was free. • Symmetrical condition at center line of the Ship in transverse direction

Load condition	Container load and ballasting condition	Loading condition at the time of accident Container loads were applied as stack loads in each bay. (Fuel oil weight was ignored because of small effect on the result.)
	Hull weight	Hull weight corresponding to double bottom structure was taken into account.
	Sea pressure	<ul style="list-style-type: none"> Hydrostatic pressure corresponding to the full draught Wave-induced pressure specified in ClassNK Guidelines ^(Note)
	Vertical bending moment	Gradually increased until the hull girder was fractured the model, i.e. hull girder ultimate strength.

Note : Guidelines for Container Carrier Strength (Guidelines for Direct Strength Analysis) in 2012

1.2 Analysis Model

The FE model used for the 3-hold elasto-plastic analysis is shown in **Fig. A2-1**. It is the same as the FE model used in Chapter 5 of JG Interim Report.

The target for the analysis was the area between the three floor spaces including the butt joint of FR151+200 mm, where it was concluded that the fracture of the Ship had originated. The plates and frames including bottom longitudinals in the target area were modeled with shell elements of around 100 mm x 100 mm in size, i.e. fine mesh elements, in the overall breadth in transverse direction, and between the base line and the neutral axis of the transverse section in vertical direction. Scallop openings in the bottom longitudinal webs for butt joint penetration were also modeled. The remaining part was modeled with shell elements of around 200 mm x 200 mm in size.

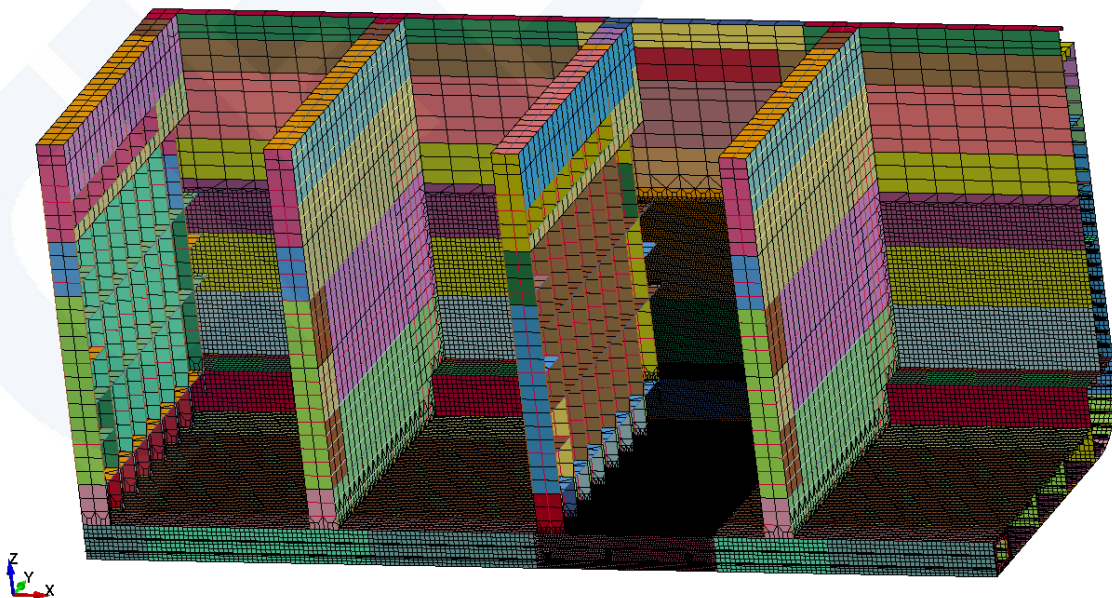


Fig. A2-1(a) Overall view of 3-hold model for the elasto-plastic analysis

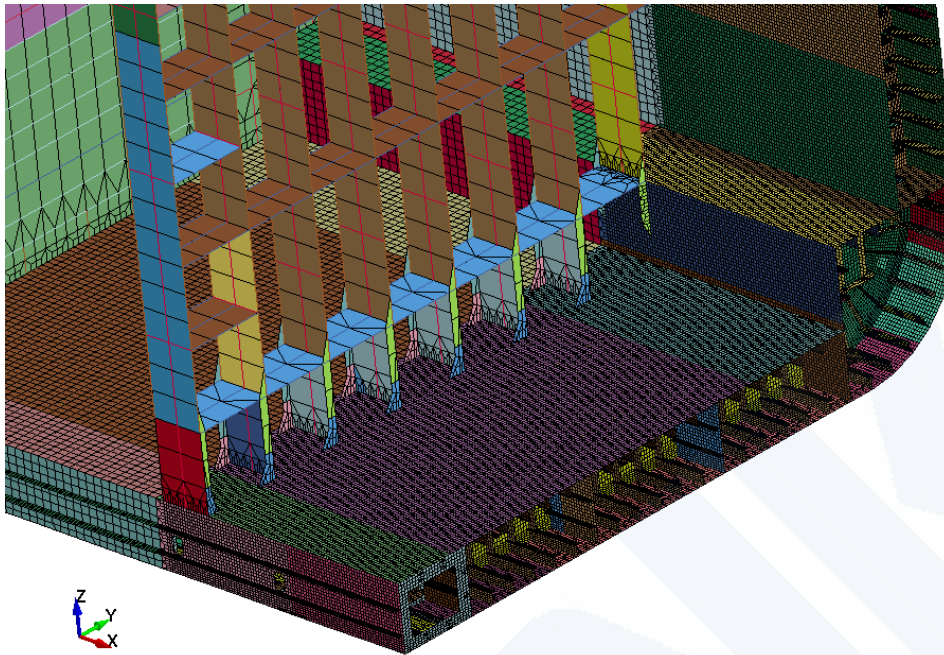


Fig. A2-1 (b) Target area for analysis with fine mesh elements in FE model

1.3 Material Property of Steel

Material properties of steel for the analysis are shown in **Table A2-2**. As described in 3.3.1 of this Report, 3-hold model elasto-plastic analyses were conducted with different values of the yield stress considering the deviation of the yield stress. The value of the yield stress for each analysis case is shown in **Table A2-3**. Elastic-perfect plasticity taking into account linear hardening was given as the condition of the relationship between stress and strain. **Fig. A2-2** shows an example of the relationship between stress and strain as a true stress and true strain curve which depends on the yield stress.

Table A2-2 Material properties of steel

Young's modulus	206,000 N/mm ²
Poisson's ratio	0.3
Mass density	7.85 ton/m ³
Yield stress	See Table A2-3
True stress and true strain curve	See Fig. A2-2

Table A2-3 Yield stress for each case of 3-hold elasto-plastic analysis

Steel strength	Yield stress of steel (N/mm ²)		
	Case where average value was calculated based on the mill sheet values of bottom shell plates of the Ship ^(See Note)	Case 1 in 3.3.1 of this Report where minimum value was estimated based on the deviation of the mill sheet values of the Ship ^(See Note)	Case 2 in 3.3.1 of this Report where minimum value was defined as specified minimum yield stress
MS	274	259	235
YP32	359	342	315
YP36	392	378	355
YP40	417	407	390
YP47	494	481	460

Note : Yield stress of the bottom shell plates was estimated by the methods described in 3.3.1 of this Report. The yield stresses of the other structural members for the analysis were estimated with the assumption that they kept the same relationship of proportion as that of the bottom shell plates between the specified minimum yield stress, the general average value and the yield stress used in the analysis. (See **Appendix 8** regarding the general average value.)

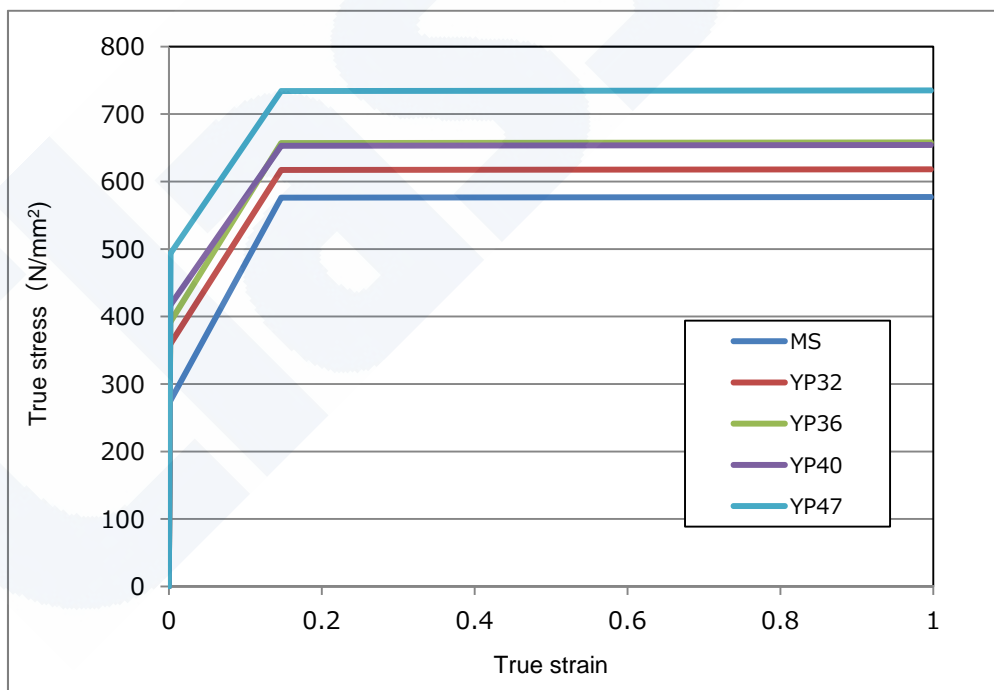


Fig. A2-2 Relationship between stress and strain (True stress and true strain curve)
An example of the case of the average yield stress based on the mill sheet values of the Ship

1.4 Condition of Initial Shape Deformation

Initial shape deformation used in this Annex considers imperfections caused in plates and longitudinals of hull structures during construction. **Appendix 3** explains the effect on the hull girder ultimate strength by local deformations generated during navigations in service, such as found in the sister ships of the Ship.

In JG Interim Report, the following two cases were taken into account as the conditions of initial shape deformation for 3-hold elasto-plastic analysis in bottom shell plates, inner bottom plates, longitudinal bulkhead, side shell plates and the longitudinals attached to them.

- Hungry horse mode simulating the imperfections during construction (deformation simulating sine curve shape with one wave length in plates and deformations simulating Euler buckling mode and lateral buckling mode in longitudinals)
- Buckling mode of bottom shell plates (deformation simulating buckling mode with four half waves in plate and deformations simulating Euler buckling mode and lateral buckling mode in longitudinals)

Initial shape deformations were given only below the neutral axis of the transverse section of the Ship in the both cases.

The result of the analysis in the latter case, i.e. the analysis with the initial shape deformation of the buckling mode of bottom shell plates was adopted as the hull girder ultimate strength of the Ship at the time of the accident in JG Interim Report.

In the investigation of this Report, this buckling mode of bottom shell plates was applied as the initial shape deformation for the analysis condition which was the same as JG Interim Report, i.e. the deformations simulating four half wave buckling mode with the amplitude of 4 mm were given to bottom shell plates, inner bottom plates, longitudinal bulkhead and side shell plates. As for initial shape deformations of the longitudinals attached to the plates, deformations simulating Euler buckling mode and lateral buckling mode were given respectively. The deformation volumes of the longitudinals for initial shape deformation were determined referring to the standard range of JSQS (Japanese Shipbuilding Quality Standard). The initial deformations were given only below the neutral axis of the transverse section of the Ship both in the plates and in the longitudinals as same as JG Interim Report.

As mentioned in the above, the condition of the initial shape deformation for estimating the hull girder ultimate strength in 3.3.1 of this Report was the same as the condition in which the hull girder ultimate strength at the time of accident was estimated in JG Interim Report.

On the other hand, various deformation modes exist in the actual imperfections generated during construction and these modes are considered to be complex ones in which many wave shape components are superimposed. The quantitative investigation about the effect of initial

shape deformation on hull girder ultimate strength taking into account this view point is considered to be an issue in the future.

1.5 Boundary Condition

As same as in Chapter 5 of JG Interim Report, the cantilever condition was applied as the boundary condition for the analysis, where the aft end of the model was fixed and the fore end was free, and symmetrical condition in transverse direction was given at the center line of the Ship. With regard to the center girder, the symmetry condition was applied only on the intersections with floors, bottom shell plates and inner bottom plates in order to make buckling behavior possible for the center girder.

The schematic of the boundary condition is shown in **Fig. A2-3** and **Fig. A2-4**, where the following symbols are used.

- u : displacement in longitudinal direction
- v : displacement in transverse direction
- w : displacement in vertical direction
- θ_x : rotation around the longitudinal axis (X axis)
- θ_y : rotation around the transverse axis (Y axis)

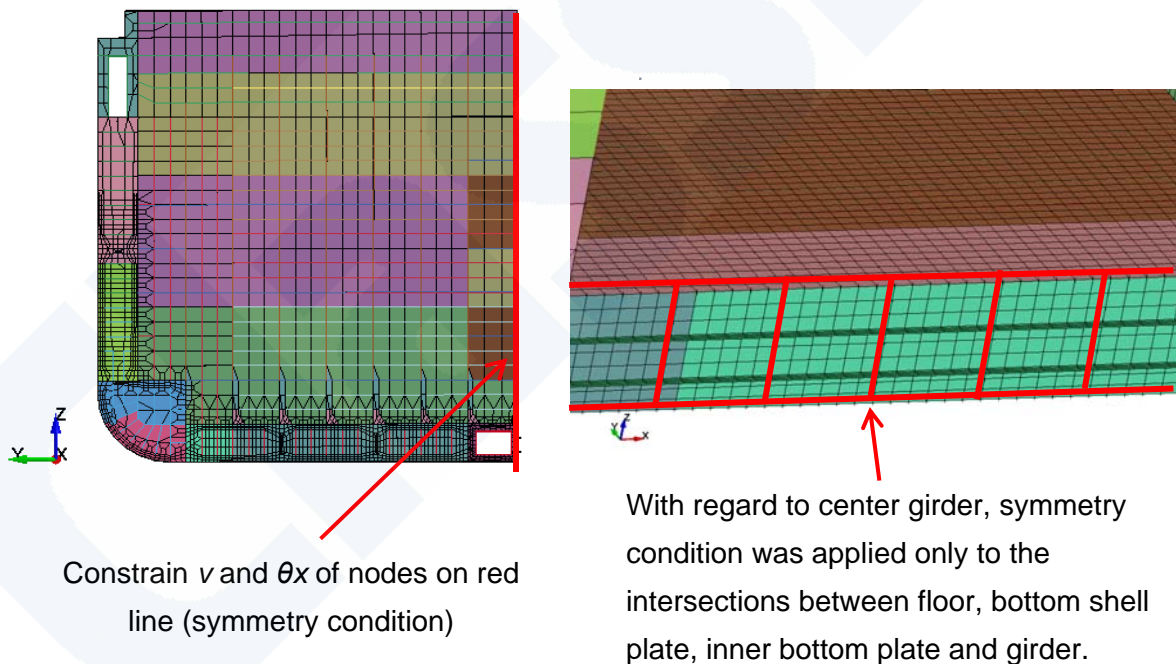
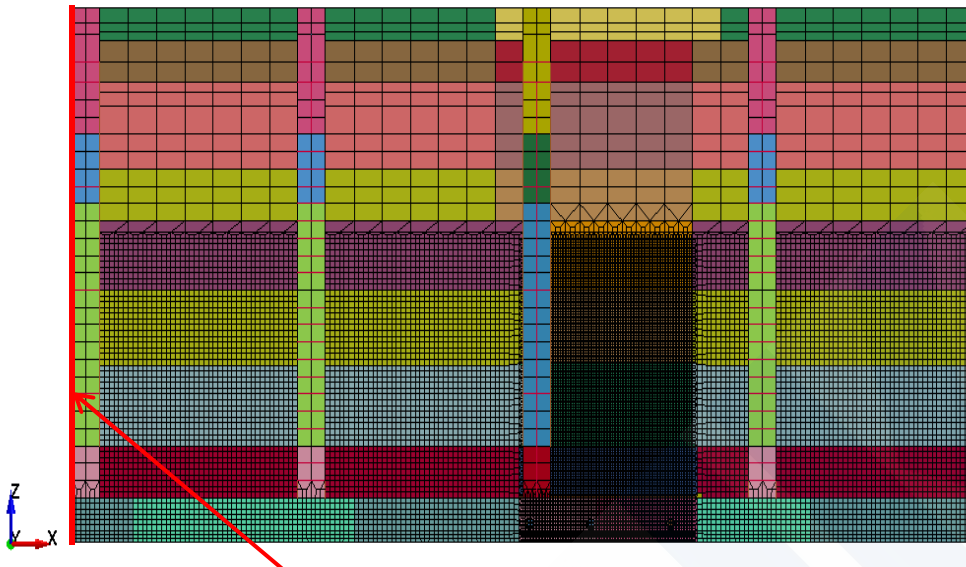
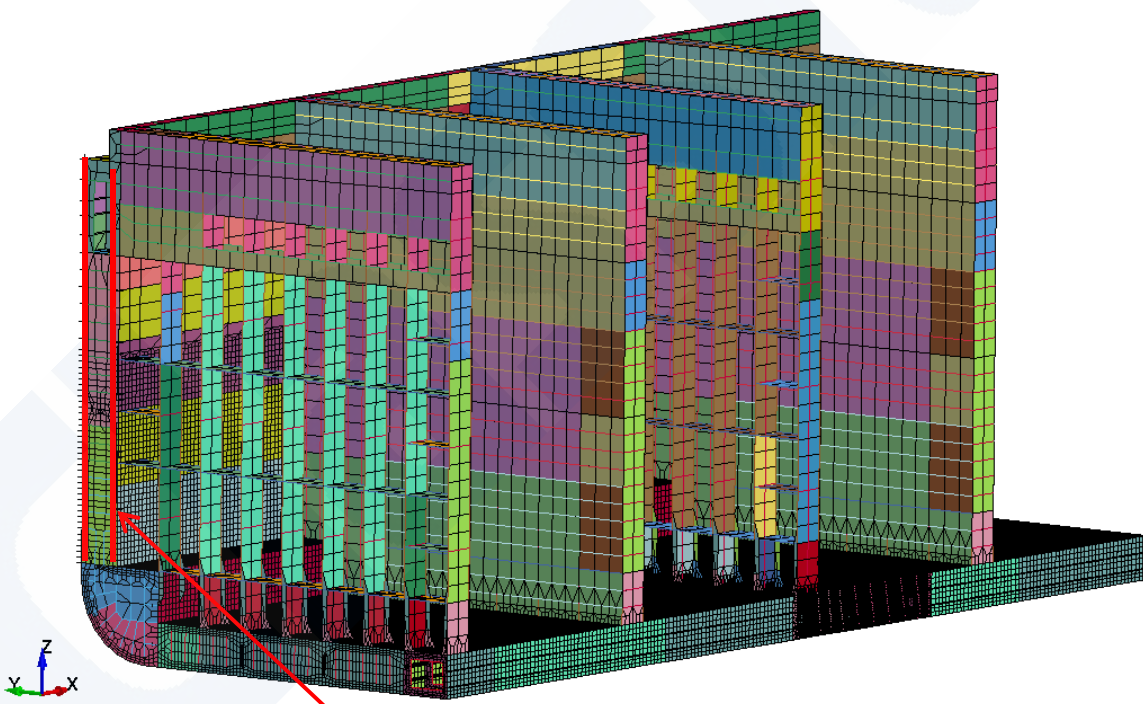


Fig. A2-3 Boundary condition at center line



Constrain u and θ_y of nodes on red line
(support condition in the longitudinal direction)

Fig. A2-4(a) Support condition in vertical and longitudinal directions



Constrain w of nodes on red line
(support conditions in the vertical direction)

Fig. A2-4(b) Support condition in vertical and longitudinal directions

1.6 Load Condition

The following loads were applied to the FE model in sequence.

- ① Hull weight corresponding to double bottom structure
- ② Hydrostatic pressure corresponding to the full draught
- ③ Container loads (based on the loading information at the time of accident) (stack loads corresponding to average container weight per unit)

Note : Ballast tanks in the midship area were empty.

- ④ Allowable still water vertical bending moment (Hogging)
- ⑤ Wave-induced pressure specified in Guidelines for Container Carrier Strength (Guidelines for Direct Strength Analysis) in 2012
- ⑥ Wave-induced vertical bending moment specified in IACS UR S11 (Hogging)
- ⑦ Additional vertical bending moment (Hogging)

First, ①, ② and ③ were applied being gradually increased in one second until reached the specified values. Next, ④, ⑤ and ⑥ were applied to the FE model in turn in one second respectively. Finally, ⑦ was applied being gradually increased until reached the hull girder ultimate strength. (See **Fig. A2-5** and **Fig. A2-6**.)

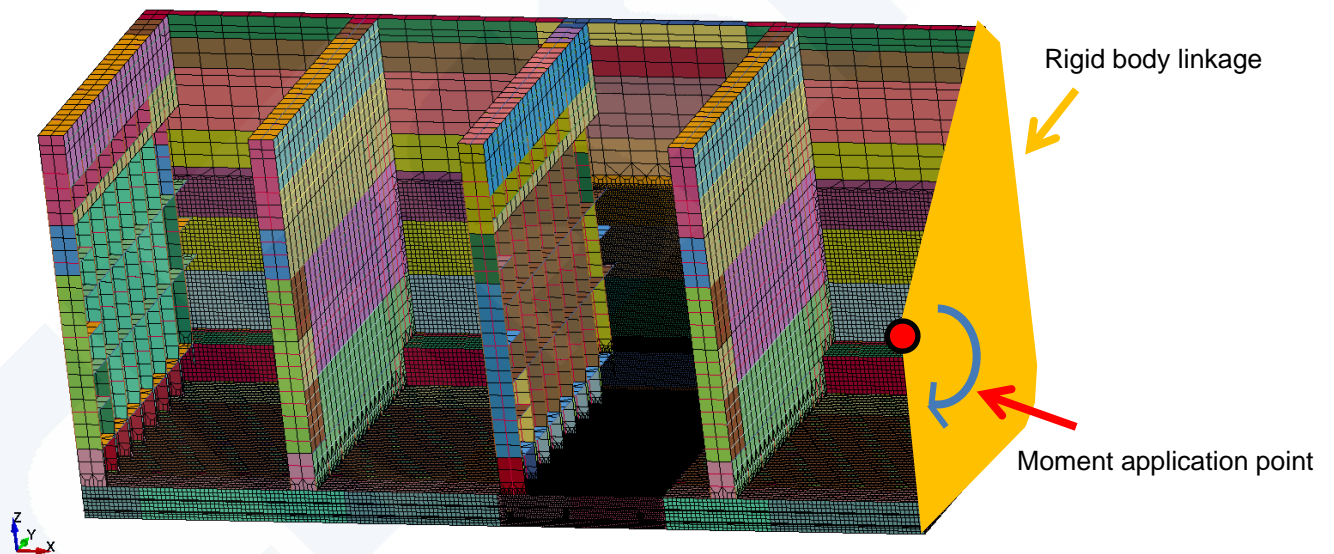


Fig. A2-5 Point where the moment was applied

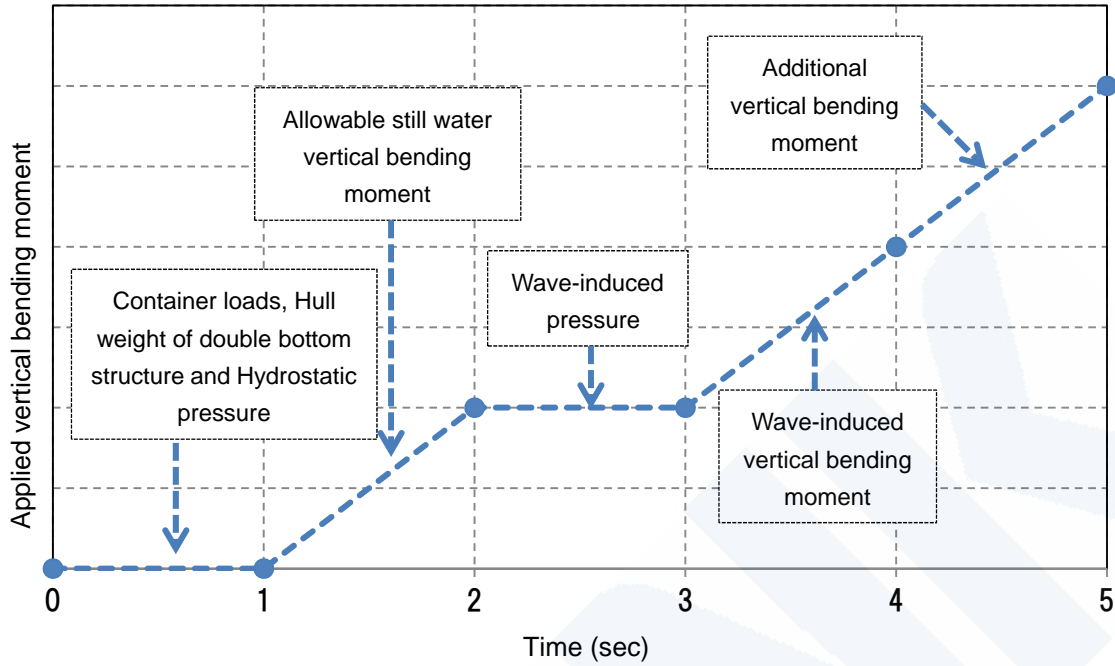


Fig. A2-6 Sequence of application of the loads

1.7 Analysis Result

Table A2-4 shows the values of the hull girder ultimate strength obtained by the 3-hold model elasto-plastic analysis in each case.

Table A2-4 Hull girder ultimate strength obtained by 3-hold model elasto-plastic analysis

Case where average yield stress was calculated based on the mill sheet values of the Ship	14.8×10^6 kN-m
Case 1 in 3.3.1 of this Report where minimum yield stress was estimated based on the deviation of mill sheet values of the Ship	14.2×10^6 kN-m
Case 2 in 3.3.1 of this Report where minimum yield stress was defined as specified minimum yield stress	13.2×10^6 kN-m

Fig. A2-7 shows an example of the history of vertical bending moment in the section where the hull girder was fractured. The peak value in the history curve was considered as to be the hull girder ultimate strength.

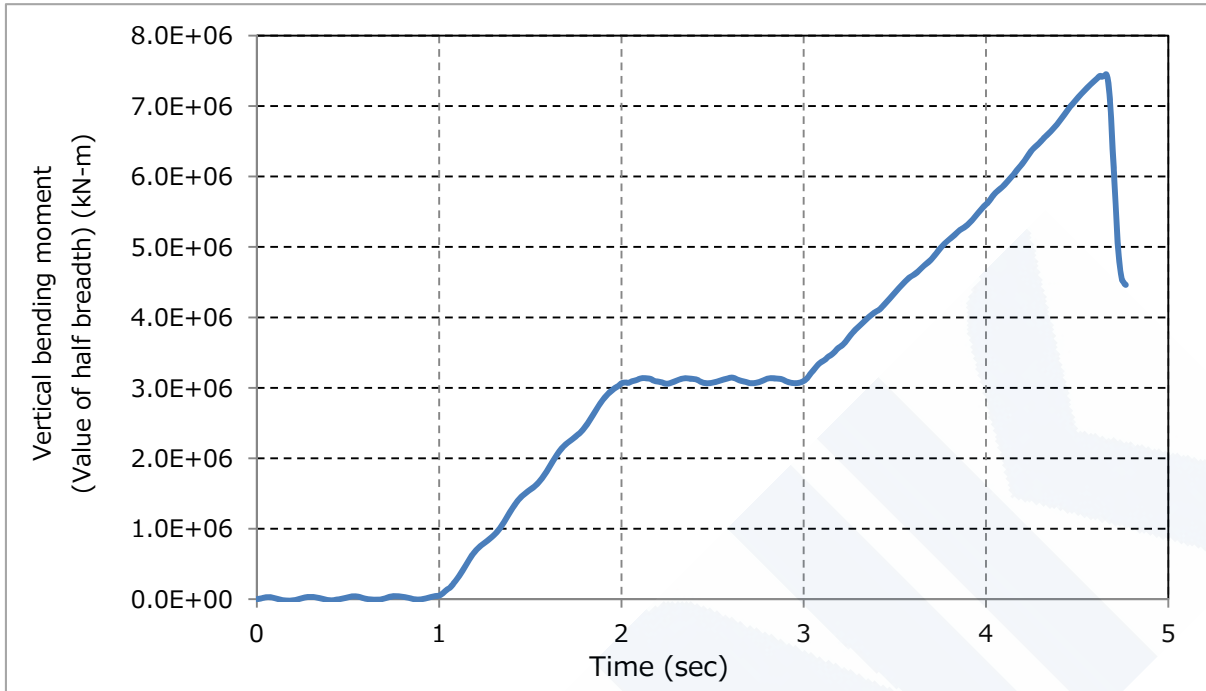


Fig. A2-7 History of vertical bending moment in the section where hull girder was fractured (in the case of the average yield stress based on the mill sheet values)

Figures from **A2-8** to **A2-11** show examples of the results of 3-hold model elasto-plastic analysis, which illustrates Mises' equivalent stress and equivalent plastic strain of the bottom shell plates at the time of the peak load equal to the hull girder ultimate strength (in **Fig. A2-8** and **Fig. A2-9**), and at the time of the post-peak load (in **Fig. A2-10** and **Fig. A2-11**).

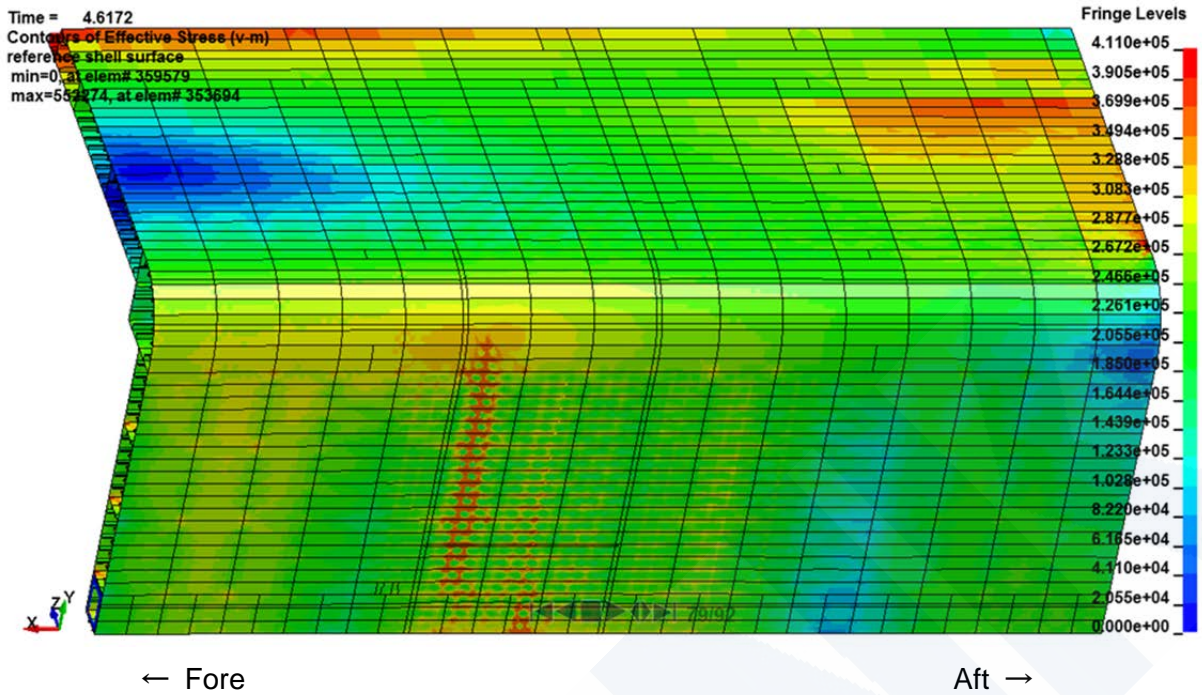


Fig. A2-8 Mises' equivalent stress at the time of the peak load equal to the hull girder ultimate strength
(In the case of the average yield stress based on the mill sheet of the Ship)

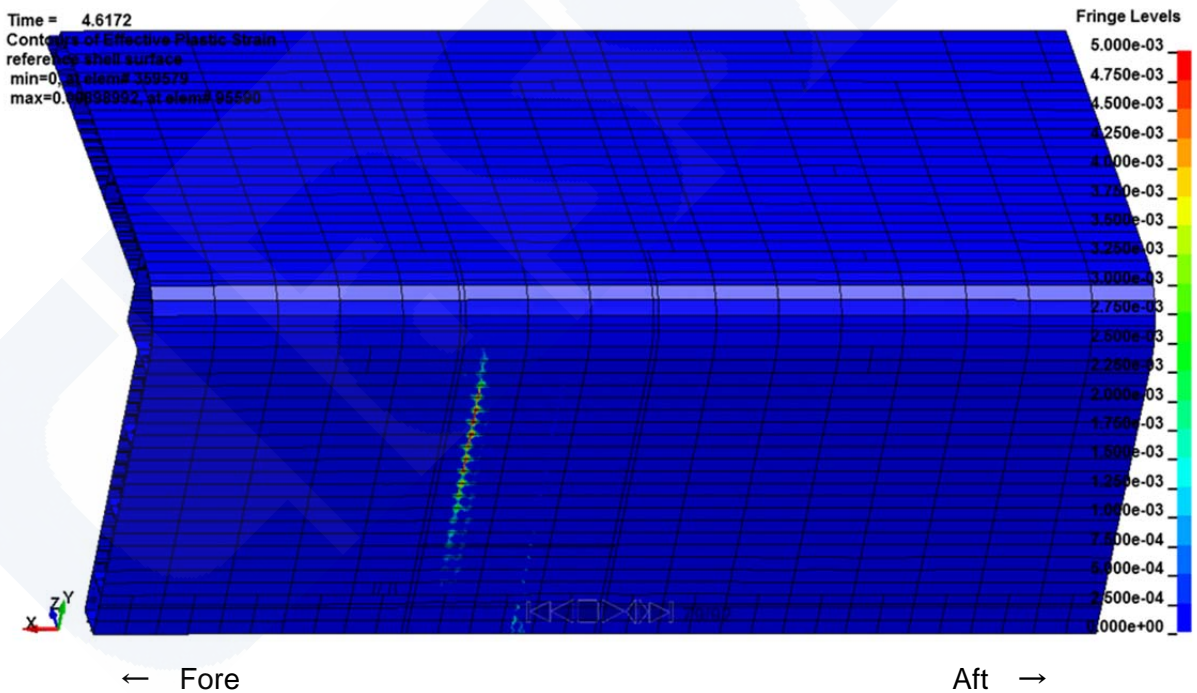


Fig. A2-9 Equivalent plastic strain at the time of the peak load equal to the hull girder ultimate strength
(In the case of the average yield stress based on the mill sheet of the Ship)

2. Local Deformations of Bottom Shell Plates found in the Sister Ships of the Ship

As stated in Chapter 4 of JG Interim Report, local deformations of around 20 mm in height were found in the bottom shell plates of the sister ships of the Ship through the inspections which were carried out just after the accident.

Through the results of the 3-hold model elasto-plastic analyses conducted in Chapter 3 and Chapter 4 of this Report, it was observed that plastic strains were generated in the bottom shell plates locally in the load condition before reaching the value of the hull girder ultimate strength. The pattern of the plastic strains is similar to the patterns of the local deformations found in the sister ships of the Ship.

Fig. A2-12 shows the history of application of the vertical bending moment in the section where the hull girder was fractured, relating to 3-hold model elasto-plastic analysis in case of estimating the *minimum hull girder ultimate strength* by the method of Case 1 shown in **Table 3-1** in 3.3.1 of this Report. The yield stress of the bottom shell plates was 342 N/mm² in this analysis

Fig. A2-13 shows the result of the analysis of the bottom shell plates and bottom longitudinals at the time of “plastic strain generated” as indicated in **Fig. A2-12**, which is just before the peak load, i.e. the hull girder ultimate strength. **Fig. A2-13** shows the distribution of equivalent plastic strains of the bottom shell plates and the bottom longitudinals at the time of “plastic strain generated” as seen from the above. In the figure, the light-blue color shows plastic strain and it can be seen that the plastic strains are locally generated in the bottom shell plates.

The outline of the bottom shell plate deformation indicated by a yellow dotted line in **Fig. A2-13** is shown in **Fig. A2-14**. The deformation with three half waves is seen in the longitudinal direction, which is similar to the local deformation in the bottom shell plates found in the sister ships of the Ship. However it should be noted that the deformation shown in **Fig. A2-14** includes elastic deformation generated under the condition where the vertical bending moment is applied, and further investigation is necessary with regard to the relationship between the residual deformation in the case of unloading the vertical bending moment and the local deformation found in the sister ships of the Ship.

There might be a possibility where plastic strains are generated in a load condition with ample time before reaching the hull girder ultimate strength, therefore it is considered to be a future task to quantitatively elucidate how the local deformations are generated in the bottom shell plates. Furthermore it would be necessary to investigate the effect where the load with limited energy such as whipping response is applied as pointed out in JG Interim Report.

Incidentally as stated in JG Interim Report, the significant reinforcements in order to increase hull girder strength had already been carried out as a preventative safety measure successively in the double bottom structure of the sister ships of the Ship.

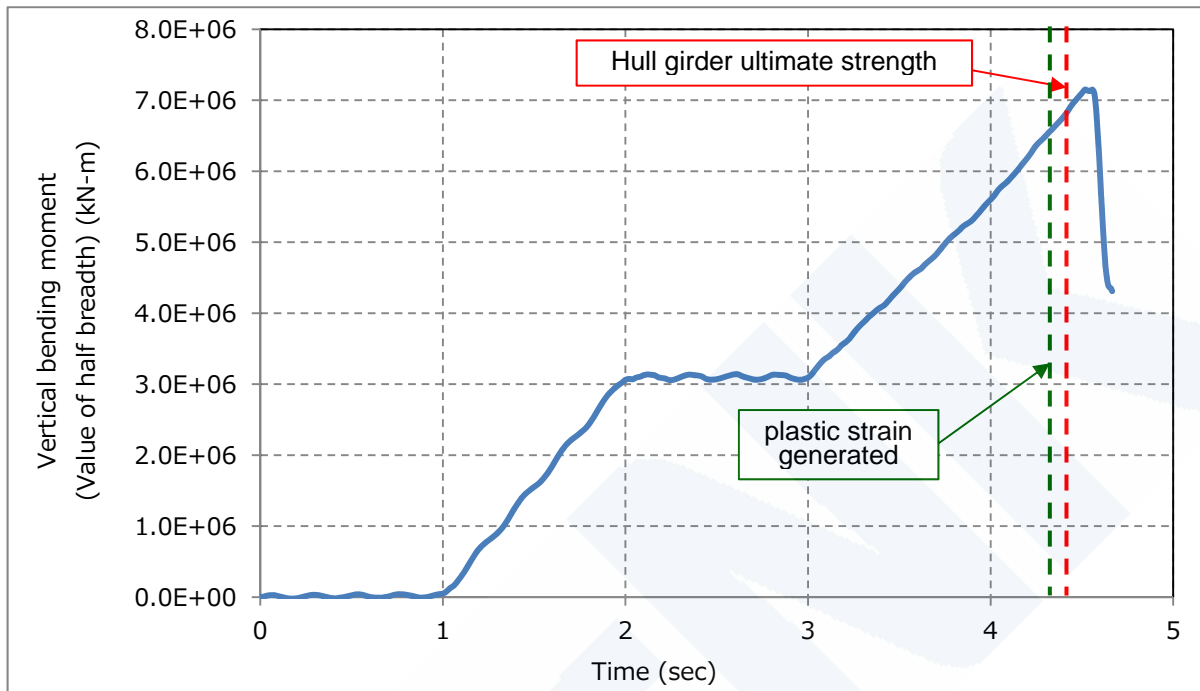


Fig. A2-12 History of application of vertical bending moment in the case of estimating the *minimum hull girder ultimate strength* by the method of Case 1 shown in **Table 3-1** in 3.3.1 of this Report

(The vertical axis shows the value corresponding to the half breadth not multiplied by 0.96 and 0.95 which are the effects of local deformation and welding residual stress respectively.)

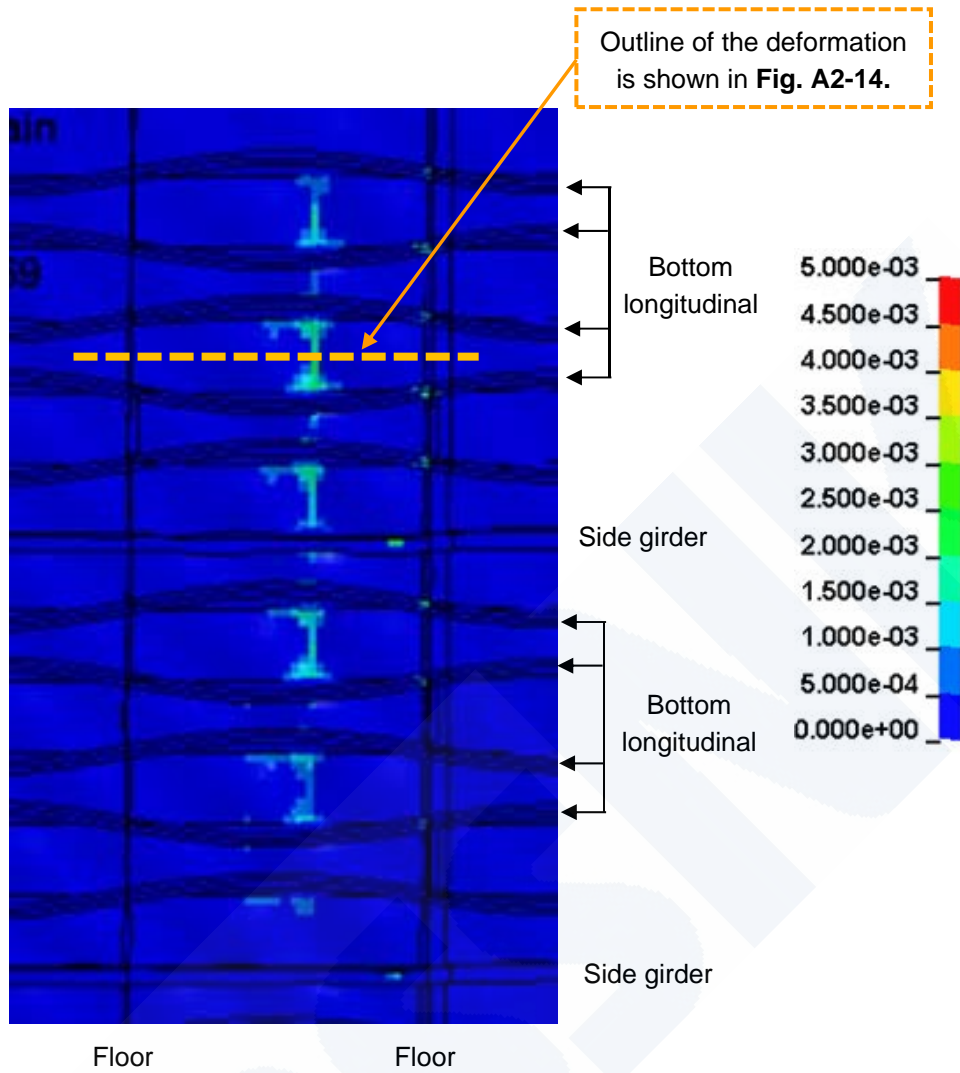


Fig. A2-13 Equivalent plastic strain in bottom shell plates and bottom longitudinals
(Plastic strain at the center of thickness)

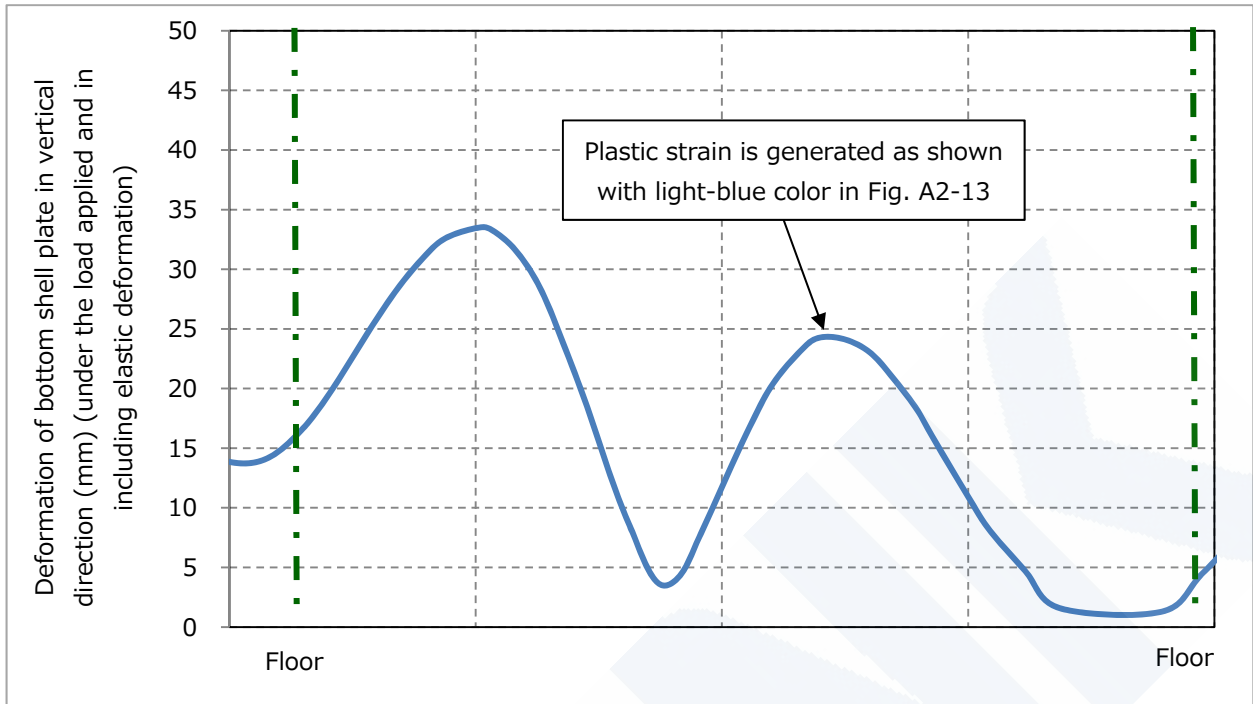


Fig. A2-14 Outline of bottom shell plate deformation where plastic strain is generated (Under the condition where load is applied)

Appendix 3 Effect of Local Deformation of Bottom Shell Plates and Welding Residual Stress of Bottom Longitudinals on Hull Girder Ultimate Strength (related to 3.3.1 of this Report)

1. Effect of Local Deformation of Bottom Shell Plate on Hull Girder Ultimate Strength

As stated in Chapter 4 of JG Interim Report, local deformations of around 20 mm in height were observed in the bottom shell plates in the midship part of the sister ships of the Ship through the inspections which were carried out after the accident.

To investigate the effect of these local deformation on the hull girder ultimate strength, JG Committee carried out a 3-hold model elasto-plastic analysis of the Ship with an condition where local circular deformations of 30 mm in height existed in the fore and aft of the butt joint at FR151+200 mm and in the overall breadth up to the bilge circle end in the transverse direction, as illustrated in **Fig. A3-1**.

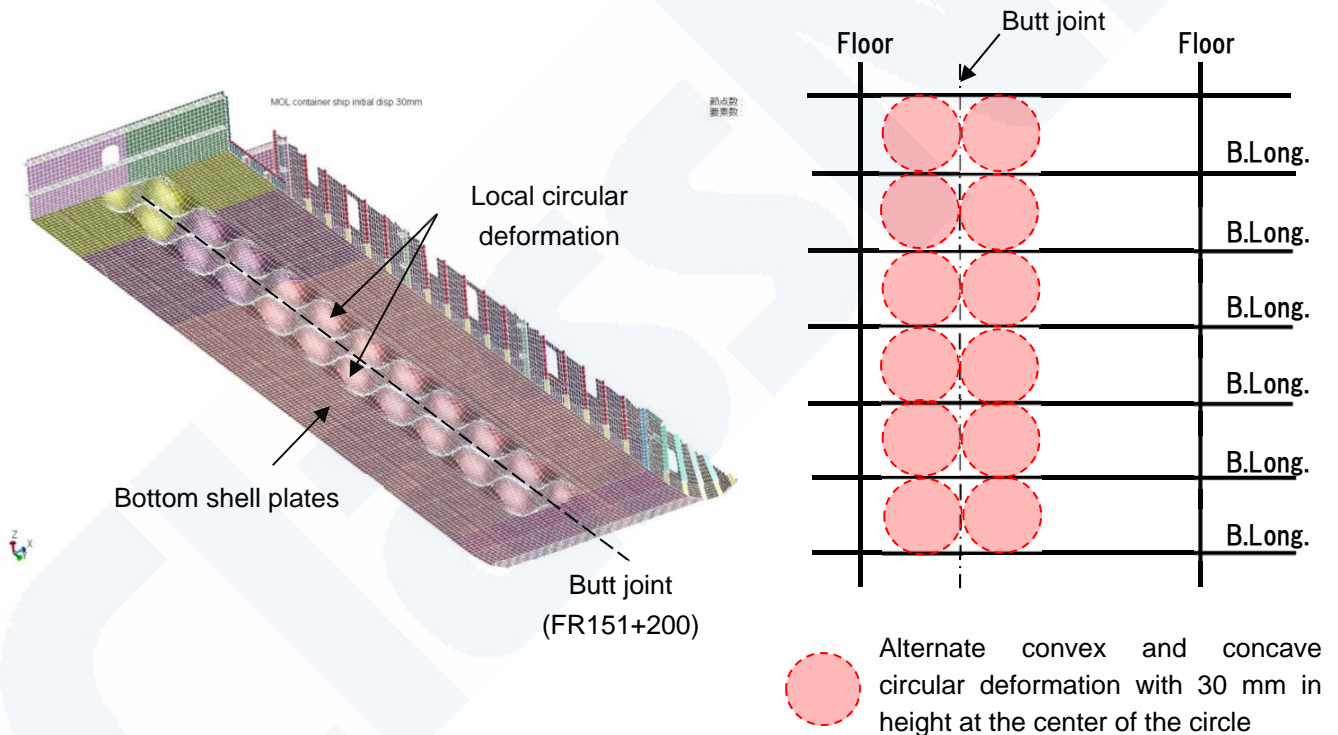


Fig. A3-1 Condition of initial shape deformation for 3-hold model elasto-plastic analysis to investigate the effect of local deformation of bottom shell plates on hull girder ultimate strength (extracted from **Fig. 5.2.8** in JG Interim Report)

The result of 3-hold model elasto-plastic analysis with the local deformations of 30 mm in height shown in **Fig. A3-1** was 96% of the hull girder ultimate strength described in 3.3.1 of this Report with 4 half-waves buckling mode deformations.

It can be said that the initial deformation condition shown in **Fig. A3-1** is an extreme case,

because 30 mm local deformations exist in the overall breadth in the transverse direction. Accordingly the effect of the local deformations of 30 mm in height, the reduction of 5% in the hull girder ultimate strength, can be considered the maximum one among the effects of various local deformations in the bottom shell plates.

2. Effect of Welding Residual Stress of Bottom Longitudinals on Hull Girder Ultimate Strength

Tensile welding residual stress in the longitudinal direction exists in the fillet welding part of bottom longitudinals. Meanwhile compressive residual stress is generated in the bottom shell plates in the longitudinal direction between the bottom longitudinals due to the equilibrium condition of residual stresses, and it is well known this compressive stress reduces the buckling strength in the longitudinal direction of the bottom shell plates.

In order to evaluate the effect of the above welding residual stress on the buckling collapse strength of the stiffened bottom panel, an elasto-plastic analysis of the stiffened bottom panel was carried out with giving welding residual stress as the analysis initial condition. **Table A3-1** shows outlines of the analysis and **Fig. A3-2** shows the analysis model.

The analysis was conducted in two different cases, i.e. with welding residual stress and without welding residual stress and the effect of the welding residual stress on the buckling collapse strength was evaluated by comparing the two results.

Table A3-1 Elasto-plastic analysis of stiffened bottom panel for the evaluation of effect of welding residual stress on buckling collapse strength

Object for analysis	Stiffened bottom panel, i.e. bottom shell plates and bottom longitudinals between No.3 Girder and No.9 Girder of the Ship
Extent of model	Longitudinal direction : 1/2 + 1 + 1/2 floor space Transverse direction : between No.3 Girder and No.9 Girder (Scallop openings on bottom longitudinal webs for the butt joint were modeled.)
Load conditions	<ol style="list-style-type: none"> 1. First, following loads were applied to the model of the stiffened bottom panel. <ul style="list-style-type: none"> • Bottom sea pressure (lateral load) was applied to the bottom shell plates. • Compressive stress in the transverse direction (double bottom local stress) was generated in the bottom shell plates by applying corresponding transverse load. • Welding residual stress shown in Fig. A3-3 was given. 2. Next, longitudinal load (forced displacement) was applied being gradually increased up to the collapse strength of the panel.

Boundary condition	Longitudinal direction : periodically continuous condition Transverse direction : simply supported in connected part of the girder and bottom shell plate (The floors were modelled in the half height and symmetrical condition was applied on the upper end in the vertical direction.)
Analysis program	MARC (implicit method)

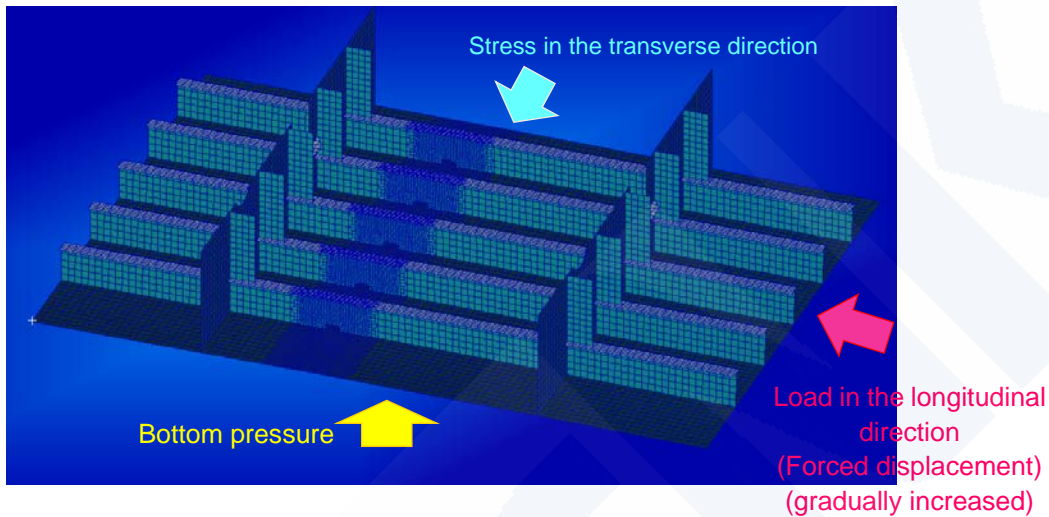


Fig. A3-2 Model of stiffened bottom panel

The distribution of welding residual stress caused by the fillet welding of bottom longitudinals was estimated as shown in **Fig. A3-3**, and it was applied to the elasto-plastic analysis of the stiffened bottom panel as the initial analysis condition. The distribution of welding residual stress was estimated in the following way.

- Heat input per one pass of fillet welding on a bottom longitudinal was presumed to be 30,000 J/cm.
- Compressive welding residual stress was estimated by the following equation based on the equilibrium condition of welding residual stress.

$$\frac{\sigma_c}{\sigma_Y} = \frac{2b_t}{b - 2b_t}$$

σ_c : Compressive welding residual stress (N/mm²)

σ_Y : Yield stress (N/mm²)

b : Space of bottom longitudinal (mm)

b_t : Breadth where tensile welding residual stress is generated (mm)

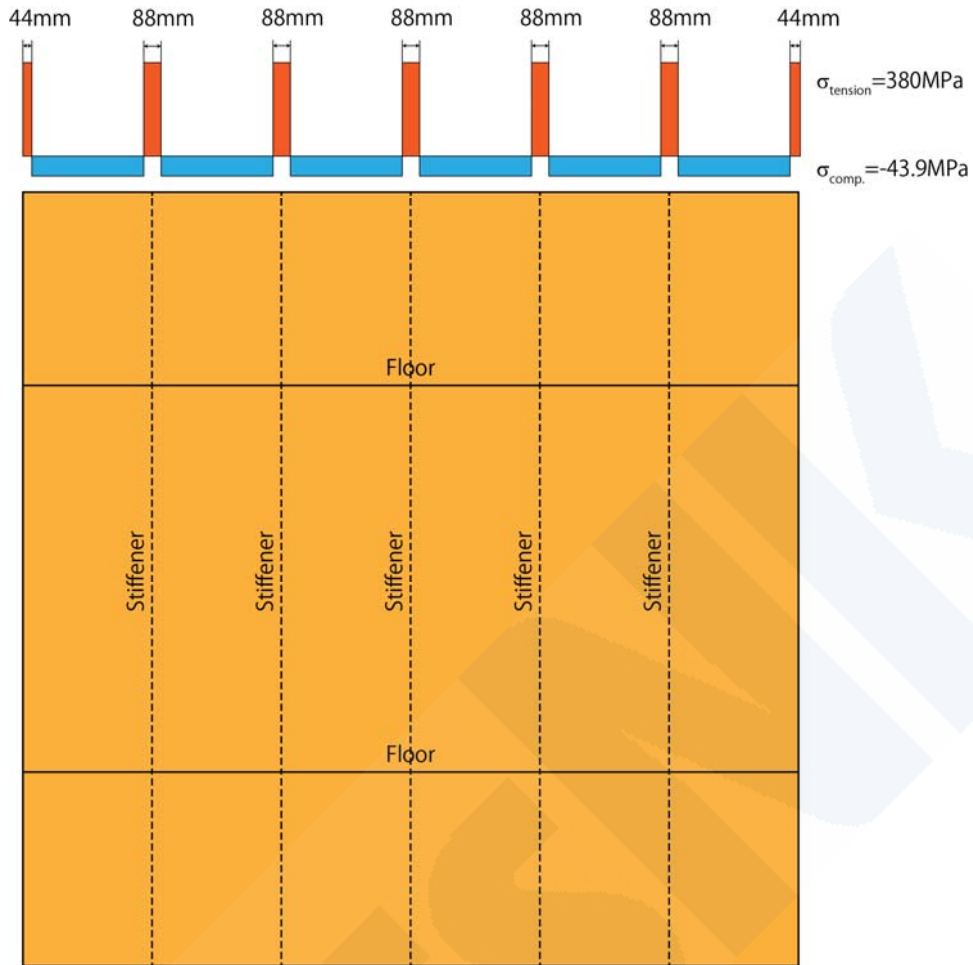


Fig. A3-3 Distribution of welding residual stress caused by fillet welding of bottom longitudinals

Fig. A3-4 shows the deformation and the equivalent stress of the panel just before the peak load, i.e. panel collapse strength. The results of analysis, i.e. the collapse strength of the stiffened bottom panel, are shown in **Table A3-2** which shows that the collapse strength of the stiffened bottom panel was decreased by around 8% in the case where welding residual stress of the bottom longitudinal is taken into account.

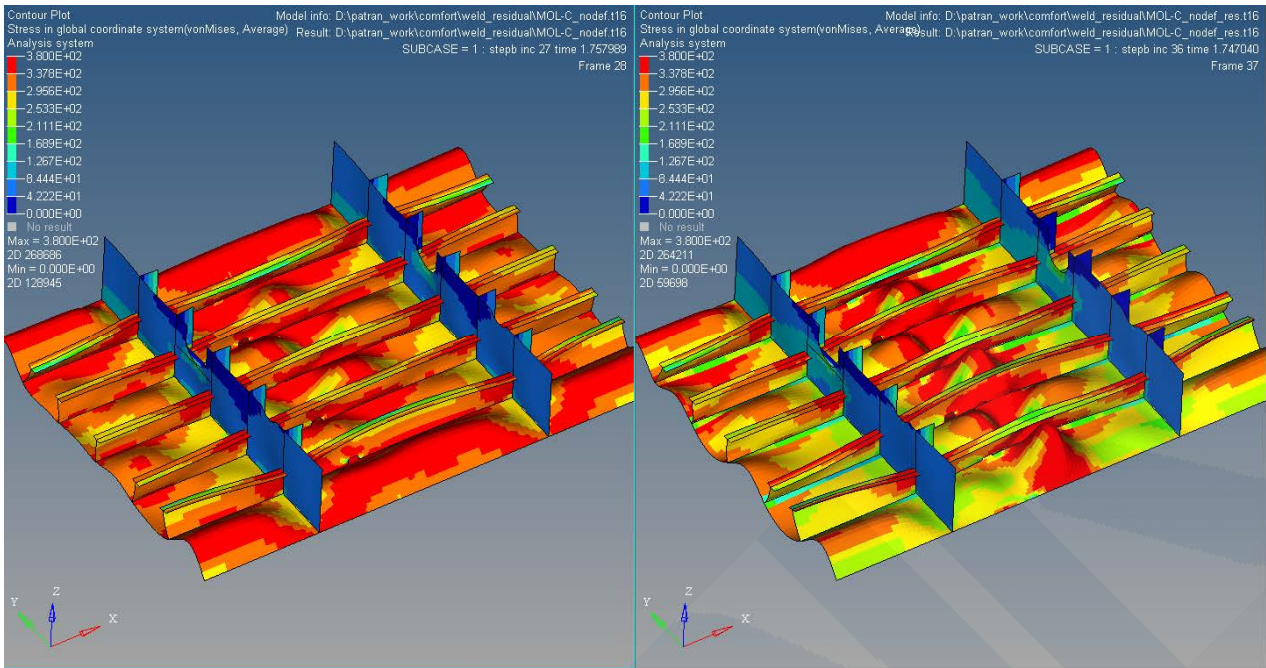


Fig. A3-4 Deformation and equivalent stress just before the collapse strength of the panel
Left : without consideration of welding residual stress
Right : with consideration of welding residual stress)

Table A3-2 Analysis results (Collapse strength of stiffened bottom panel)

	Without consideration of welding residual stress	With consideration of welding residual stress
Collapse strength of stiffened bottom panel (N/mm ²)	318	293

The above is the result of the strength analysis on the stiffened bottom panel. In general the effect of welding residual stress on the post-collapse strength is less than that of the collapse strength and it is known that the effect of welding residual stress on the hull girder ultimate strength, the total sum of the load bearing capacity of each panel, is less than the effect on the collapse strength of one panel only.

Therefore maximum 5% reduction was considered as the effect of welding residual strength of bottom longitudinals on the hull girder ultimate strength in the investigation in 3.3.1 of this Report.

Appendix 4 Simulation of Wave Vertical Bending Moment at the Time of Accident with Consideration of the Deviation of Sea States (related to 3.3.2 of this Report)

Although JG Interim Report estimated the sea state at the time of accident to be a significant wave height of 5.5 m, an mean wave period of 10.5 seconds and an encountered wave direction of 114 degrees (oblique sea from bow and Port side), JG Interim Report stated that the significant wave height might have had the deviation between around 0.5 m and 2 m from the estimated height because of the error of the weather and the sea states data based on the estimation. JG Interim Report also said the error of the mean wave period to be between around 0.5 seconds and 2 seconds with the explanation that there were not many cases of wave periods being comprehensively verified. Furthermore JG Interim Report pointed out the possibility of further wave period deviations due to differences of applied numerical wave prediction models.

In light of these remarks of JG Interim Report, the NK Panel considered the deviation of the sea states at the time of accident as follows;

- Significant wave height : from 5.5 m to 7.5 m
- Mean wave period : from 10.3 seconds to 15 seconds
- Encountered wave direction : from 120 degree (oblique sea from bow and Port side) to 180 degree (head sea) (whipping response is maximum at 180 degree)

Simulations of wave-induced load were performed in 27 (=3×3×3) different cases of short-term sea states as shown in **Table A4-1** specifically in order to estimate the maximum value of the wave-induced vertical bending moment including whipping response in each short-term sea state.

The simulations were carried out in the same way as JG Interim Report by using the non-linear strip method developed and owned by the Japanese National Maritime Research Institute (NMRI).

Table A4-1 Conditions of wave-induced load simulations considering deviation of sea states

Significant wave height	5.5 m, 6.5 m, 7.5 m
Mean wave period	10.3 seconds, 12.5 seconds, 15 seconds
Encountered wave directions	120 deg., 150 deg., 180 deg. (head sea)
Ship speed	17 knots (identical with that in JG Interim Report)
Loading condition	Loading condition at the time of accident (identical with that in JG Interim Report)

Fig. A4-1 shows the results of the wave-induced load simulations. It shows the maximum value of the response (wave-induced vertical bending moment) in each short-term sea state (so-called the maximum expected value in 1000 waves) obtained through the simulations in 27 cases.

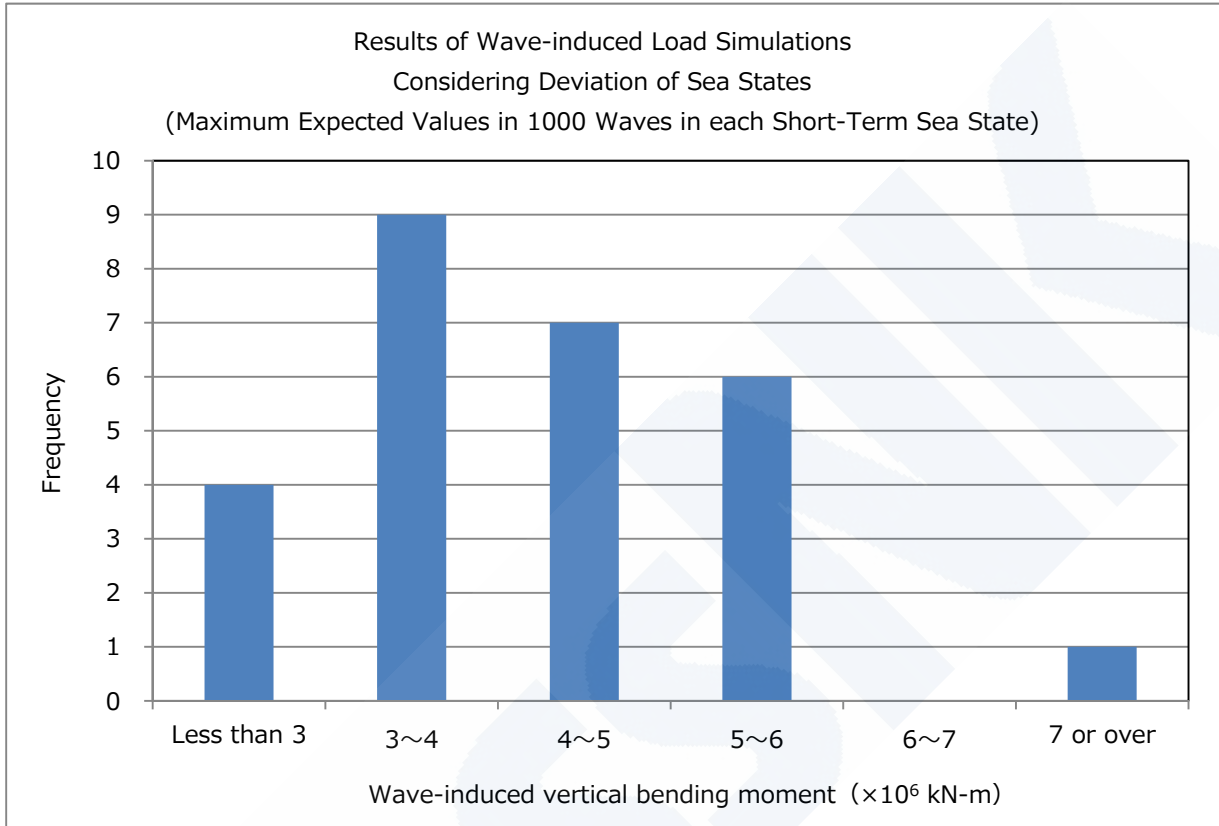


Fig. A4-1 Results of wave-induced load simulations considering deviation of sea states

Table A4-2 shows the results of the simulations in two cases in which the wave-induced vertical bending moment (maximum expected value in 1000 waves) is maximum and minimum.

Table A4-2 Results of wave-induced load simulations considering deviation of sea states
(In cases where wave-induced vertical bending moment is maximum and minimum)

		Case with the maximum moment	Case with the minimum moment
Sea States	Significant wave height	7.5 m	5.5 m
	Mean wave period	15 seconds	15 seconds
	Encountered wave direction	180 deg. (head sea)	120 deg. (oblique sea from bow and Port side)
Total wave-induced vertical bending moment including whipping response		7.23×10^6 kN-m	2.50×10^6 kN-m
Wave-induced vertical bending moment (Wave component only)		4.18×10^6 kN-m	2.47×10^6 kN-m
Wave-induced vertical bending moment (Whipping response only)		3.05×10^6 kN-m	0.03×10^6 kN-m

Appendix 5 Investigation based on Draught Measurements at Ship's Departure (related to 3.3.3 of this Report)

Investigation Related to the Possibility of Deviation of Still Water Vertical Bending Moment due to Deviation (Gap between Declared Weight and Actual Weight) in the Weight (Load) of Container Cargo

1. Objectives of the Investigation

The objectives of this investigation were to investigate the possibility of deviation in the maximum still water vertical bending moment (hereinafter "Ms maximum value") caused by the gap in the weight distribution of container cargo due to the difference between the "sum total of actual weight of container cargo" calculated from draught measurements and the "sum total of declared weight of container cargo" obtained from the results of loading calculations by a loading computer.

2. Data Used in the Investigation

"Results of loading calculation by a loading computer based on declared weight of container cargo" have been extracted for the total of 58 loading cases, based on "results of draught measurement" carried out at the departure loading conditions of four (4) sister ships of the Ship within the period of 7th September 2013 to 4th February 2014, i.e. a period after the Ship's accident.

2.1 Relative Difference between Declared and Actual Weight of Container Cargo (in Sequence)

Fig. A5-1 shows the distribution of relative difference between the "sum total of actual weight of container cargo" calculated from draught measurements and the "sum total of declared weight of container cargo" obtained from loading calculations carried out by loading computer based on the declared weight of container cargo, shown in sequence for the measured period.



Fig. A5-1 Sequential distribution of relative difference between the “sum total of actual weight of container cargo” and “sum total of declared weight of container cargo”

2.2 Relative Difference in the Total Weight of Container Cargo (for Each Port)

Draught measurements for the 58 extracted loading cases were performed at 12 ports in the Europe-Asia navigation route, which is the same route as the one taken by the Ship. **Fig. A5-2** shows the distribution of relative difference, which is shown in **Fig. A5-1** in sequence, categorized by ports where the draught measurements have been performed. **Table A5-1** shows the number of measurements performed at each port along with the mean relative difference between the “sum total of actual weight of container cargo” and the “sum total of declared weight of container cargo”.

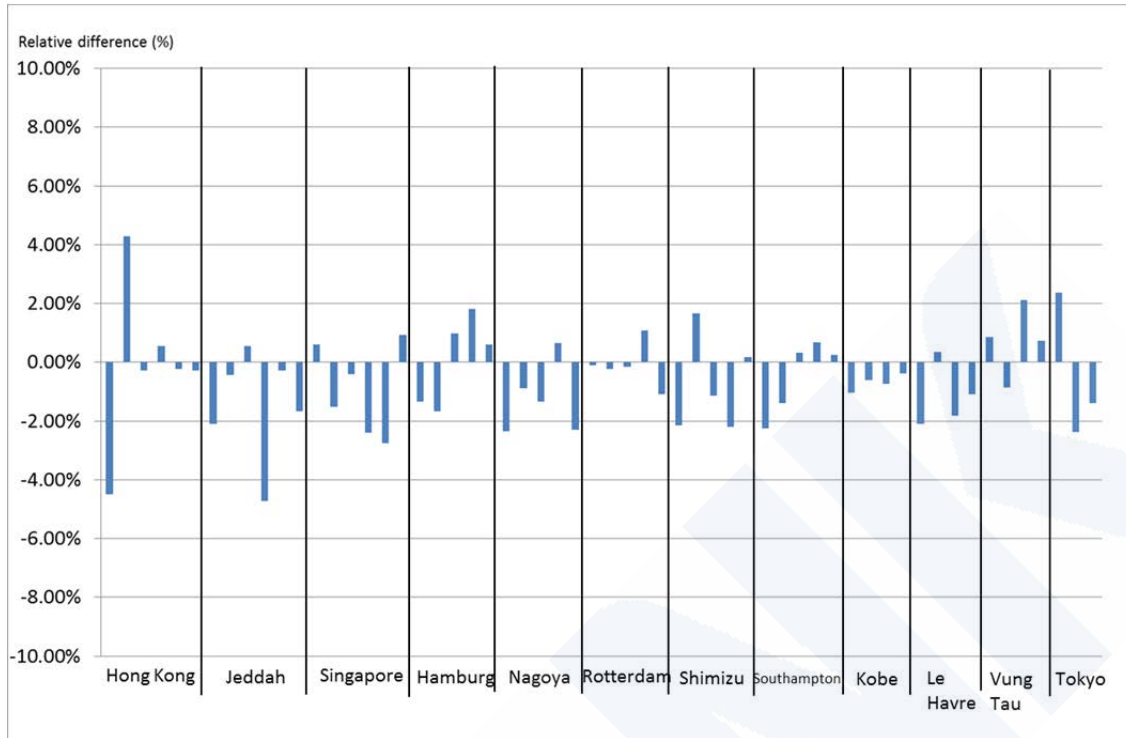


Fig. A5-2 Trend of relative difference between the “sum total of actual weight of container cargo” and the “sum total of declared weight of container cargo”

Table A5-1 Number of measurement cases and mean relative difference between the “sum total of actual weight of container cargo” and the “sum total of declared weight of container cargo” by port

Port	No. of cases	Mean relative difference
Hong Kong	6	-0.077%
Jeddah	6	-1.444%
Singapore	6	-0.924%
Hamburg	5	0.080%
Nagoya	5	-1.242%
Rotterdam	5	-0.107%
Shimizu	5	-0.728%
Southampton	5	-0.478%
Kobe	4	-0.687%
Le Havre	4	-1.157%
Vung Tau	4	0.712%
Tokyo	3	-0.472%

According to **Fig. A5-2**, the maximum relative difference is within $\pm 5\%$ at any port. Since the mean relative difference by port showed no specific difference in **Table A5-1**, no specific trend was observed in the relative difference between the “sum total of actual weight of container

cargo” and the “sum total of declared weight of container cargo” by port.

Table A5-2 shows the mean relative difference between the “sum total of actual weight of container cargo” and the “sum total of declared weight of container cargo” categorized by regions where the ports are located. The difference in sum total weight of container cargo did not show any specific trend even when compared by regions.

Table A5-2 Mean relative difference between the “sum total of actual weight of container cargo” and the “sum total of declared weight of container cargo” by region

Region	Port	No. of cases	Mean relative difference
Europe and West Asia	Jeddah	25	-0.633%
	Rotterdam		
	Hamburg		
	Southampton		
	Le Havre		
South East Asia	Hong Kong	16	-0.197%
	Vung Tau		
	Singapore		
Japan	Kobe	17	-0.824%
	Nagoya		
	Shimizu		
	Tokyo		

2.3 Normal Distribution of Relative Difference

Based on the relative differences of the 58 cases, relative frequency distribution (taking the sum total of areas as 1) is approximated by normal distribution, as shown in **Fig. A5-3**.

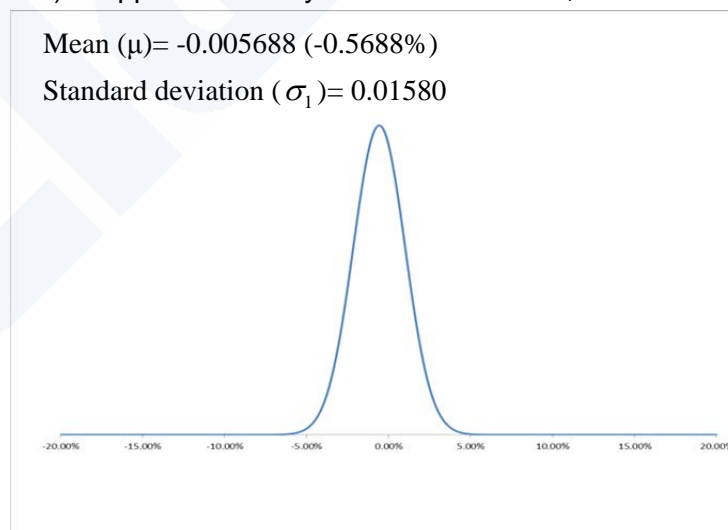


Fig. A5-3 Normal distribution of relative difference between the “sum total of actual weight of container cargo” and the “sum total of declared weight of container cargo”

2.4 Validating the Normal Distribution Approximation

The relative frequency distribution of relative difference was approximated by normal distribution in 2.3 of this appendix. To confirm its validity, normal probability (normal Q-Q plot and normal P-P plot) were plotted, as shown in **Fig. A5-4** and **Fig. A5-5**.

Correlation coefficients between the actual values plotted in blue and the red straight line that perfectly coincides with the normal distribution were found to be very close to 1.0 for both normal Q-Q plot and normal P-P plot, where the correlation coefficient for normal Q-Q plot is at 0.9968 and that for normal P-P plot is at 0.9864. This shows a strong correlation between the approximated normal distribution curve and the actual relative difference distribution. Therefore, it can be concluded that the approximation using normal distribution in the investigation in 2.3 of this appendix is acceptable in statistical point of view.

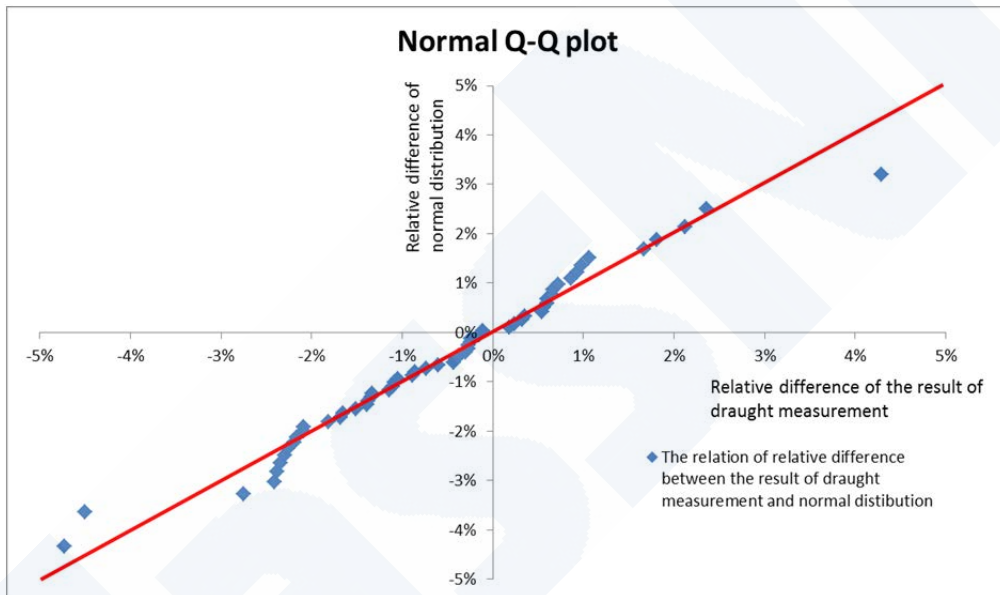


Fig. A5-4 Normal Q-Q Plot (correlation coefficient: 0.9968)

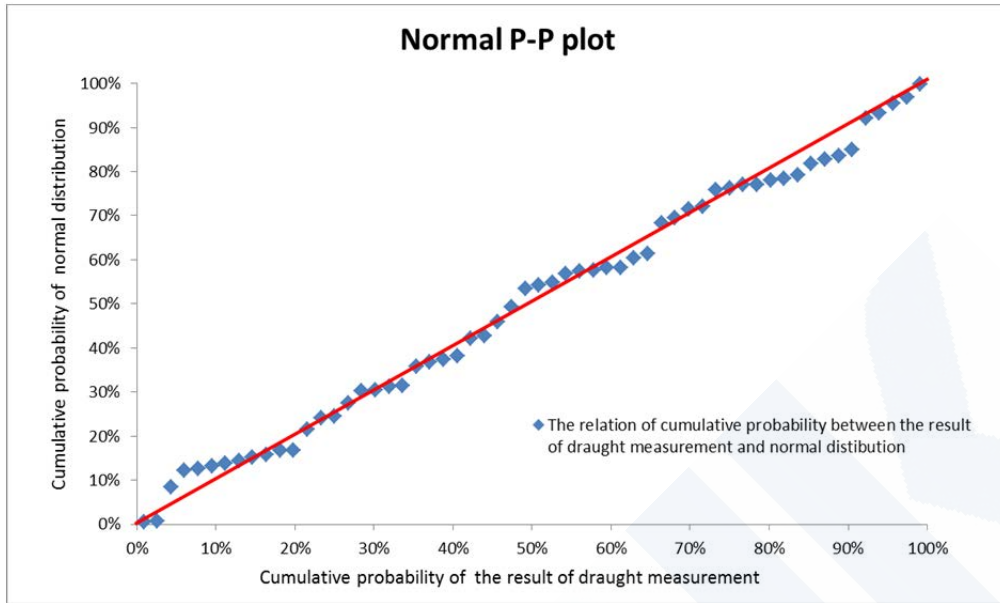


Fig. A5-5 Normal P-P Plot (correlation coefficient: 0.9864)

2.5 Occurrence Probability of Deviation of the “Sum Total of Actual Weight of Container Cargo” from the “Sum Total of Declared Weight of Container Cargo”

Table A5-3 shows the calculation results for occurrence probability of deviation of the “sum total of actual weight of container cargo” from the “sum total of declared weight of container cargo”, which was calculated using the normal distribution in Fig. 5-3.

Table A5-3 Occurrence probability of deviation of the “sum total of actual weight of container cargo” from the “sum total of declared weight of container cargo”

Deviation of the “sum total of actual weight of container cargo”	Occurrence probability
below -12.5%	$0.220 \times 10^{-13}\%$
-12.5% to below -7.5%	$0.058 \times 10^{-2}\%$
-7.5% to below -2.5%	11.089%
-2.5% to below +2.5%	86.300%
+2.5% to below +7.5%	2.610%
+7.5% to below +12.5%	$0.002 \times 10^{-2}\%$
+12.5% and above	$0.681 \times 10^{-14}\%$

3. Considerations on Occurrence Probability of the Container Loading Cases in Chapter 6 of JG Interim Report

The occurrence probability was estimated for two loading case examples in 6.3.1 of JG Interim Report—one as shown in Fig. 6.3.1 “loading case example in which Ms maximum value becomes 126% of allowable value” and the other as shown in Fig. 6.3.2 “loading case example in which Ms maximum value becomes 115% of allowable value”—that were shown

as examples of container loading cases calculated from hull deflection of the Ship.

Since JG Interim Report did not report the actual weight for each container cargo in the loading case examples, the deviation in the weight of container cargo in this Report was assumed in accordance with the occurrence probability (**Table A5-3**) determined from draught measurements of the 58 loading cases.

3.1 Division of Container Cargo into Three Groups: Fore/Mid/Aft Groups of Container Cargo

The weight of container cargo in the Ship’s loading condition at departure from Singapore was divided into three container groups in the longitudinal direction: Fore/Mid/Aft. The deviation in weight of container cargo in each of these groups was taken into consideration. As in JG Interim Report, the Fore/Mid/Aft boundaries were taken at locations where the Ms maximum value increases/decreases as the weight of container cargo in each bay increases (see **Fig. A5-6**).

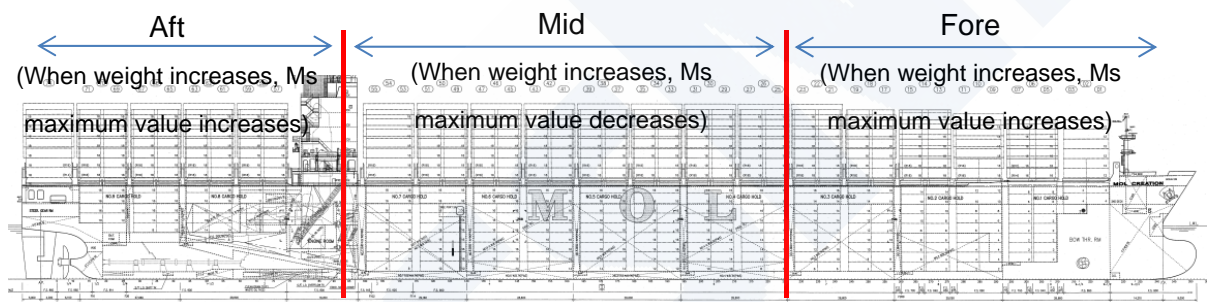


Fig. A5-6 Fore/Mid/Aft boundaries

3.2 Estimating the Deviation of the “Sum Total of Actual Weight of Container Cargo” for Containers in Each Container Group from the Deviation of the “Sum Total of Actual Weight of Container Cargo” for all Containers

The occurrence probability of deviation of the “sum total of actual weight of container cargo” for all containers has been determined as shown in **Table A5-3**. As for the occurrence probability of deviation of the “sum total of actual weight of container cargo” for containers in each of the three divided container groups, the standard deviation should be corrected as shown in **Fig. A5-6** in order to use the occurrence probability determined for all containers.

The reason is that as the total number of containers increases, the deviation of the actual weight of each container cargo which differs in weight tends to be canceled out, and the deviation of the sum total of actual weight of container cargo gradually decreases. Conversely, however, as the total number of containers decreases, the cancelation effect diminishes, and the degree of deviation of the weight increases. Since the total number of containers in this case has been divided into three parts, the standard deviation of the “sum total of actual weight of container cargo” within the number of containers in each container group is

estimated approximately to be $\sqrt{3}$ times the standard deviation of the “sum total of actual weight of container cargo” for all containers. The basis of assuming $\sqrt{3}$ times the standard deviation and its validity are described at the end of this appendix as “Technical Background”.

By taking $\sqrt{3}$ times the standard deviation of the “sum total of actual weight of container cargo” for all containers, the normal distribution for the occurrence of relative difference between the “sum total of actual weight of container cargo” and the “sum total of declared weight of container cargo” in the containers of each container group was determined for each container group as shown in **Fig. A5-7** by the blue line. **Table A5-4** shows the occurrence probability of deviation of the “sum total of actual weight of container cargo” in each container group determined from the aforementioned normal distribution.

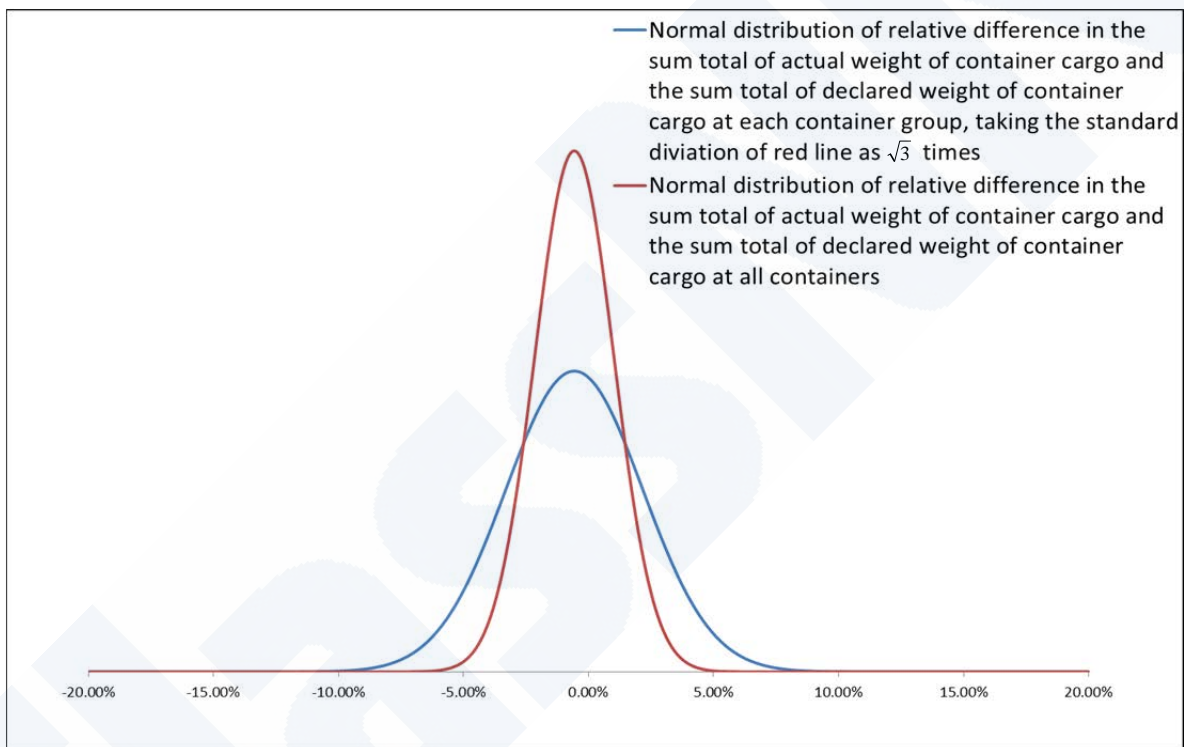


Fig. A5-7 Normal distribution for occurrence of relative difference between the “actual weight of container cargo” and “declared weight of container cargo”

Table A5-4 Occurrence probability of deviation of the “sum total of actual weight of container cargo” in each container group

Deviation in the “Sum Total of Actual Weight of Container Cargo”	Occurrence probability
below -12.5%	$0.653 \times 10^{-3}\%$
-12.5% to below -7.5%	0.566%
-7.5% to below -2.5%	23.457%
-2.5% to below +2.5%	62.866%
+2.5% to below +7.5%	12.951%
+7.5% to below +12.5%	0.160%
+12.5% and above	$0.090 \times 10^{-3}\%$

3.3 Occurrence Probability for Container Loading Case Examples Shown in JG Interim Report

The effects of loading container cargo are mentioned in 6.3.1 of JG Interim Report. According to the report, Ms maximum value was estimated to be 126% of the allowable value (118% when the buoyancy effect due to deflection is taken into account) from the results of direct calculations by whole FEM model using hull deflection value of the Ship, measured at the time of departure from Singapore just before the accident.

For the two loading case examples in the aforementioned report, where Ms maximum value for one is at 126% of the allowable value (Case 1) and the other is at 118% of the allowable value (Case 2), the occurrence probability of each loading case is calculated using the occurrence probability of deviation of the “sum total of actual weight of container cargo” in each container group shown in **Table A5-4**. The results of this calculation are shown in **Table A5-5**.

Table A5-5 Occurrence probability of loading case examples shown in 6.3.1 of JG Interim Report

	Change in weight of container cargo (occurrence probability)			Occurrence probability (Aft x Mid x Fore)
	Aft	Mid	Fore	
Case 1	14% increase ($0.001 \times 10^{-2}\%$) ^{*1}	14% decrease ($0.005 \times 10^{-2}\%$) ^{*1}	13% increase ($0.004 \times 10^{-2}\%$) ^{*1}	$8.451 \times 10^{-19}\%$
Case 2	5% increase (2.095%) ^{*1}	7% decrease (0.940%) ^{*1}	7% increase (0.284%) ^{*1}	$5.599 \times 10^{-5}\%$

*1) % value within parentheses is the occurrence probability of change in weight of container cargo in each group.

Since the deviation of the “sum total of actual weight of container cargo” for each container group was estimated from that for all containers as shown in 3.2 of this appendix, the calculated occurrence probability is based on certain assumptions. However, the occurrence probability for these cases can be practically ignored from statistical point of view, considering that the said value for both cases is extremely small ($8.451 \times 10^{-19}\%$ and $5.599 \times 10^{-50}\%$).

4. Estimation of Probability Distribution of Ms Maximum Value with Respect to Deviation of the Weight of Container Cargo

The probability distribution of deviation of Ms maximum value in the Ship’s loading condition at departure from Singapore was estimated using the occurrence probability of deviation of the “sum total of actual weight of container cargo” in each container group shown in **Table A5-4**.

4.1 Establishing Seven Deviation Values of the “Sum Total of Actual Weight of Container Cargo” in Each of Fore/Mid/Aft Container Groups

The deviations (**Table A5-4**) of the “sum total of actual weight of container cargo” in each of Fore/Mid/Aft container groups were represented by seven deviation values, namely “-15%, -10%, -5%, 0%, +5%, +10%, +15%” as shown in **Table A5-6**.

Table A5-6 Deviation and occurrence probability of the “sum total of actual weight of container cargo” in each container group

Deviation of the “sum total of actual weight of container cargo” in each container group	Occurrence probability
-15%	$0.653 \times 10^{-3}\%$
-10%	0.566%
-5%	23.457%
0%	62.866%
+5%	12.951%
+10%	0.160%
+15%	$0.090 \times 10^{-3}\%$

4.2 Calculating Occurrence Probability of Deviation of the Ms Maximum Value

In the case of the Ship’s loading conditions at departure from Singapore, the 7 combinations of deviations of the “sum total of actual weight of container cargo” in the three Fore/Mid/Aft container groups, that is, 343 (7 x 7 x 7) loading conditions were assumed, and the occurrence probability of deviation in the weight of container cargo was determined using **Table A5-6**. On the other hand, the Ms maximum value for each condition was calculated, and the relative difference from the Ms maximum values was determined using declared

weight of container cargo at departure from Singapore.

For instance, if the deviation of “sum total of actual weight of container cargo” in the container groups for a certain loading condition are Aft (0%), Mid (-10%), and Fore (0%), then the probability that such deviation occurs would become $62.9\% \times 0.566\% \times 62.9\% = 0.224\%$. The relative difference in the Ms maximum values at this loading condition is +7.57%. This means that such probability is 0.224% as relative difference of Ms maximum value is +7.57%.

The mean value and standard deviation were determined from the relative difference of 343 kinds of Ms maximum value and its occurrence probability. These are plotted as normal distribution in **Fig. A5-8**. **Table A5-7** shows the occurrence probability in every 5% of deviation of Ms maximum values using this normal distribution.

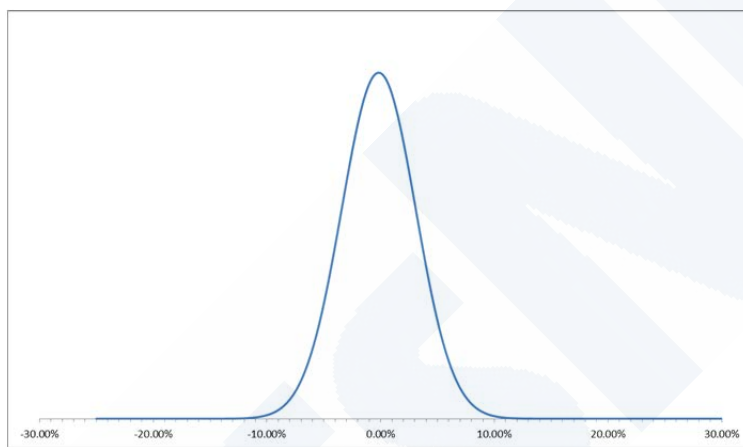


Fig. A5-8 Normal distribution of deviations in Ms maximum value that occurs due to deviation in the “weight of container cargo”

Table A5-7 Occurrence probability of deviation of Ms maximum values

Deviation of Ms maximum values	Occurrence probability
below -10%	0.126%
-10% to below -5%	7.171%
-5% to below 0%	44.789%
0% to below +5%	42.316%
+5% to below +10%	5.510%
+10% to below +15%	0.088%
+15% to below +20%	$0.016 \times 10^{-2}\%$
+20% to below +25%	$2.811 \times 10^{-8}\%$
+25% and above	$5.059 \times 10^{-13}\%$

In **Table A5-7**, the range of deviation where the occurrence probability is more than 1% (the range of deviation where the deviation of Ms maximum value is from -10% to +10%) covers 99.8% of the range of all data. Accordingly, the actual Ms maximum values conceivably

deviate approximately $\pm 10\%$ from the Ms maximum values determined from the declared weight of container cargo at most.

5. Conclusions of the Investigation

Deviation of Ms maximum values was estimated from the deviation (difference between declared weight and actual weight) of the weight (load) of the container cargo, based on the results of draught measurement at departure from ports for four sister ships of the Ship. It is estimated from the results that a possibility of maximum deviation is $\pm 10\%$ approximately in Ms maximum values based on the declared weight of container cargo.

—Technical Background: Basis for Taking $\sqrt{3}$ Times the Standard Deviation and Its Validity—

When considering the weight of a certain number of containers in relation to the deviation of the “weight of container cargo”, as the number of containers increases, the deviation in the weight of container cargo cancels out, and the degree of deviation decreases. Conversely, if the number of containers decreases, the degree of deviation increases. Since the actual weight of each container cargo was not included in the data for the 58 cases used in this investigation, it became necessary to estimate the deviation of the “sum total of actual weight of container cargo” in each container group of the three groups, namely Fore/Mid/Aft, from two types of data: the “sum total of declared weight of container cargo” obtained from the loading calculation results by the loading computer based on the declared weight of container cargo and the “sum total of actual weight of container cargo” calculated from result of the actual ships’ draught measurement at departure from port. The procedure used in the estimation is described below.

1. Relationship between Number of Containers and Degree of Deviation

According to the statistics, the probability distributions of the difference between declared weight and actual weight for each container cargo are mutually independent. When such distributions are assumed to follow the normal distribution $N(w, \sigma^2)$, then the probability distribution followed by the total $\sum W_i$ of n containers is $N(nw, n\sigma^2)$. Here, the probability distribution corresponding to $N(w, \sigma^2)$ becomes:

$$f(x) = \frac{1}{\sqrt{2\pi}\sigma} e^{-\frac{(x-w)^2}{2\sigma^2}}$$

Therefore, the probability distribution related to the total $\sum W_i$ of n containers will be as follows:

$$F(X) = \frac{1}{\sqrt{2n\pi}\sigma} e^{-\frac{(x-nw)^2}{2n\sigma^2}}$$

If we assume that the standard deviation σ_a of the difference between declared weight and actual weight of n container cargo is known, then the standard deviation σ_b per container from the above becomes $\sigma_b = \sigma_a / \sqrt{n}$. This leads to the relationships in **Table R5-1** based on the assumptions of normal distribution and the definition of standard deviation.

Table R5-1 Relationships of statistical quantities of differing number of containers and statistical quantities obtained from the difference between declared weight and actual weight of n containers

	1 container	n/3 containers	n containers
A. Total weight of container cargo	\bar{W}	$\frac{n\bar{W}}{3}$	$n\bar{W}$
B. Standard deviation of difference between declared weight and actual weight	σ	$\sqrt{\frac{n}{3}}\sigma$	$\sqrt{n}\sigma$
(B/A) Standard deviation of the relative differences between the declared weight and actual weight	$\frac{\sigma}{\bar{W}}$	$\frac{\sqrt{3}\sigma}{\sqrt{n}\bar{W}}$	$\frac{\sigma}{\sqrt{n}\bar{W}}$

Here, \bar{W} is the mean weight of one container.

2. Estimating the Degree of Deviation of the “Sum Total of Actual Weight of Container Cargo” with Respect to Number of Containers in Each of the Groups Fore/Mid/Aft

By taking $1/\sqrt{n}$ times the standard deviation of the total weight of n containers, the standard deviation for one container can be determined. On the other hand, since the total weight of the container cargo would be $1/n$ at the same time, the standard deviation of “weight difference/declared weight” for each of n containers can be determined by taking \sqrt{n} times the standard deviation of the “weight difference/total declared weight” for n number of containers, taking into account the standard deviation of relative difference between declared weight and actual weight in **Table R5-1**. Accordingly, when all containers loaded on the ship are divided into the three groups of Fore/Mid/Aft, and if all containers are simply assumed as three large containers, then the number of containers becomes $n=3$. Although this is a very rough estimate since it includes many assumptions, it was decided to use $\sqrt{3}$ times the standard deviation of the “sum total of actual weight of container cargo” for all containers from above as the standard deviation of the “sum total of actual weight of container cargo” in each of Fore/Mid/Aft container groups.

3. Confirming the Validity of Estimation Method Using $\sqrt{3}$ Times

For each of the Fore/Mid/Aft groups, occurrence probabilities of deviation of the “sum total of actual weight of container cargo” were determined from normal distribution taking into consideration the deviation of the “sum total of actual weight of container cargo” of containers in each of the Fore/Mid/Aft groups (**Table A5-6**), where each was calculated by taking $\sqrt{3}$ times the standard deviation of the “sum total of actual weight of container cargo” for all containers. Occurrence probability of deviation of the “sum total of actual weight of container cargo” for all containers was calculated as shown in **Table R5-2**.

Table R5-2 Occurrence probability of deviation of the “sum total of actual weight of container cargo” in all containers

Relative difference between the total weight of laden containers and the total declared weight of containers	Occurrence probability (A) calculated from normal distribution of deviation of the “sum total of actual weight of container cargo” at each container group, estimated by taking $\sqrt{3}$ times the standard deviation	Occurrence probability (B) calculated from normal distribution of deviation of the “sum total of actual weight of container cargo” from draught measurements (Values in Table A5-3)
below -12.5%	$1.070 \times 10^{-9}\%$	$0.220 \times 10^{-13}\%$
-12.5% to below -7.5%	$0.468 \times 10^{-2}\%$	$0.058 \times 10^{-2}\%$
-7.5% to below -2.5%	13.619%	11.089%
-2.5% to below +2.5%	82.302%	86.300%
+2.5% to below +7.5%	4.073%	2.610%
+7.5% to below +12.5%	$0.029 \times 10^{-2}\%$	$0.002 \times 10^{-2}\%$
+12.5% and above	$0.109 \times 10^{-10}\%$	$0.681 \times 10^{-14}\%$

Occurrence probability (A) calculating from the normal distribution of deviation of the “sum total of actual weight of container cargo” at each container group taking standard deviation as $\sqrt{3}$ times was compared with occurrence probability (B) calculating from the normal distribution of deviation of the “sum total of actual weight of container cargo” from draught measurement by plotting **Table R5-2** in a graph as shown in **Fig. R5-1**. The comparison showed that the distributions were practically the same. This suggests that, in this investigation, it is valid to assume the standard deviation of the “sum total of actual weight of container cargo” in the containers in each container group of Fore/Mid/Aft as the standard deviation of the “sum total of actual weight of container cargo” in all containers.

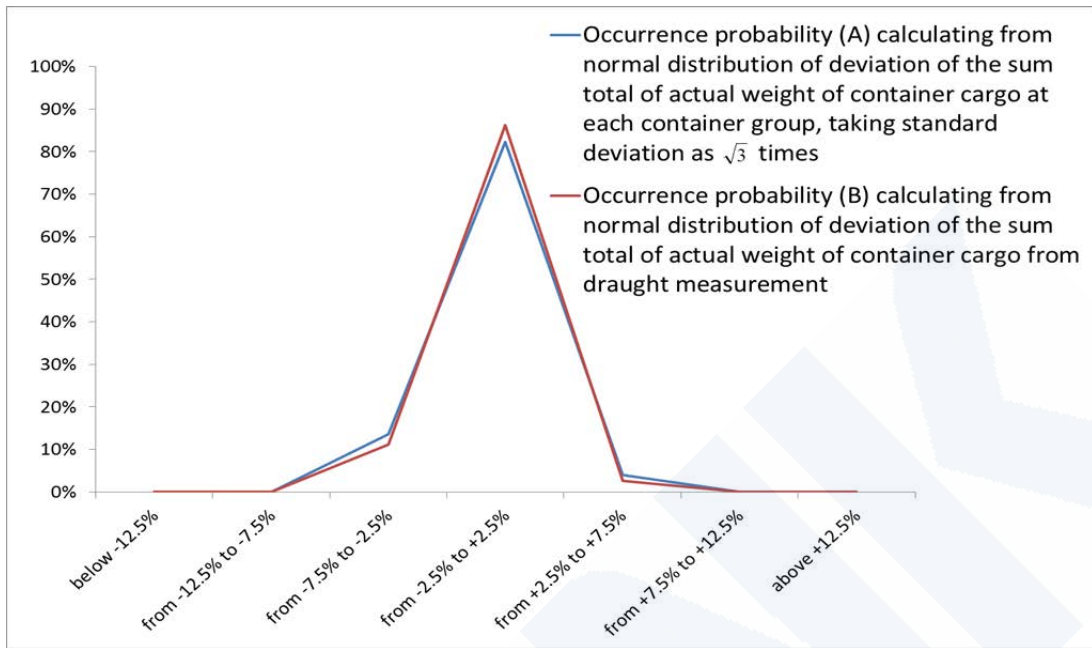


Fig. R5-1 Comparison of occurrence probability

Note that $\sqrt{3}$ is the multiplication factor assumed when the number of containers in each of the groups Fore/Mid/Aft is the same. However, the positions where the Ship is divided into Fore/Mid/Aft groups in **Fig. A5-6** are not the positions at which the number of containers in each group becomes equal. By 20-ft conversion, the actual number of containers in each group is Fore=2177TEU, Mid=3368TEU, Aft=1496TEU (total 7041TEU), and thus the number is not the same in all of the groups. For this reason, considering the number of containers in each group, the following assumptions were made to evaluate the standard deviation of each “weight of the container group” in Fore/Mid/Aft: Fore= $\sqrt{7041/2177} = \sqrt{3.234}$ times, Mid= $\sqrt{7041/3368} = \sqrt{2.091}$ times, Aft= $\sqrt{7041/1496} = \sqrt{4.707}$ times. With these assumptions, the normal distribution at which deviation occurs in Ms maximum values was determined as shown in **Fig. R5-2**.

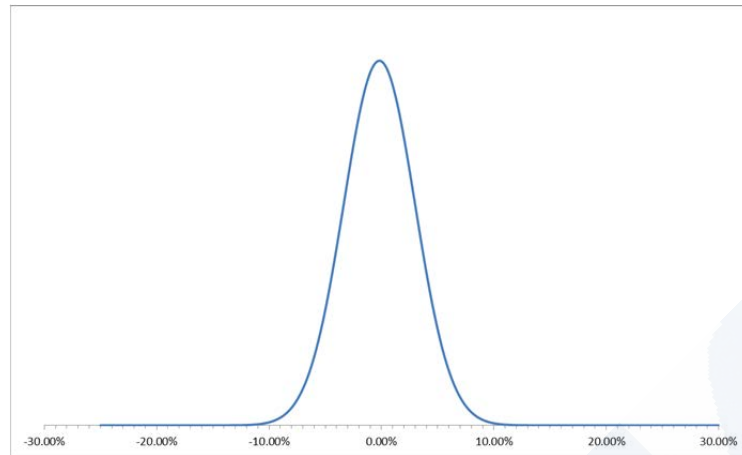


Fig. R5-2 Normal distribution at which deviation of the “Ms maximum value” occurs considering the number of containers in each container group

Comparing **Fig. R5-2** with **Fig. A5-8**, it is seen that the possibility of Ms maximum value deviating is approximately $\pm 10\%$ in both results. Accordingly, the estimation of the occurrence possibility of deviation of Ms maximum value by the deviation of the weight of the container cargo in this section was found to give the same result as the estimation obtained by correcting the standard deviation using $\sqrt{3}$ times and simply assuming that each group has the same number of containers. Therefore, it can be concluded that the use of $\sqrt{3}$ times in the estimation method in the investigation is valid.

-----End of Technical Background-----

Appendix 6 Estimation of Probability Distribution of Strength and Loads (related to 3.4 of this Report)

This appendix describes the ways how to estimate the probability distribution of the strength and of the loads stated in 3.4 of this Report.

1. Estimation of Probability Distribution of Strength

The probability distribution of the strength (Hull girder ultimate strength) is presumed to be a normal distribution. Given that the data for estimating probability distribution were limited, the mean value and the lower limit of strength were estimated first and then the deviation of the strength was estimated based on the mean value and the lower limit estimated in this Report.

1.1 Estimation of Mean Value of Strength

As mentioned in 3.3.1 of this Report, the mean value of the hull girder ultimate strength of the Ship was estimated in the following ways.

The average value of the yield stress was estimated by averaging the yield stress values in the mill sheets of the bottom shell plates in the transverse section of the Ship where it was concluded that the fracture had been originated.

A 3-hold model elasto-plastic analysis was carried out by using the above mean yield stress (for the bottom shell plates) and the result of the analysis was considered to be the mean value of the hull girder ultimate strength of the Ship. The values of the mean yield stress of other structural members for the analysis were estimated with the assumption that they kept the same relationship of proportion as that of the bottom shell plates between the specified minimum yield stress, the general average value of yield stress and the yield stress used in the analysis. (Refer to **Appendix 8** on the general average value of yield stress.) In the estimation of the mean value of the hull girder strength, the effect of the local deformation of the bottom shell plates and the effect of welding residual stress of the bottom longitudinals were not considered.

1.2 Estimation of Lower Limit of Strength

The minimum yield stress was estimated according to the following two ways, which was used for the 3-hold model elasto-plastic analysis in order to estimate the minimum hull girder ultimate strength.

Case 1 : Way based on the mill sheet values of the bottom shell plates of the Ship

In the process of calculating the mean strength, the average in the mill sheet values of the bottom shell plates where it was concluded the fracture had originated was defined as the average yield stress as mentioned in 1.1 of this appendix. Although it can be considered that the deviation of the yield stress of the bottom shell plates was considerably limited, there still exists some deviation

between the mill sheet values and the actual values of yield strength because the tensile tests were not conducted on individual steel plates to issue a mill sheet.

Furthermore as noted in 1.1 of this appendix, the yield stress values of other structural members were not checked against the corresponding mill sheet values, which means the deviation of the yield stress is also to be considered on other structural members. Considering these deviations as mentioned above, the minimum yield stress was estimated in the following manner.

First, the standard deviation (σ) of the mill sheet values of the bottom shell plates of the Ship was calculated. Next, the value lower by three times the standard deviation (3σ) than the average steel yield stress of the mill sheets of the bottom shell plates was presumed to be the minimum yield stress value. It can be said that the presumed minimum yield stress is the realistic minimum value in the deviation of the yield stress, in other words any value below the presumed minimum yield stress would occur at an approximate probability of 1/1000 or less.

Case 2 : Way to use specified minimum yield stress

The specified minimum yield stress was used as the minimum yield stress for the 3-hold elasto-plastic analysis.

With the use of the minimum yield stress values estimated in the above two cases, 3-hold model elasto-plastic analyses were conducted to calculate the minimum hull girder ultimate strength corresponding to the minimum yield stress respectively. As mentioned in 3.3.1 of this Report, the deviation of the yield strength of Case 1 was estimated smaller than that of Case 2.

The lower limit of hull girder ultimate strength was determined by multiplying the minimum hull girder ultimate strength obtained through the above by following two coefficients;

- (1) Lower limit of the coefficient of the effect of local deformations of the bottom shell plates (0.96)
- (2) Lower limit of the coefficient of the effect of welding residual stress of bottom longitudinals (0.95)

Table 3-1 in 3.3.1 of this Report shows the individual value of the hull girder ultimate strength estimated in the above ways.

1.3 Estimation of Deviation of Strength (Standard Deviation in Normal Distribution)

On the assumption that the difference between the mean value and the minimum value of the hull girder ultimate strength estimated in 1.1 and 1.2 of this appendix corresponded to three times the standard deviation (3σ) in normal distribution, the form of the normal distribution was estimated. It means that the probability of the hull girder ultimate strength being less than the minimum value is approximately 1/1000, which can be considered

sufficiently small, i.e. the probability is nearly equal to zero.

2. Estimation of Probability Distribution of Load

The vertical bending moment acting on the hull girder is the total sum of the wave-induced vertical bending moment and the still water vertical bending moment. The probability distribution of the wave-induced vertical bending moment was presumed to follow the Gumbel distribution as stated in 3.4 of this Report, which is one of the extreme-value distributions and is used to model the distribution of maximums of various distributions. The cases where the probability distribution of the wave-induced vertical bending moment is presumed to follow the normal distribution are also shown in this appendix for reference. The probability distribution of the still water vertical bending moment was presumed to follow the normal distribution according to the outcome of **Appendix 5**.

Given that the data for the estimation of the probability distribution of the loads were limited as well as the case of the strength, first the mean value and the upper limit of the wave-induced vertical bending moment and the still water vertical bending moment was estimated individually and next the deviation of each moment was estimated by using the mean value and the upper limit.

2.1 Probability Distribution of Wave-Induced Vertical Bending Moment

【Case to follow the Gumbel distribution】

The mode of the Gumbel distribution for the wave-induced vertical bending moment was presumed to be 3.4×10^6 kN-m, which was the simulation result (the maximum expected value) at the sea state of significant wave height of 5.5 m, mean wave period of 10.3 seconds and encountered wave direction of 114 degrees, estimated as the sea state at the time of accident in JG Interim Report. The form of the Gumbel distribution was determined so that the maximum simulation result among 27 cases described in **Appendix 4** (7.23×10^6 kN-m) would be practically the upper limit of the distribution.

【Case to follow the normal distribution】

The mean value of the normal distribution for the wave-induced vertical bending moment was presumed to be 4.45×10^6 kN-m, which was the simulation result at the sea state of the significant wave height of 6.5 meters, mean wave period of 12.5 seconds and the wave direction of 150 degrees, the middle sea state among 27 cases described in **Appendix 4**.

The standard deviation of the normal distribution was set to be 0.927×10^6 kN-m so that the difference between the maximum simulation result among 27 cases (7.23×10^6 kN-m) and the mean value of the distribution (4.45×10^6 kN-m) would be three times the standard deviation.

It also can be said that the simulation maximum result among 27 cases would be practically the upper limit of the distribution.

2.2 Probability Distribution of Still Water Vertical Bending Moment

According to the outcome of **Appendix 5**, it was presumed that the probability distribution would follow the normal distribution and the mean value was presumed to be 6.0×10^6 kN-m, the still water vertical bending moment at the time of accident stated in JG Interim Report. 10% of the mean value, which was considered to be maximum deviation of the still water vertical bending moment according to **Appendix 5**, was presumed to be three times the standard deviation of the estimated normal distribution of the still water vertical bending moment so that it could give the upper and lower limit of the deviation practically.

2.3 Probability Distribution of Total Vertical Bending Moment (Total sum of wave-included vertical bending moment and still water vertical bending moment)

The coefficient of variation, i.e. the value of dividing the standard deviation by the mean, of the simulation results of wave-induced vertical bending moment of 27 sea state cases as shown in **Appendix 4** was estimated to be 28%. Meanwhile **Appendix 5** estimated the probability that the distribution between the still water bending moment calculated based on declared container weights and the actual still water bending moment existed within $\pm 10\%$ of the mean value was approximately 99.8%, which means the coefficient of variation is around 3%.

According to the above it can be said that the deviation of the wave-induced vertical bending moment is much larger than that of the still water vertical bending moment. Therefore the probability distribution of the total vertical bending moment, the total sum of the wave-induced vertical bending moment and the still water bending moment, was presumed to follow the distribution of the wave-induced vertical bending moment. It is evident that in the case where the two vertical bending moments follow the normal distribution, the sum of the two vertical bending moments also follows the normal distribution according to the reproductive property of the normal distribution.

In the case of the probability distribution of the wave-induced vertical bending moment being the Gumbel distribution, the total vertical bending moment, i.e. total sum of the wave-induced vertical moment and the still water vertical bending moment, was presumed to follow the Gumbel distribution. The mode of the total vertical bending moment in the Gumbel distribution was presumed to be 9.4×10^6 kN-m, which was the sum of the mode of the wave-induced vertical bending moment (the Gumbel distribution) of 3.4×10^6 kN-m and the mean value of the still water vertical bending moment (the normal distribution) of 6.0×10^6 kN-m. The upper limit of the total vertical bending moment (the Gumbel distribution) was presumed to be 13.83×10^6 kN-m, which was the sum of the upper limit of the wave-induced vertical bending moment (7.23×10^6 kN-m) and the upper limit of the still water vertical bending moment ($6.0 \times 1.1 = 6.6 \times 10^6$ kN-m).

In the case where the probability distribution of the wave-induced vertical bending moment was presumed to follow the normal distribution, the total vertical bending moment, combining the two different moments, was considered to follow the normal distribution in accordance with the reproductive property of the normal distribution because the still water vertical bending moment was also presumed to follow the normal distribution.

In this case the mean value of the total vertical bending moment was defined to be the sum of the mean values of the wave-induced vertical bending moment and the still water vertical bending moment, and the variance, i.e. the square of the standard deviation, of the total vertical bending moment was defined to be the sum of the variances of the two vertical bending moment.

3. Relationship between Probability Distribution of Strength and that of Load

The relationship between the estimated probability distributions of the strength (hull girder ultimate strength) and the load (wave-induced vertical bending moment and still water vertical bending moment) was shown in from **Fig. A6-1** to **Fig. A6-4**. The probability distributions shown in from **Fig. A6-1** to **Fig. A6-4** are explained in the following table. **Fig. A6-1** is identical with **Fig. 3-1** in 3.4 of this Report.

Fig.	Case	Probability distribution of Strength	Probability distribution of load
A6-1	A	<p><i>Normal distribution</i> Distribution was estimated in the way of Case 1 explained in 1.2 of this appendix, based on the mill sheet values of the bottom shell plates of the Ship</p>	<p><i>Gumbel distribution</i> for the wave-induced vertical bending moment, <i>Normal distribution</i> for the still water vertical bending moment</p>
A6-2	B		<p><i>Normal distribution</i> for both the wave-induced vertical bending moment and the still water vertical bending moment</p>
A6-3	C	<p><i>Normal distribution</i> Distribution was estimated in the way of Case 2 explained in 1.2 of this appendix, with the specified minimum yield stress defined as minimum yield stress.</p>	<p>Same as Case A</p>
A6-4	D		<p>Same as Case B</p>

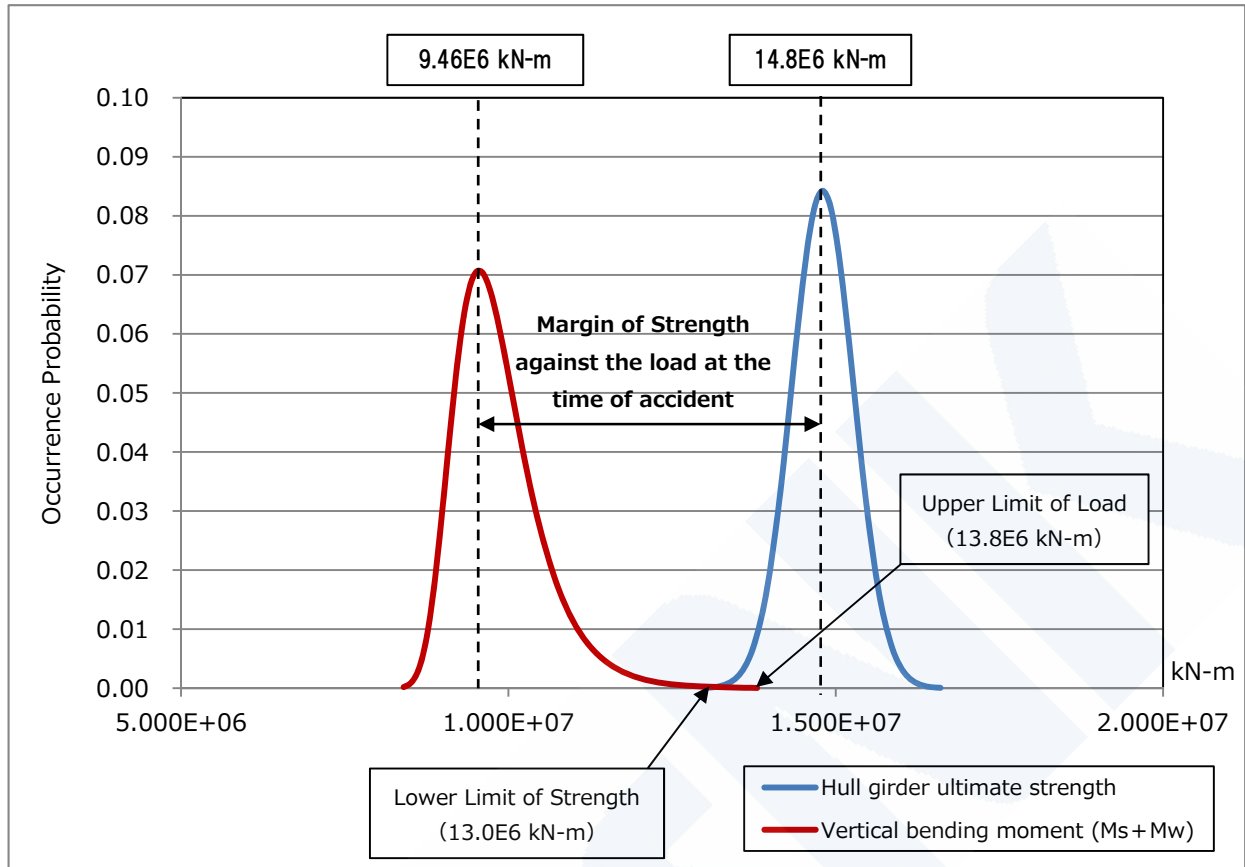


Fig. A6-1 Relationship between strength and load at the time of the accident (Case A)

Probability distribution of the strength : Normal distribution

(deviation estimated from the distribution of the mill sheet values of the Ship)

Wave-induced vertical bending moment : Gumbel distribution

Still water vertical bending moment : Normal distribution

(The vertical axis represents the occurrence probability

corresponding to the band of 1×10^5 kN-m of the strength and the load respectively.)

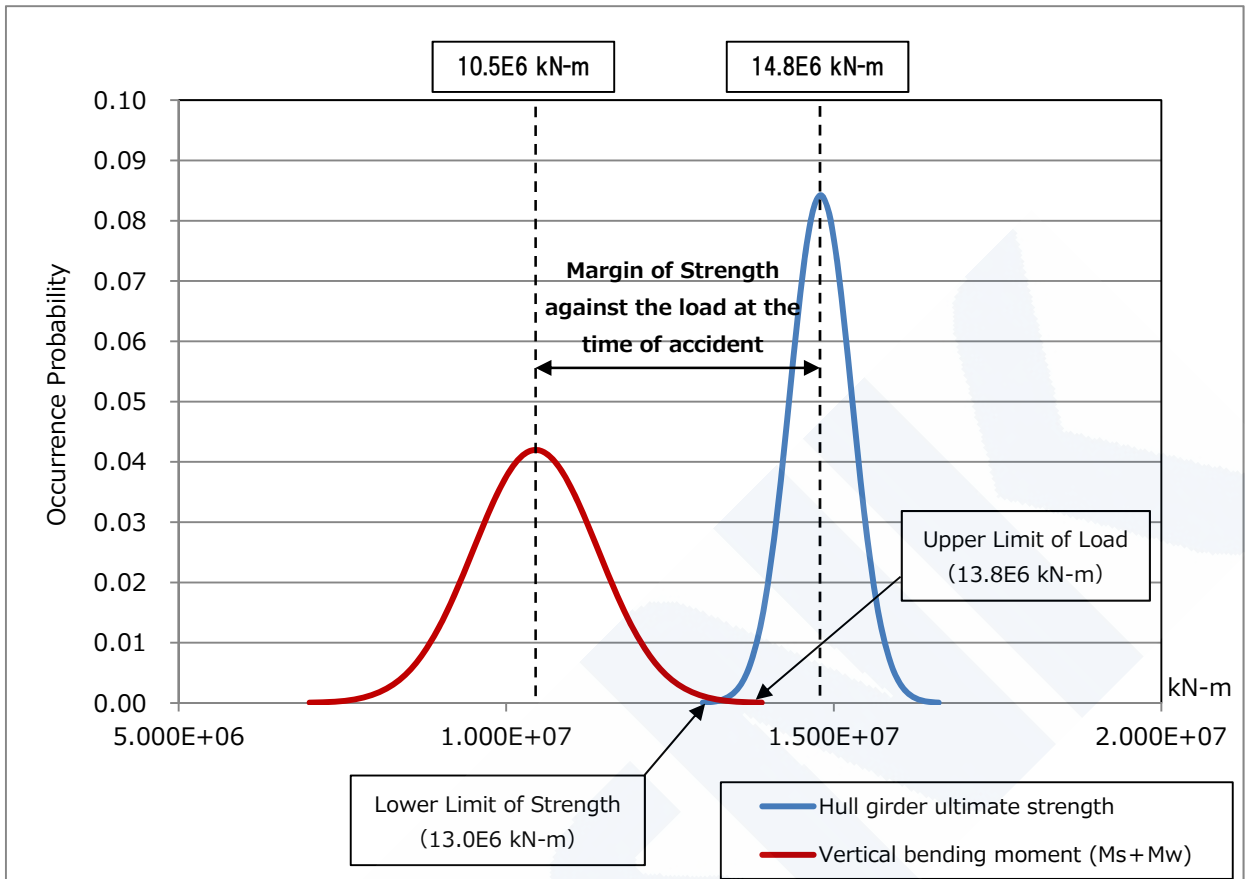


Fig. A6-2 Relationship between strength and load at the time of the accident (Case B)

Probability distribution of the strength : Normal distribution

(deviation estimated from the distribution of the mill sheet values of the Ship)

Wave-induced vertical bending moment : Normal distribution

Still water vertical bending moment : Normal distribution

(The vertical axis represents the occurrence probability

corresponding to the band of 1×10^5 kN-m of the strength and the load respectively.)

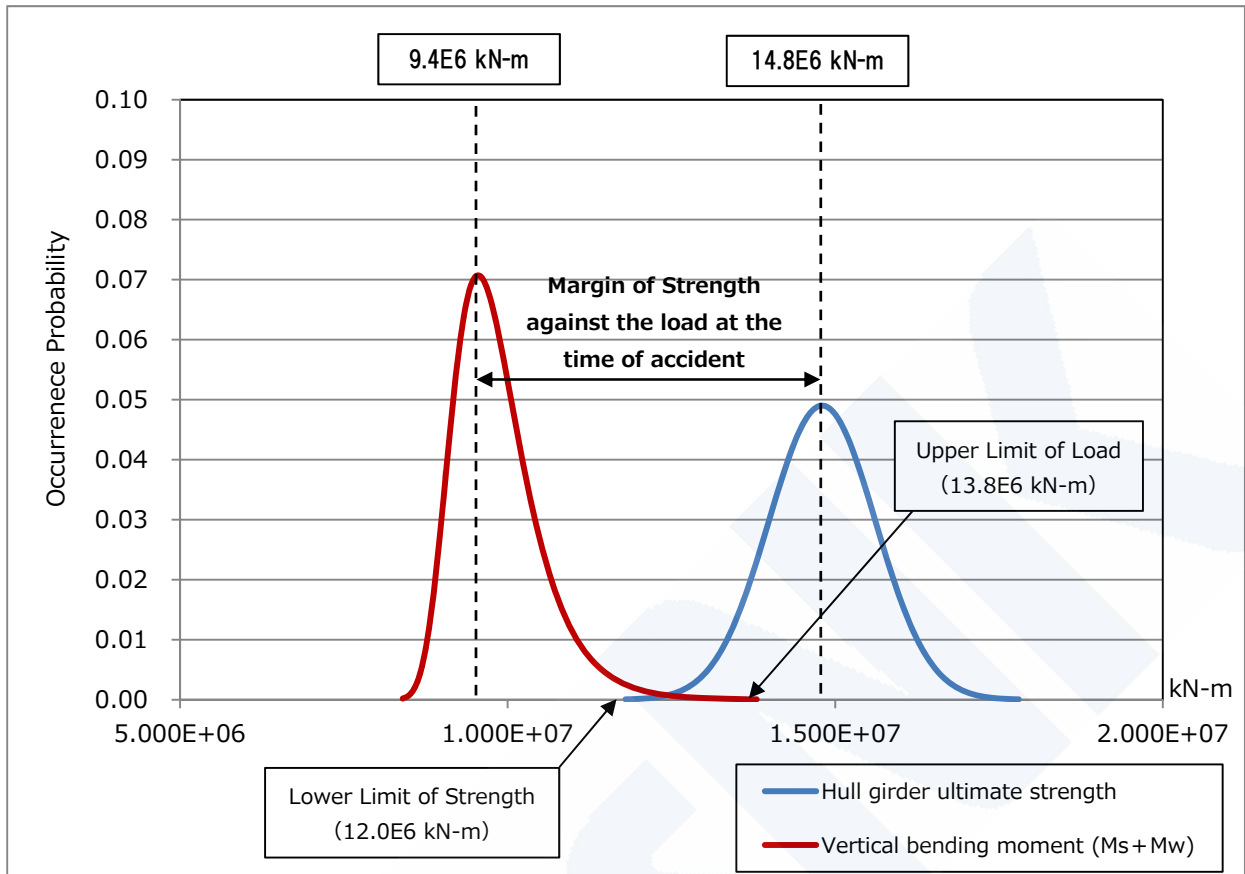


Fig. A6-3 Relationship between strength and load at the time of the accident (Case C)

Probability distribution of the strength : Normal distribution

(lower limit of strength estimated from the required minimum yield stress)

Wave-induced vertical bending moment : Gumbel distribution

Still water vertical bending moment : Normal distribution

(The vertical axis represents the occurrence probability corresponding to the band of 1×10^5 kN-m of the strength and the load respectively.)

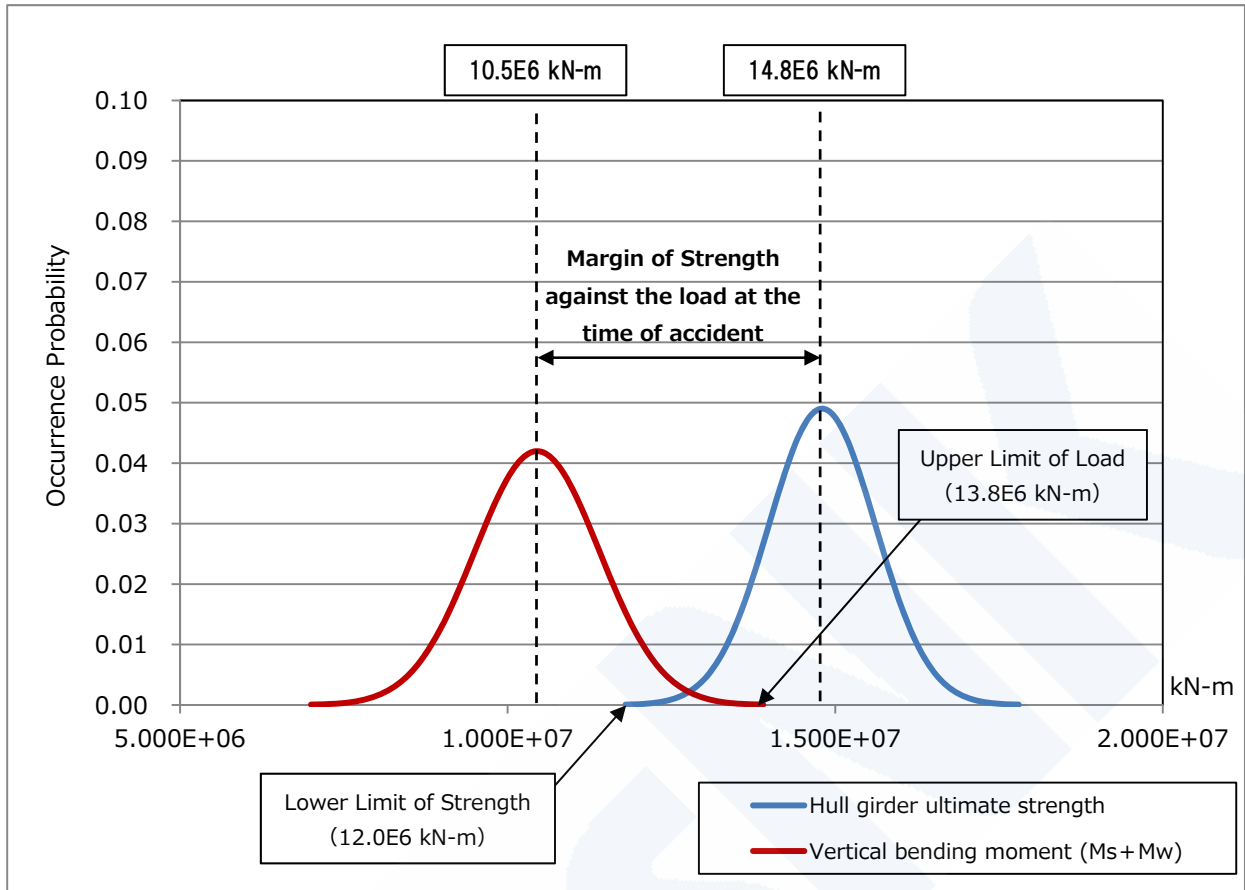


Fig. A6-4 Relationship between strength and load at the time of the accident (Case C)

Probability distribution of the strength : Normal distribution

(lower limit of strength estimated from the required minimum yield stress)

Wave-induced vertical bending moment : Nominal distribution

Still water vertical bending moment : Normal distribution

(The vertical axis represents the occurrence probability corresponding to the band of 1×10^5 kN-m of the strength and the load respectively.)

Appendix 7 Stresses of Transverse Strength Occurring in Double Bottom Structure of Post-Panamax Container Ships (related to 4.2.3 of this Report)

Post-Panamax container ships have improved their stability and have gained more cargo loading flexibility in complying with the stability requirements. For this reason, various loading conditions that could not be carried out in Panamax container ships are possible in Post-Panamax container ships, such as the loading of light containers in weight in the cargo holds. On the other hand, ship-breadth of Post-Panamax container ships becomes large and the lateral load by upward load from bottom sea pressure becomes relatively increased, meanwhile, container weight even under the normal loading condition is not so heavier than the lateral load to balance out. Therefore, the stress occurring to the double bottom structure tends to be higher, when light containers in weight are loaded in the cargo holds.

In such various loading conditions, the stresses occurring in the bottom shell plates were calculated when light containers in weight are loaded in the cargo hold, and the possibilities were investigated whether such stresses could be similar to those under One-bay empty condition. One-bay empty condition is used for the structural design of the container ships with the assumptions that one of the bays of the hold is not loaded with containers in the hold and on the hatch cover and that the other bays of the hold and adjacent holds are loaded with containers including those on the hatch covers.

Various kinds of container loading arrangements can be planned in the actual operation of Post-Panamax container ships. Therefore, the investigation was carried out with the assumption that the containers are loaded in the holds and on the hatch covers homogeneously and calculating a number of container loading cases with changing the container weights. Various container loads were assumed for this investigation up to the maximum design load, with seven (7) container load scenarios in the holds and three (3) container load scenarios on the hatch covers, and the total of twenty one (21) combined loading conditions were simulated as shown in **Table A7-1**.

Table A7-1 Loading conditions used in the examination

	One-bay empty condition (One-bay of the hold is empty and other bays are loaded.)	Loading condition studied (All bays are loaded.)
Container load in hold	30.0 Ton/FEU (Design load)	0 to 30.0 Ton/FEU (Total 7 scenarios at 5-ton interval)
Container load on hatch cover	130.0 Ton/Stack (Design load for 40 feet container loading)	- Design load (130 Ton/Stack) - 2/3 Design load (87 Ton/Stack) - 1/3 Design load (43 Ton/Stack) (Total 3 scenarios)

The result of the investigation is shown in **Fig. A7-1**. Container loads in the hold are displayed along the horizontal axis, and the transverse stress occurred in the bottom shell plates displayed along the vertical axis. Then, maximum value of the transverse stresses for each loading condition is plotted on the graph and connected by the three lines for each container load scenario on the hatch cover e.g. Design load, 2/3 Design load and 1/3 Design load. For comparison, the maximum value of transverse stress occurred in the bottom shell plates under One-bay empty condition is about between 85 and 90 N/mm² and represented by the red belt in **Fig. A7-1**.

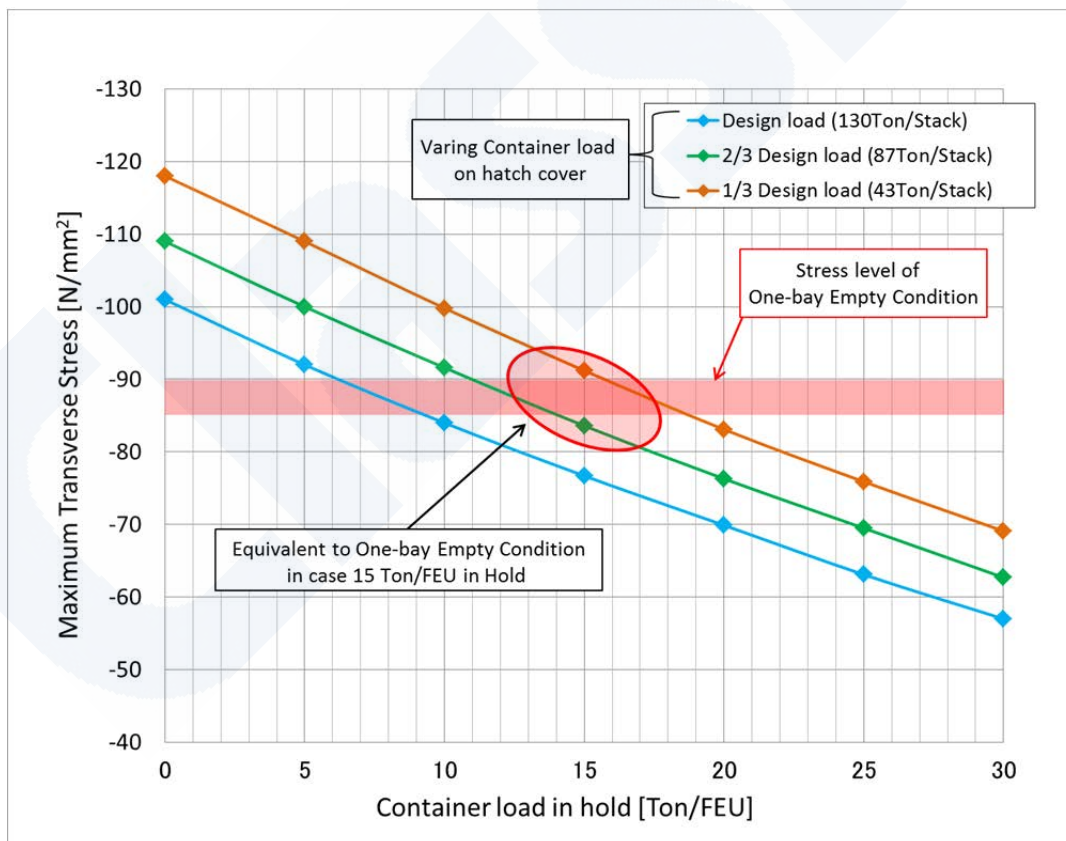


Fig. A7-1 Comparison of transverse stresses at the bottom shell plates for each loading condition

This figure shows that the transverse stress levels equal to those under One-bay empty condition where the lines cross the red belt area.

For instance, when the container loads on the hatch cover are between 1/3 Design load and 2/3 Design load and the container loads in the hold are about 15 Ton/FEU, the transverse stress is equal to the stress level under One-bay empty condition.

As a result, for Post-Panamax container ships which have gained more cargo loading flexibility, it was verified that there may exist a certain possibility of the occurrence of the transverse stress in the bottom shell plates being equal to the stress level found in One-bay empty condition, even in the simulated loading conditions close to the normal loading conditions in the actual operation.

Appendix 8 3-Hold Model Elasto-Plastic Analysis (Investigation of the Hull Girder Ultimate Strength for Target Ships including the Ship) (related to 4.2.3 of this Report)

As stated in 4.2.3 of this Report, 3-hold model elasto-plastic analyses were conducted taking into account the lateral loads on the target ships including the Ship in order to estimate the hull girder ultimate strength, and the strength margin was investigated.

The outline of the 3-hold model elasto-plastic analyses stated in 4.2.3 of this Report is explained hereinafter.

1. Target Ships

3-hold model elasto-plastic analyses were conducted on the target ships (five 8,000TEU class container ships and two 6,000TEU class container ships) as stated in 4.1 of this Report. The target ships except the Ship have sufficient service records on the hull structure safety.

2. Outline of Analysis Condition

Table A8-1 shows the analysis conditions for the 3-hold model elasto-plastic analyses stated in 4.2.3 of this Report.

Table A8-1 Analysis conditions for 3-hold model elasto-plastic analysis in 4.2.3 of this Report

Analysis program		LS-DYNA (explicit method)
Extent of model		<ul style="list-style-type: none"> Longitudinal direction : 1/2 + 1 + 1/2 holds Transverse direction : Half breadth
Condition of initial shape deformation		No initial shape deformation was given.
Thickness		Gross thickness
Boundary condition		<ul style="list-style-type: none"> Simply supported at fore end and aft end of the model Symmetrical condition at the center line in transverse direction
Load condition	Container load and ballasting condition	One-bay empty condition without ballast in double bottom (Target bay of the analysis was empty.)
	Hull weight	Hull weight of the whole model was considered.
	Sea pressure	<ul style="list-style-type: none"> Hydrostatic pressure corresponding to the full draught Wave-induced pressure specified in ClassNK Guidelines ^(Note)
	Vertical bending moment	Gradually increased until the hull girder was fractured in the model, i.e. the hull girder ultimate strength

Note : Guidelines for Container Carrier Strength (Guidelines for Direct Strength Analysis) in 2012

Some conditions for the analysis shown in **Table A8-1** were different from those of the 3-hold model elasto-plastic analysis of the Ship stated in **Appendix 2** carried out for investigation on the possibility of the occurrence of the accident due to the reason mentioned below.

The main purpose of 3-hold elasto-plastic analyses of 4.2.3 in this Report is relative comparison of margin of the hull girder ultimate strength in the target ships. Therefore the conditions of initial shape deformation and boundary condition were chosen so that their effects could be made minimized in the analysis results for the comparison.

Relating to the container load and ballasting condition, One-bay empty condition without ballast in double bottom was chosen due to following reasons as also explained in 4.2.3 of this Report.

First reason is that One-bay empty condition without ballast in double bottom is one of the most severe loading conditions for the strength of double bottom structure and it was expected to be effective to compare the strength margin of the target ships. Second reason is that it sometimes happens that the stress of the transverse strength of double bottom structure in the normal loading conditions becomes nearly equal to the stress corresponding to the One-bay empty condition without ballast in double bottom in the case of Post-Panamax container ships, since various loading conditions are available for Post-Panamax container ships, as detailed in 4.4 and **Appendix 7**.

The 3-hold elasto-plastic analyses in this Report were conducted by LS-DYNA (explicit method) where the period of applying total loads was around 5 seconds. Therefore it is considered that the analyses in this Report were carried out in the quasi-static condition. It is expected that quasi-static analyses give safer results in general because applied loads are certainly transmitted inside the structures.

2.1 Analysis Model

Fig. A8-1 and **Fig. A8-2** show the models for the 3-hold model elasto-plastic analyses. In general, they have the same specifications as the analysis model used for the investigation of the possibility of the occurrence of the accident of the Ship described in **Appendix 2**.

The part of the half breadth of $1/2 + 1 + 1/2$ holds was modeled and a bay in the middle hold where a butt joint existed was taken as the target bay for the analysis. In the case where a butt joint existed in both bays, i.e. the fore bay and the aft bay, the bay subjected to higher double bottom local stress was chosen as the target bay for the analysis.

The plates and frames including bottom longitudinals in the target bay were modeled with shell elements of around 100 mm x 100 mm in size, i.e. fine mesh elements, in the overall breadth in transverse direction, and between the base line and the neutral axis of the transverse section in vertical direction. Scallop openings in the bottom longitudinal webs for butt joint penetration were also modeled. The remaining part was modeled with shell elements of around 200 mm x 200 mm in size.

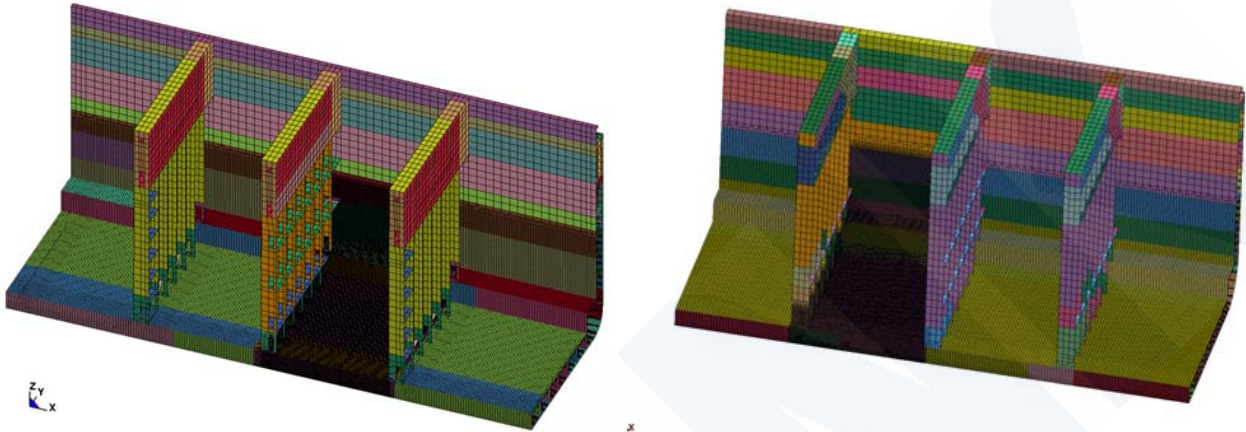


Fig. A8-1 Overview of hold model

Left : In the case where the fore bay in the middle hold is the target bay for the analysis

Right : In the case where the aft bay in the middle hold is the target bay for the analysis

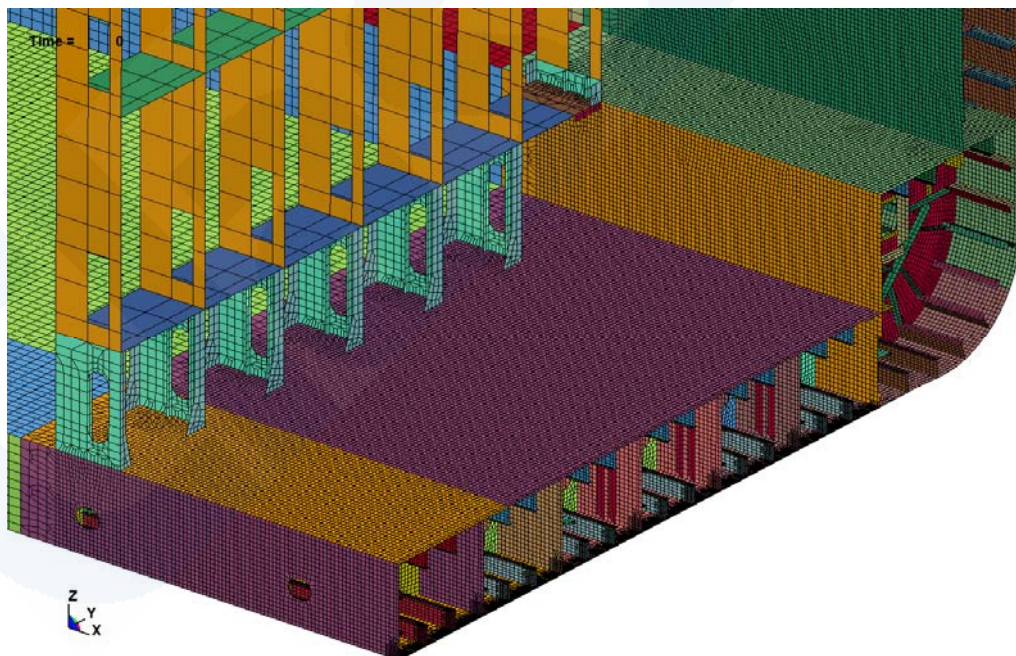


Fig. A8-2 Target bay for analysis with fine mesh elements in FE model

2.2 Material Property of Steel

Table A8-2 shows the material properties of steel for the analyses. The general average value used in JG Interim Report was also used as the yield stress, which means an expected value of the yield stress of actual steel plates in the sense of the general and the average, not the specified minimum yield stress. **Table A8-3** shows the general average values of the yield stress applied to the analyses in 4.2.3 of this Report.

Elastic-perfect plasticity taking into account linear hardening was given as the condition of the relationship between stress and strain as same as **Appendix 2. Fig. A8-3** illustrates the relationship between true stress and true strain.

Table A8-2 Material properties of steel

Young's modulus	206,000 N/mm ²
Poisson's ratio	0.3
Mass density	7.85 ton/m ³
Yield stress (General average value)	See Table A8-3 .
True stress and true strain curve	Elastic-perfect plasticity taking into account linear hardening (see Fig. A8-3 .)

Table A8-3 Yield stress (General average value)

Steel	Yield stress (N/mm ²)
MS	292
YP32	380
YP36	410
YP40	430
YP47	510

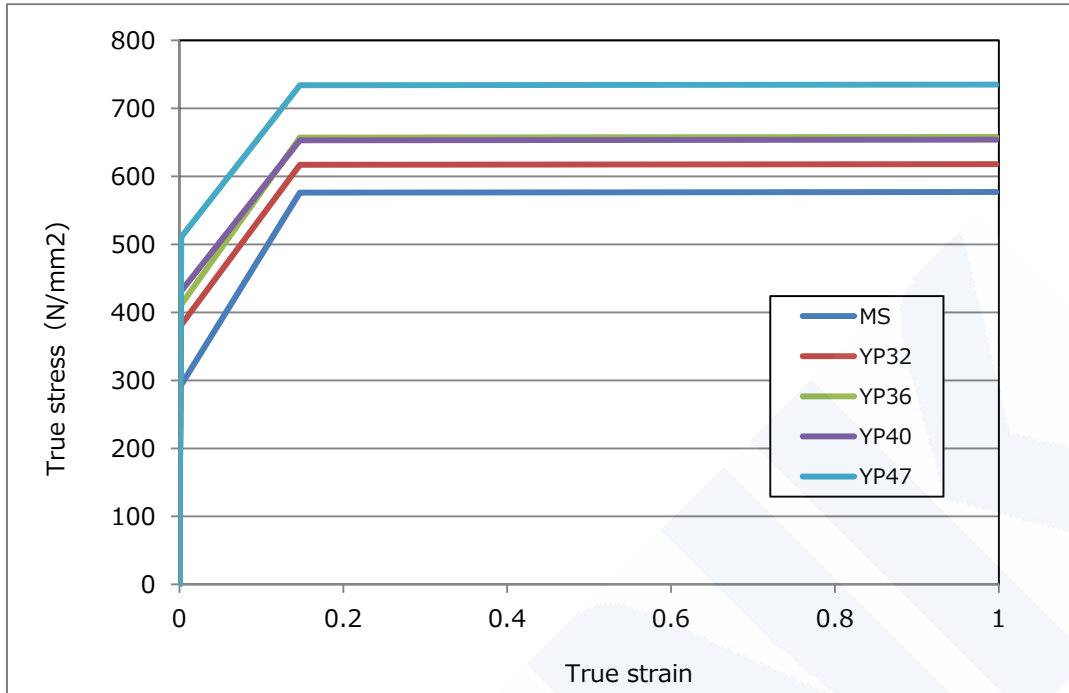


Fig. A8-3 Relationship between stress and strain (True stress and true strain curve)

Comparative investigations were conducted in 4.2.3 of this Report regarding the hull girder ultimate strength corresponding to the specified minimum yield stress. Meanwhile 3-hold model elasto-plastic analyses were conducted with the general average values of the yield stress. The hull girder ultimate strength corresponding to the specified minimum yield stress for the investigations was estimated by the following formula expression,

$$M_{U,minimum \sigma_y} = \alpha \times M_{U,average \sigma_y}$$

where :

$M_{U,minimum \sigma_y}$: Hull girder ultimate strength corresponding to the specified minimum yield stress

$M_{U,average \sigma_y}$: Hull girder ultimate strength corresponding to the general average values of the yield stress

α : Ratio of the specified minimum yield stress to the general average value of the yield stress of the bottom shell plates

The above way for the estimation of the hull girder ultimate strength corresponding to the specified minimum yield stress was confirmed by comparing the results of the 3-hold model elasto-plastic analyses in both cases where the yield stress for the analysis was the general average value and the yield stress for the analysis was the specified minimum yield stress on some of the target ships.

2.3 Boundary Condition

Both ends, i.e. fore end and aft end, of the FE model were simply supported in vertical direction, and symmetry condition in transverse direction was applied at the center line. With regard to the center girder, the symmetrical condition was applied only on the intersections with floors, bottom shell plates and inner bottom plates in order to make buckling behavior possible for the center girder.

The schematic of the boundary condition is shown in **Fig. A8-4** and **Fig. A8-5**, where the following symbols are used.

- u : displacement in longitudinal direction
- v : displacement in transverse direction
- w : displacement in vertical direction
- θ_x : rotation around the longitudinal axis (X axis)
- θ_y : rotation around the transverse axis (Y axis)

The aft end and the fore end of the model were linked with a rigid body respectively and the boundary condition of “ $u, v, w, \theta_x, \theta_z = 0$ ” was applied to the aft end and the condition of “ $v, w, \theta_x, \theta_z = 0$ ” was applied to the fore end.

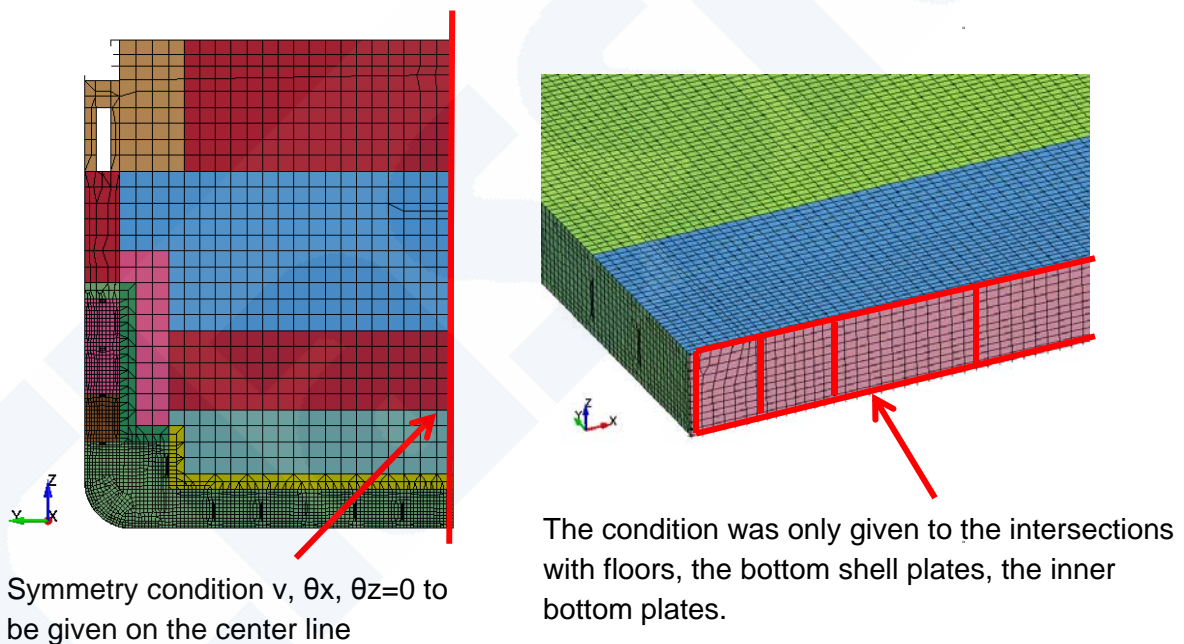


Fig. A8-4 Symmetrical condition at the center Line

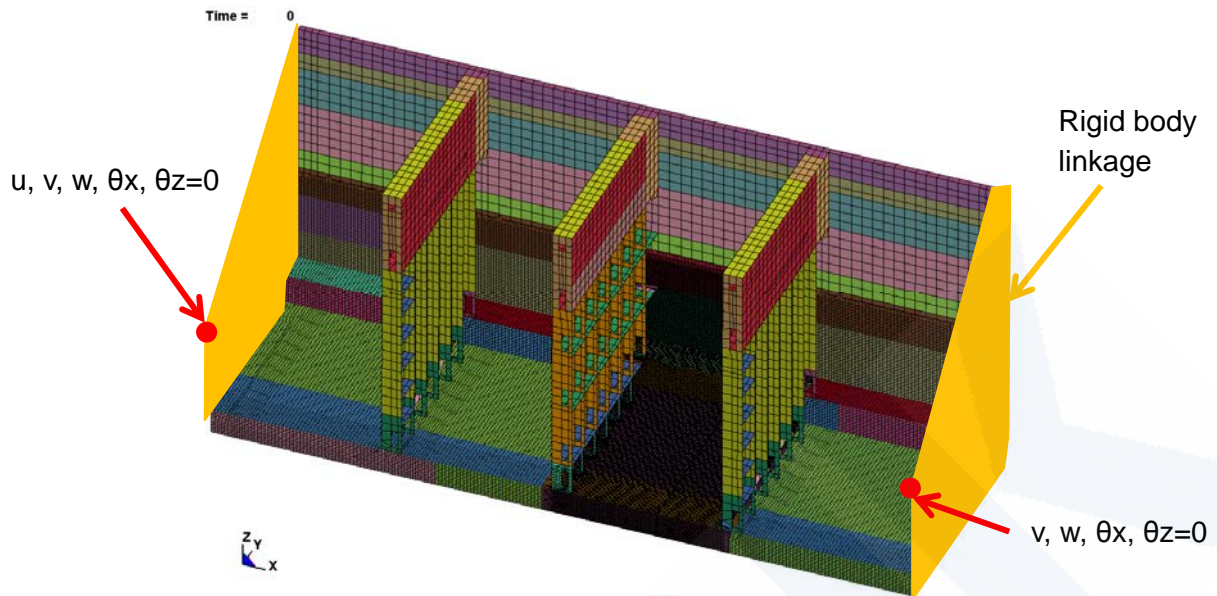


Fig. A8-5 Linkage of rigid body and boundary conditions at the ends of the model

2.4 Load Condition

The following loads were applied to the FE model in sequence.

- A) Container loads in One-bay empty condition without ballast in double bottom (Note)
- B) Hull weight corresponding to the whole model
- C) Hydrostatic pressure corresponding to the full draught
- D) Wave-induced pressure specified in Guidelines for Container Carrier Strength (Direct Strength Analysis) in 2012
- E) Allowable still water vertical bending moment (Hogging)
- F) Wave-induced vertical bending moment specified in IACS UR S11 (Hogging)
- G) Additional vertical bending moment (Hogging)

Note : One-bay empty condition was given in accordance with Guidelines for Container Carrier Strength (Direct Strength Analysis) in 2012. The target bay was empty.

First, A), B) and C) were applied being gradually increased up to the specified value in one second. Next, E), D) and F) were applied to the FE model in turn in one second respectively. Finally, G) was applied being gradually increased until reached the hull girder ultimate strength. (See Fig. A8-6, Fig. A8-7 and Fig. A8-8.)

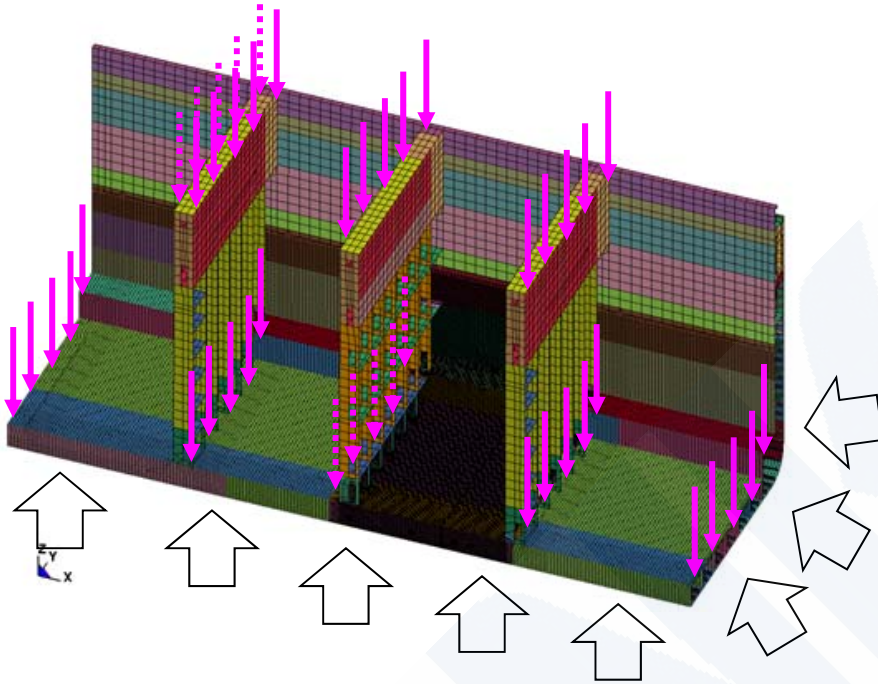


Fig. A8-6 Schematic of hydrostatic pressure, wave-induced pressure and container load

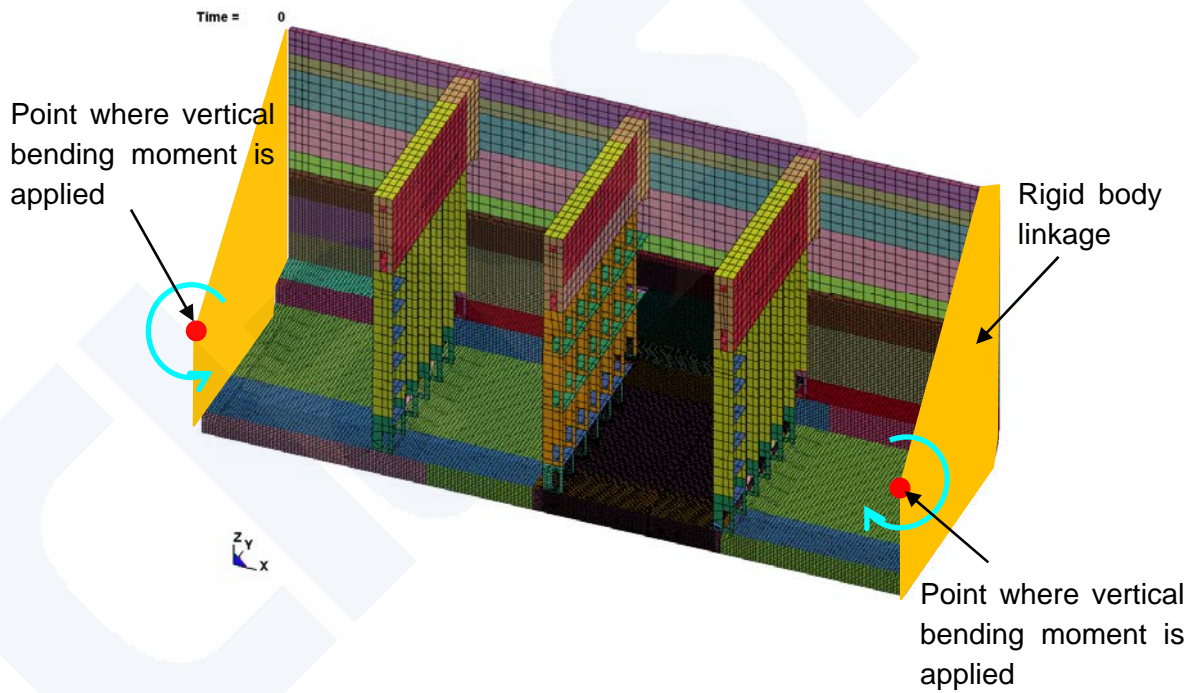


Fig. A8-7 Schematic of applying vertical bending moment

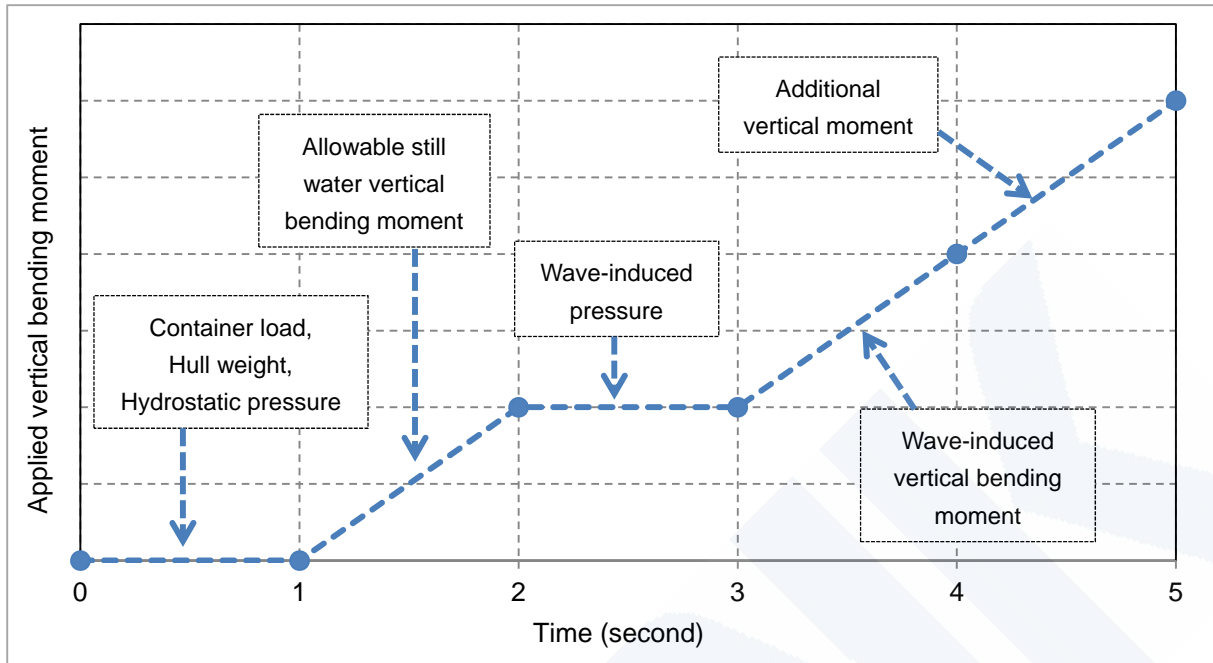


Fig. A8-8 Sequence of application of the load

2.5 Analysis Result

Fig. A8-9 shows an example of the history of vertical bending moment in the section where the hull girder was fractured. The peak value in the history curve was considered to be the hull girder ultimate strength.

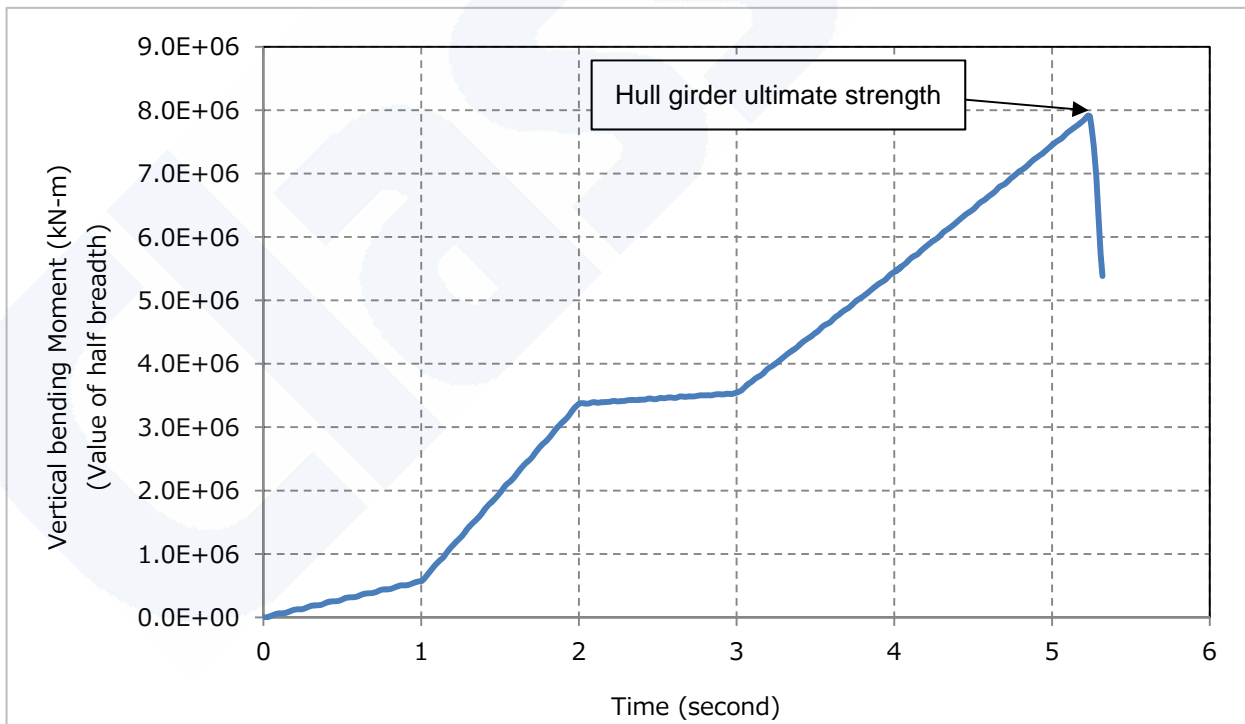


Fig. A8-9 Example of history of vertical bending moment in the section where hull girder was fractured

Figures from **A8-10** to **A8-13** show examples of the results of 3-hold elasto-plastic analyses, which illustrate Mises' equivalent stress and equivalent plastic strain at the time of the peak load, i.e. the hull girder ultimate strength.

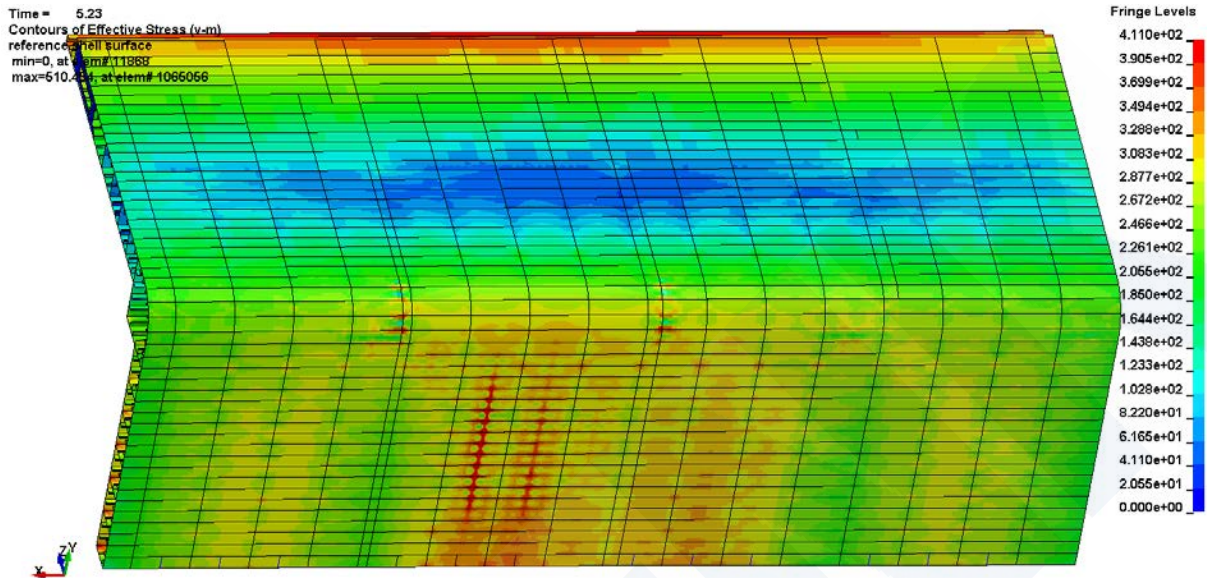


Fig. A8-10 Mises' equivalent stress at the time of the peak load, i.e. hull girder ultimate strength
(View of looking up at the bottom shell plates)

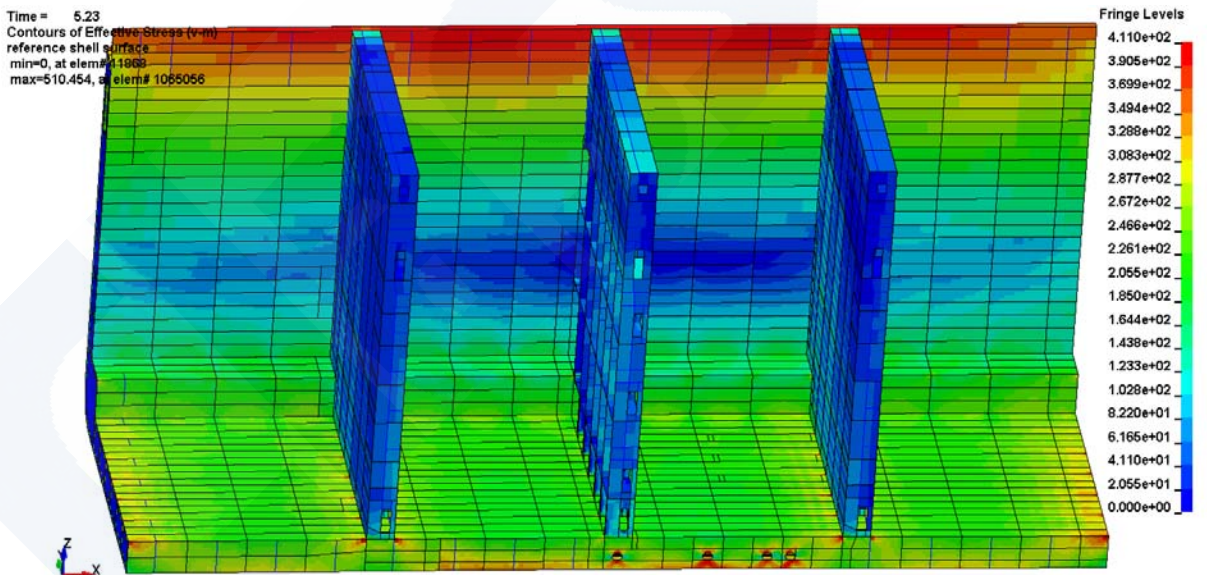


Fig. A8-11 Mises' equivalent stress at the time of the peak load, i.e. hull girder ultimate strength
(View of looking down at the inner bottom plates)

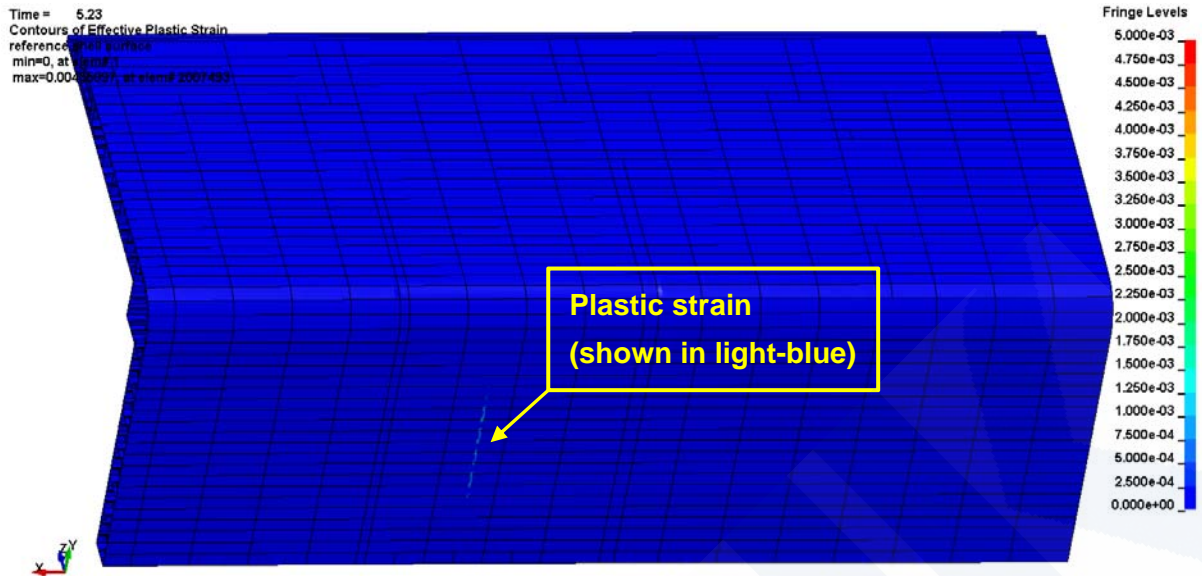


Fig. A8-12 Equivalent plastic strain at the time of the peak load, i.e. hull girder ultimate strength
(View of looking up at the bottom shell plates)

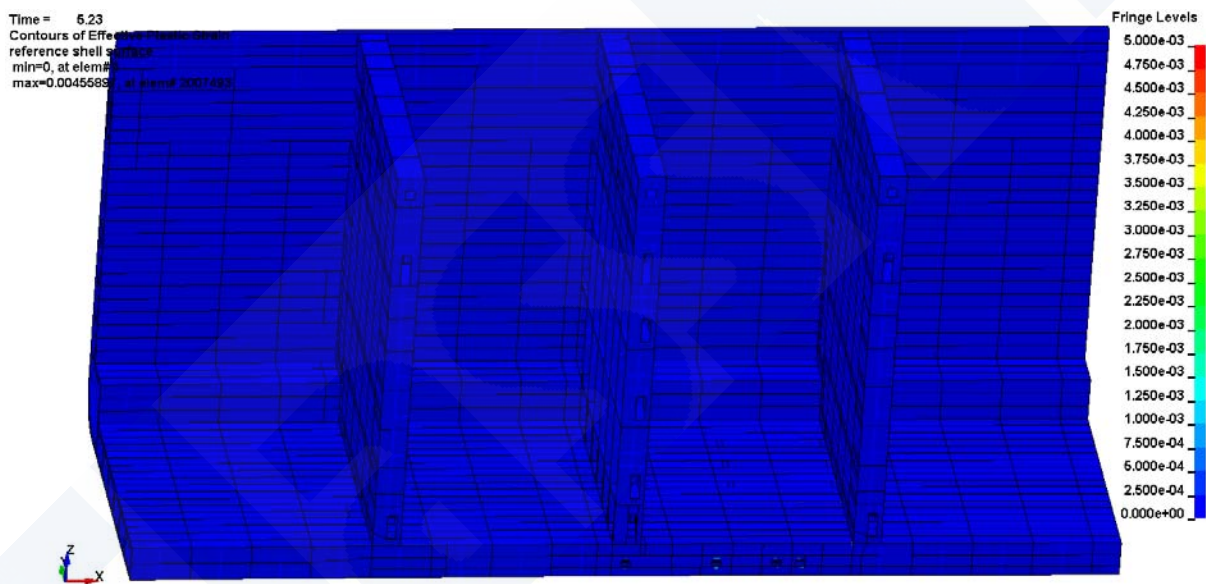


Fig. A8-13 Equivalent plastic strain at the time of the peak load, i.e. hull girder ultimate strength
(View of looking down at the inner bottom plates)
(No plastic strains are observed in inner bottom plates.)

Appendix 9 Loads acting on the Double Bottom Structure of Container Ships (related to 4.3.1 of this Report)

In general, hogging is a major condition of vertical bending in container ships. The tension load acts at the deck side, and the compressive load acts at the bottom side almost all the time in service. The tendency is remarkable particularly in container ships of up to the 10,000TEU class with the engine room and the deckhouse located semi-aft.

Bottom sea pressure, container load and the weight of ballast water and fuel oil in double bottom structure are listed as the load acting on the double bottom structure. The upward load due to bottom sea pressure is a major load as the lateral load acting on the double bottom structure because the cargo weight is relatively smaller than the load due to bottom sea pressure. The bottom sea pressure comprises hydrostatic pressure corresponding to the draught and wave-induced pressure. This upward load due to bottom sea pressure is relaxed when ballast or fuel oil is loaded in double bottom structure because the load due to them is downward, i.e. the effect due to ballast is larger than that of fuel oil because of the specific gravity.

And the compressive load due to sea pressure acting on side shell is generated in the transverse direction.

Hence, it can be said that the following 3 loads almost always act on the double bottom structure as shown in **Fig. A9-1**;

- ① Compressive load due to vertical bending
- ② Upward load due to bottom sea pressure
- ③ Transverse compressive load due to side sea pressure

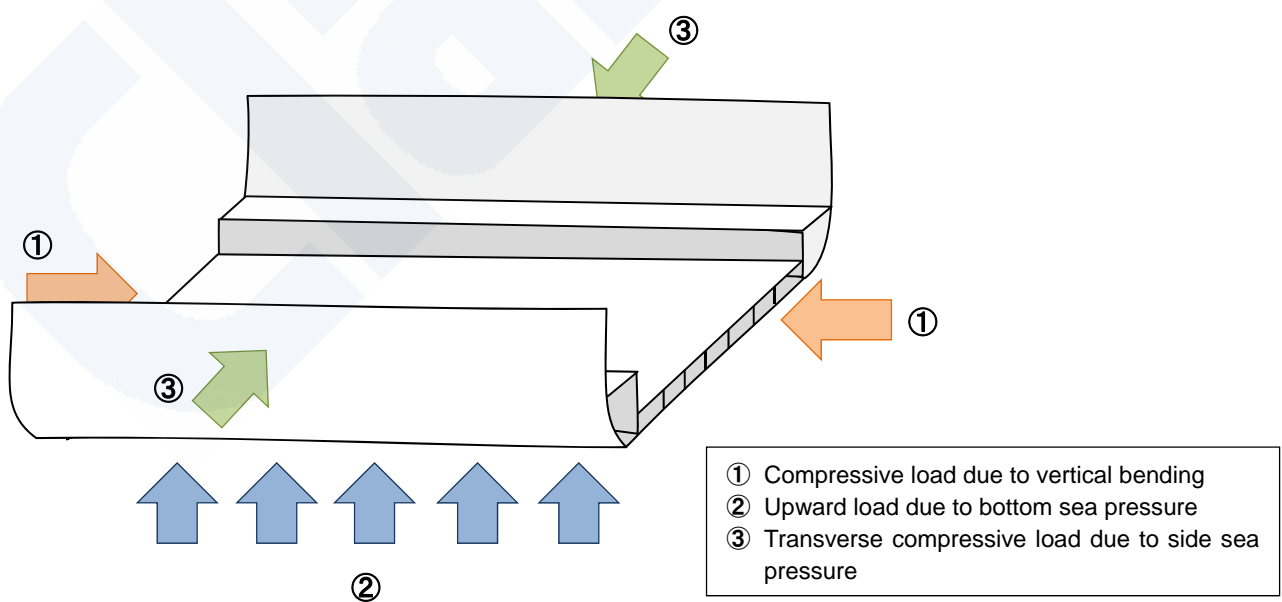


Fig. A9-1 Load acting on double bottom structure of container ships

The compressive load due to vertical bending shown in ① causes longitudinal compressive stress to the bottom shell plate. And the transverse compressive load due to ③ causes transverse compressive stress to the bottom shell plate.

On the other hand, the upward load due to bottom sea pressure shown in ② makes convex deformation as shown in **Fig. A9-2** on the double bottom structure consisting of bottom shell plate with bottom longitudinal, inner bottom shell plate with inner bottom longitudinal, girder and floor. As the result, transverse compressive stress on the bottom shell plate is generated near the center line. The deformation of the double bottom structure is maximized near the partial bulkhead within the longitudinal direction and therefore longitudinal compressive stress is generated in the bottom shell plate around the partial bulkhead.

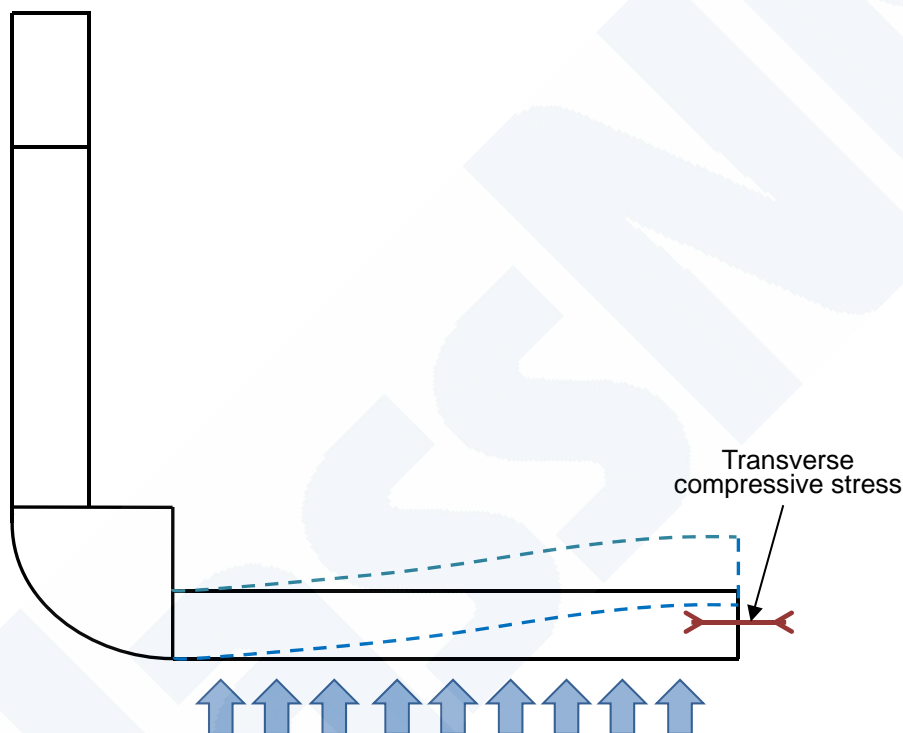


Fig. A9-2 Stress generated in the bottom shell plate due to bottom sea pressure

Consequently, in the bottom shell plate at the center of the hold, i.e. near the center line and near the partial bulkhead, compressive stress due to ① compressive load due to vertical bending and due to ② upward load from bottom sea pressure are superimposed in the longitudinal direction, and compressive stress due to ② upward load due to bottom sea pressure and due to ③ compressive load due to side sea pressure are superimposed in the transverse direction.

Appendix 10 Relationship between Buckling Collapse Strength of Stiffened Bottom Panel and Stresses generated in the Panel (related to 4.3.1 of this Report)

1. Introduction

The comparative investigation was performed regarding the relationship between the buckling collapse strength of stiffened bottom panels under the bi-axial compression, i.e. longitudinal and transverse compression, and the stress generated in the stiffened bottom panels on the target ships.

Buckling collapse analyses, i.e. elasto-plastic analyses by a non-linear FE analysis program under the bi-axial compression were carried out on the stiffened bottom panels. The analysis results were compiled into the curves of the buckling collapse strength of the stiffened bottom panels of the target ships respectively as shown from **Fig. A10-3** to **Fig. A10-9**, which indicate combinations of longitudinal compressive stress and transverse compressive stress corresponding to the buckling collapse strength. The details on the buckling collapse analyses and the curves of the buckling collapse strength are explained later in 2 of this Appendix.

In addition, the stresses generated in the stiffened bottom panels in the typical load conditions calculated by the method with elastic FE analysis described in **Appendix 11** were plotted over the curves in order to make the comparison between the buckling collapse strength and the generated stresses on the target ships.

Furthermore the investigation was carried out regarding the effect of the initial shape deformation on the buckling collapse strength as explained at the end of this Appendix.

2. Buckling Collapse Strength of Stiffened Bottom Panel and Stresses generated in the Panel

2.1 Analysis Model

The stiffened bottom panel adjacent to the keel plate panel, i.e. between No.3 Girder and No.9 Girder or between No.3 Girder and No.6 Girder, was modeled on each target ship. The modelling extent in the longitudinal direction is $1/2 + 1 + 1/2$ floor space, and the extent in the vertical direction is up to the middle of the double bottom height. The bottom shell plates, the bottom longitudinals, the floors and the stiffeners attached to the floors were modelled by the shell elements. Furthermore scallop openings in bottom longitudinal webs for the butt joint were also modelled. An example of the FE model is shown in **Fig. A10-1**.

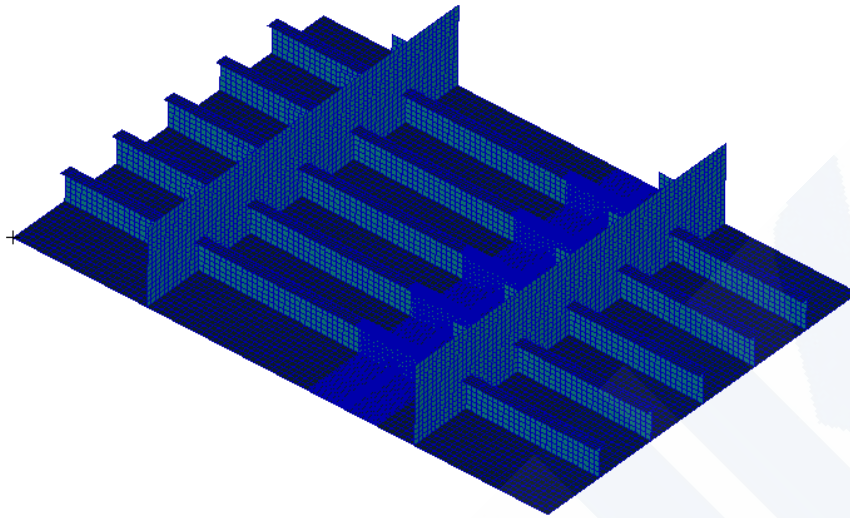


Fig. A10-1 Example of FE model of stiffened bottom panel

2.2 Analysis Program

Marc, a non-linear FE analysis program of the implicit method, was used.

2.3 Material Property of Steel

The general average values were used for the analyses instead of the specified minimum yield stress related to the yield stress of the steel. The general average values are expected values of actual steel plates in the sense of the average and the general, which had been adopted in JG Interim Report. Material properties of the steel for the analyses are shown in the below table. Elastic-perfect plasticity was given as the condition of the relationship between stress and strain.

Young's modulus	206,000 N/mm ²
Poisson's ratio	0.3
Yield stress (General average value)	MS : 292 N/mm ² YP32 : 380 N/mm ² YP36 : 410 N/mm ²

2.4 Boundary Condition

Outline of boundary condition is shown as follows.

Longitudinal direction (fore and aft end of the model)	Periodically continuous condition
Top end of floor	Symmetrical condition in the vertical direction
Connected part of side girder and bottom shell plate	Simply supported (Vertical displacement was constrained and rotation around longitudinal axis was free.)

2.5 Load Condition

Hydrostatic pressure corresponding to the full draught and wave-induced pressure specified in ClassNK Guidelines ^(Note) were applied to the model at the initial stage of the analyses as the lateral load acting on the bottom shell plates.

Note : Guidelines for Container Carrier Structures (Guidelines for Direct Strength Analysis) in 2012 of ClassNK

The compressive loads in the longitudinal direction and in the transverse direction were applied in the combination of the load and the forced displacement being gradually increased until the panel collapsed.

2.6 Condition of Initial Shape Deformation

Bottom shell plate deformations and lateral buckling mode deformations of bottom longitudinals were given as the initial deformation condition for the analyses.

The following 2 patterns were taken into account as the condition of initial shape deformation of the bottom shell plate.

- Pattern A : Deformation being convex upward on all bottom shell plates simulating sine curve shape of one wave length in the both spaces of the longitudinal and transverse, which simulated hungry horse mode (See **Fig. A10-2.**)
- Pattern B : Deformation being convex and concave in reverse direction between the adjacent bottom shell plates deformation simulating sine curve shape of a half wave in the both spaces of the longitudinal and transverse (See **Fig. A10-2.**)

On the both patterns, 4 mm as maximum deformation volume was given, which was equal to the standard range specified in the Japanese Ship Quality Standard (hereinafter “JSQS”). (See **Fig. A10-2.**)

On the condition of initial shape deformation of the bottom longitudinal, the lateral buckling mode specified in JSQS was applied with the maximum deformation volume equal to the standard range specified in JSQS both for Pattern A and Pattern B mentioned above.

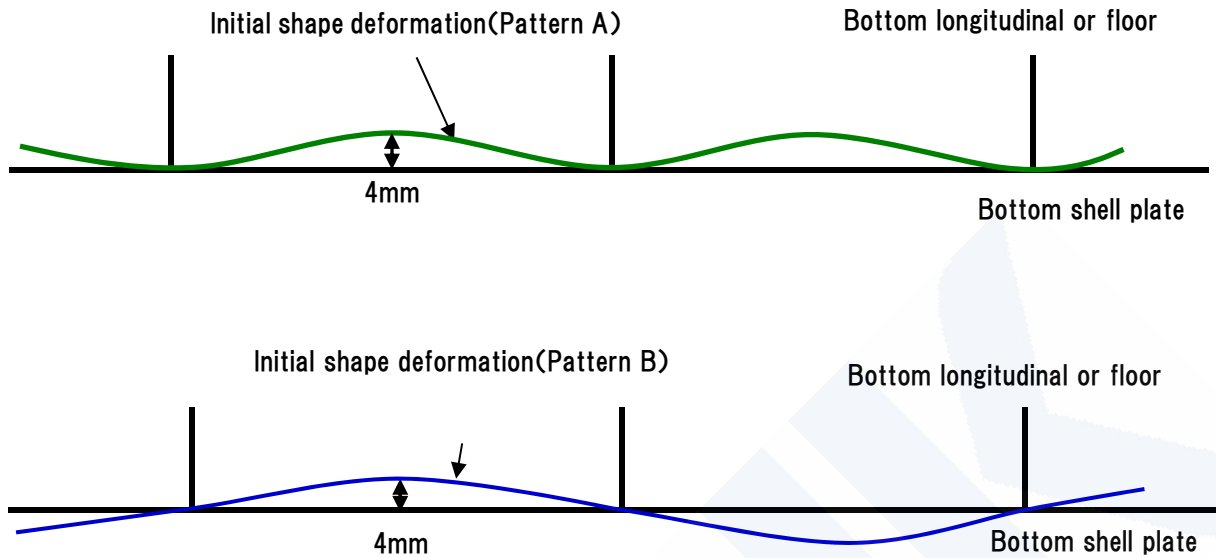


Fig. A10-2 Condition of initial shape deformation of bottom shell plates

While Pattern B can be considered as safer assumption than that of Pattern A concerning the buckling collapse strength of stiffened bottom panels, actual deformations of bottom shell plates are more complex composed of various wave patterns. Furthermore the number of half waves of buckling modes depends on the ratio of the two directions stresses under bi-axial compression. Hence, additional buckling collapse analysis was conducted in the case where minute deformations from one half-wave to five half-waves were superimposed as the initial shape deformation in order to investigate the effects of initial shape deformations. The result is described in 3 of this Appendix.

2.7 Relationship between Buckling Collapse Strength of Stiffened Bottom Panel and the Stresses generated in the Panel

Figures from A10-3 to A10-9 show the curves of the buckling collapse strength of the stiffened bottom panels of the target ships. Furthermore combinations of the longitudinal and transverse compressive stresses generated in the stiffened bottom panels in the typical load conditions are also plotted in the figures. The following 2 cases were considered as the typical load conditions to calculate the stress of the panel.

Load condition	Applied load
Case I	Lateral loads such as hydrostatic pressure corresponding to the full draught, wave-induced pressure specified in ClassNK Guidelines, hull weight, container loads
Case II	Case I + Allowable still water vertical bending moment + Wave-induced vertical bending moment specified in IACS UR S11

The two curves in the figures from **A10-3** to **A10-9** show the buckling collapse strength of the stiffened bottom panels with the condition of the initial shape deformation of Pattern A and Pattern B respectively. In the case where a combination of the longitudinal and transverse stresses generated in the panel is located outside the curves it indicates the buckling collapse occurs in the panel.

As described in 4.3.1 of this Report, it is observed that the buckling collapse strength in the longitudinal direction, i.e. a critical stress of σ_x sharply falls when the transverse compression stress (σ_y) exceeds around 100 N/mm² on any ship. And it is also confirmed that the stresses generated in the stiffened bottom panel in the case of Case II exist inside the strength lines for the target ships other than the Ship (Ship A).

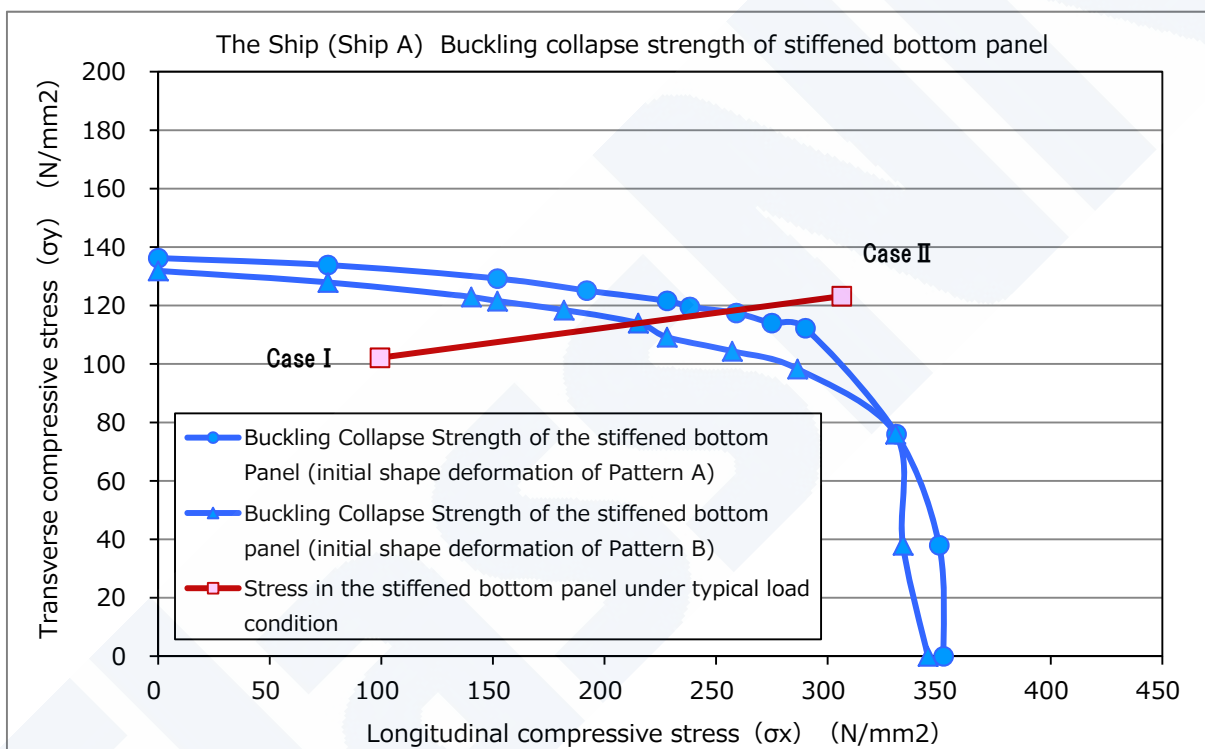


Fig. A10-3 Buckling collapse strength of stiffened bottom panel and stress generated in the panel under typical load conditions (the Ship, i.e. Ship A / No.3 Girder - No.9 Girder / in way of butt joint in midship part)

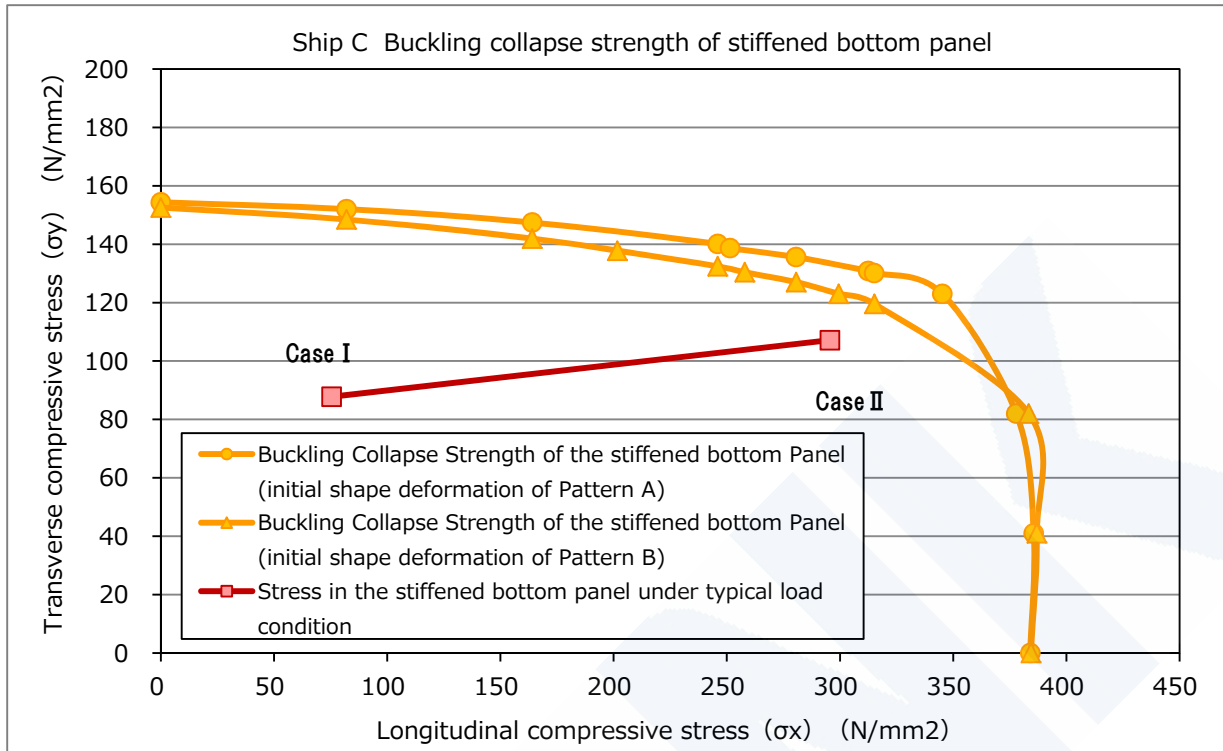


Fig. A10-4 Buckling collapse strength of stiffened bottom panel and stress generated in the panel under typical load conditions (Ship C / No.3 Girder - No.9 Girder / in way of butt joint in midship part)

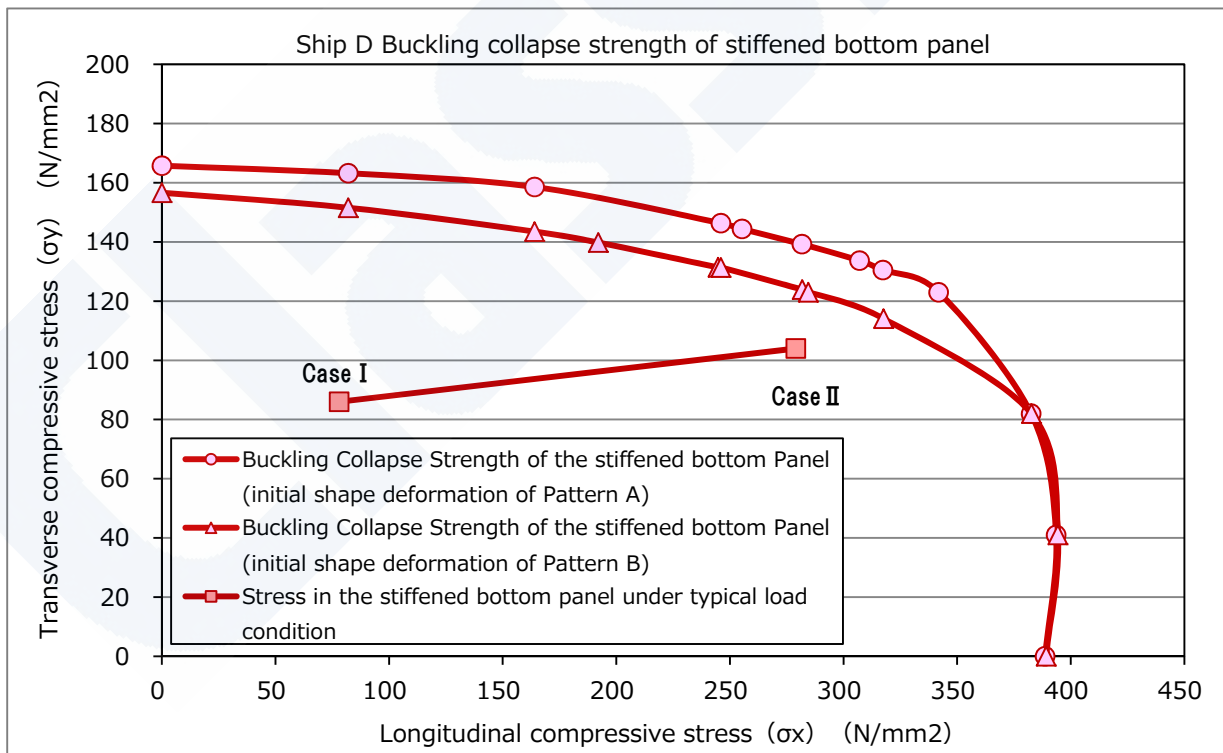


Fig. A10-5 Buckling collapse strength of stiffened bottom panel and stress generated in the panel under typical load conditions (Ship D / No.3 Girder - No.9 Girder / in way of butt joint in midship part)

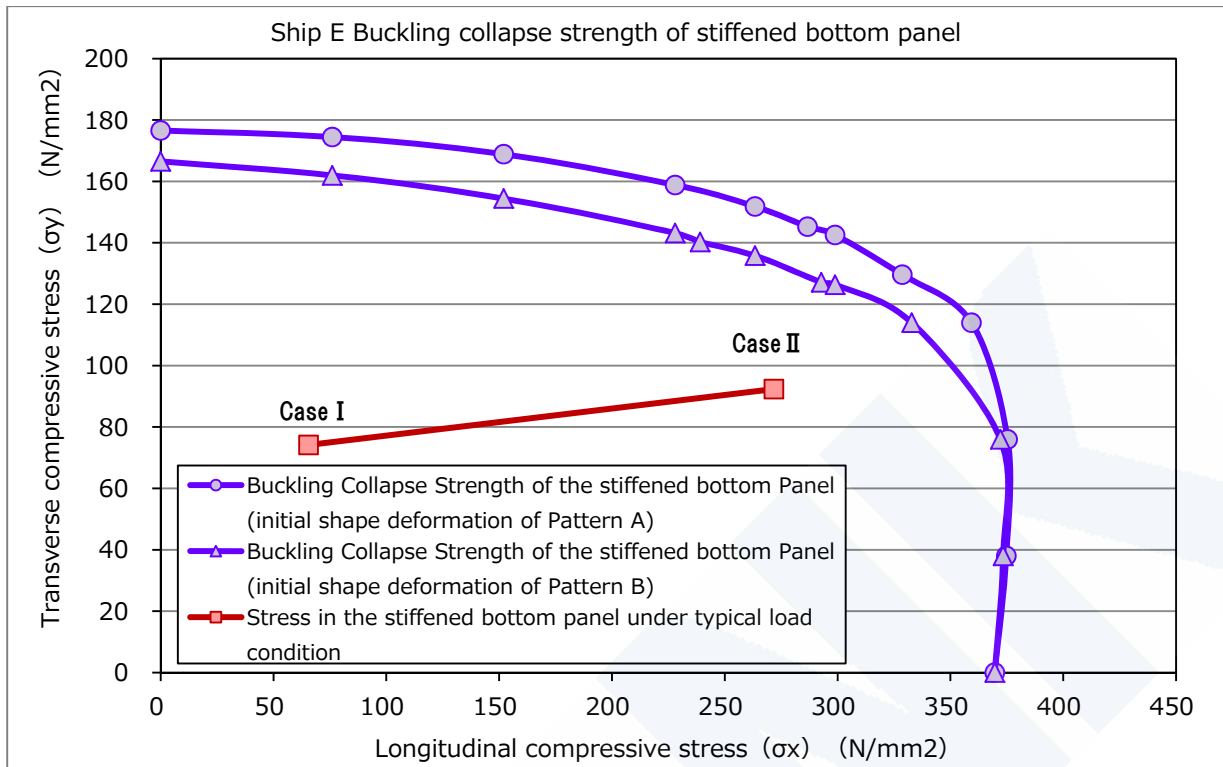


Fig. A10-6 Buckling collapse strength of stiffened bottom panel and stress generated in the panel under typical load conditions (Ship E / No.3 Girder - No.6 Girder / in way of butt joint in midship part)

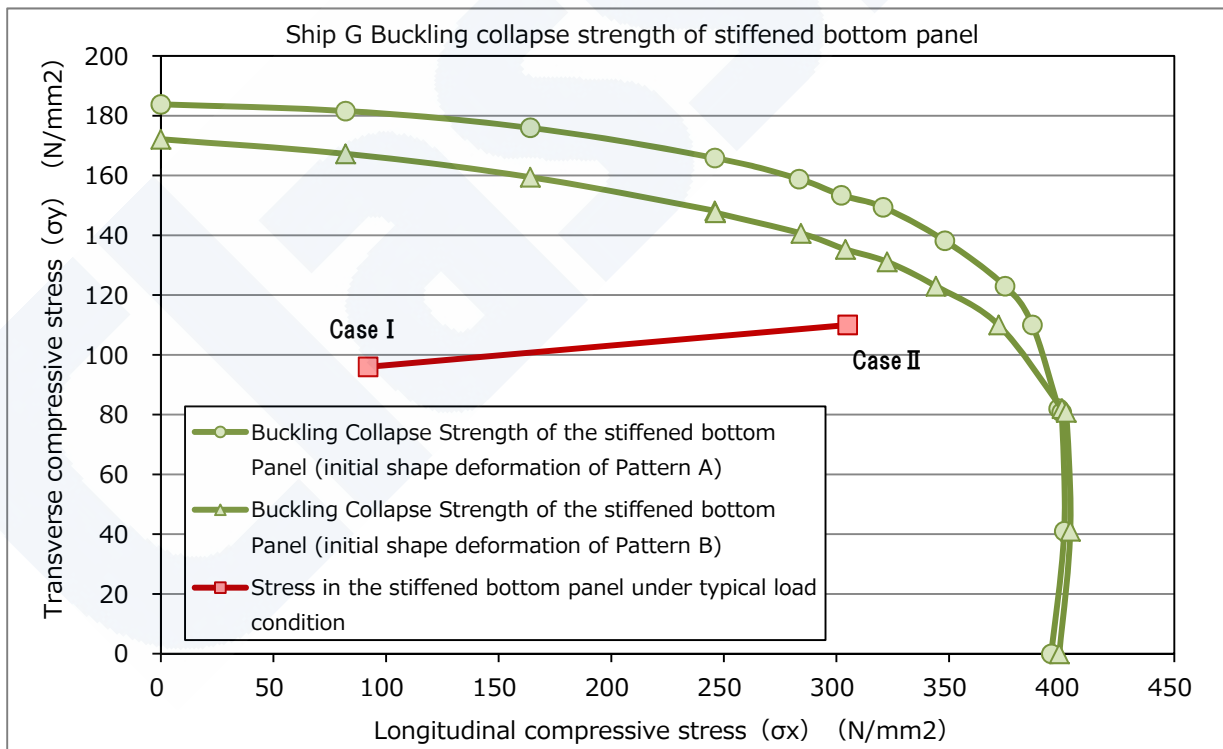


Fig. A10-7 Buckling collapse strength of stiffened bottom panel and stress generated in the panel under typical load conditions (Ship G / No.3 Girder - No.6 Girder / in way of butt joint in midship part)

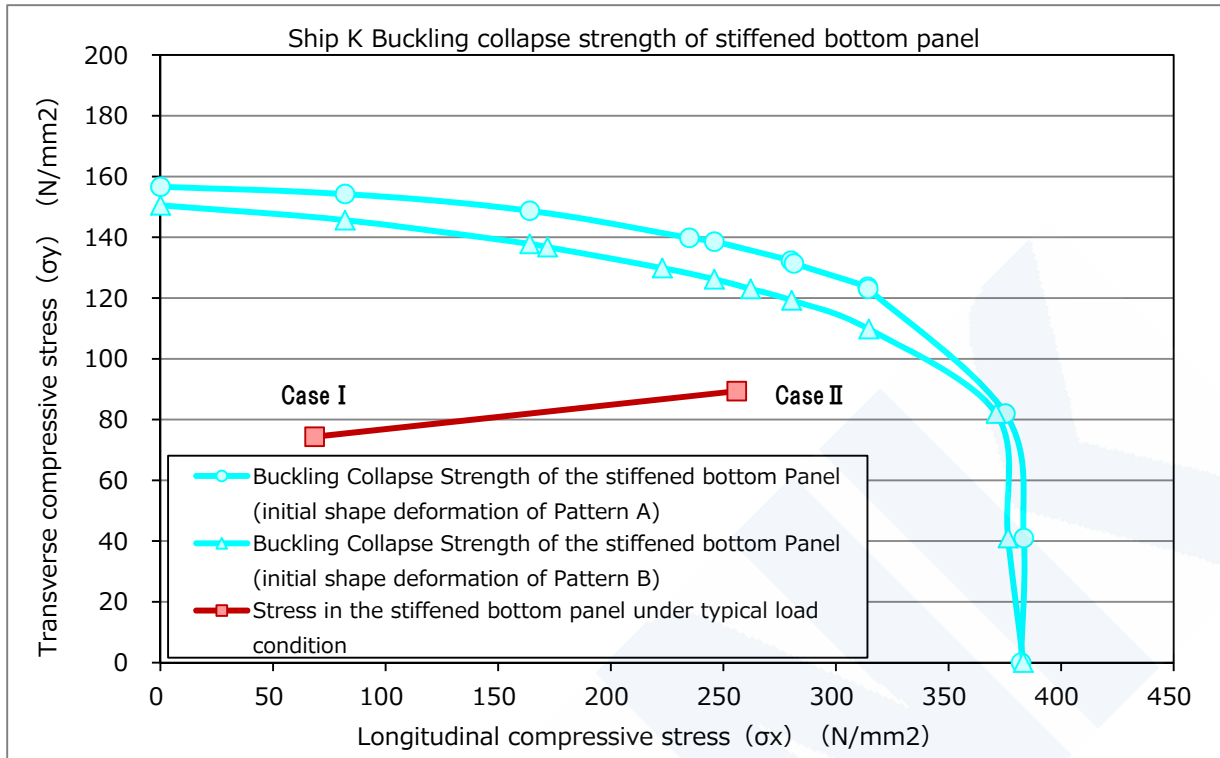


Fig. A10-8 Buckling collapse strength of stiffened bottom panel and stress generated in the panel under typical load conditions (Ship K / No.3 Girder - No.6 Girder / in way of butt joint in midship part)

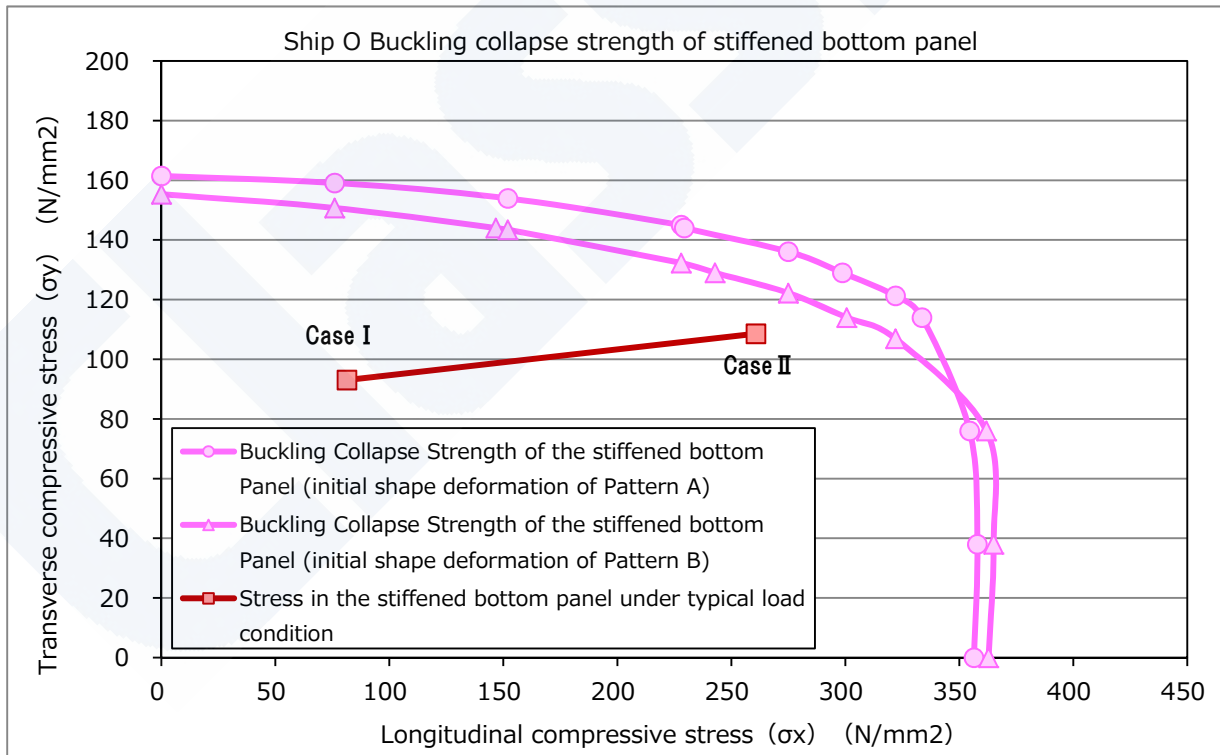


Fig. A10-9 Buckling collapse strength of stiffened bottom panel and stress generated in the panel under typical load conditions (Ship O / No.3 Girder - No.6 Girder / in way of butt joint in midship part)

3. Effect of the Initial Shape Deformation Condition on the Buckling Collapse Strength

In the above investigation, the buckling collapse strength of stiffened bottom panel was estimated in the two conditions of initial shape deformation, i.e. Pattern A and Pattern B. Pattern A is the deformation being convex upward on all plates with one wave length simulating hungry horse mode and Pattern B is the convex and concave deformation in the reverse direction between the adjacent plates.

Here, the buckling collapse analysis was carried out in the case where minute deformations from one half-wave to five half-waves were superimposed as the condition of the initial shape deformation in the stiffened bottom panel of the Ship (Ship A). The result was compared with those of the pattern A and of the pattern B in order to investigate how the condition of initial shape deformation affected the buckling collapse strength. The deformation amplitude was taken as 1/50 of the thickness of the bottom shell plates in the case of the minute deformation superimposing mode from one half-wave to five half-waves.

The result is shown in **Fig. A10-10**. Pattern B basically gives lower buckling collapse strength of the stiffened bottom panel than that of Pattern A and the difference is prominently visible in the range where transverse compressive stress is more than 100 N/mm^2 , which makes the buckling mode one half-wave. The case of minute deformation superimposing mode of from one half-wave to five half-waves gives higher buckling collapse strength than that of pattern B when the transverse compressive stress exceeds 100 N/mm^2 . On the other hand, this case gives lower buckling collapse strength than those of pattern A and B where the transverse compressive stress is less than 100 N/mm^2 .

As stated in 4.3.1 of this Report, the difference is observed between the Ship and the other target ships concerning the relationship between the buckling collapse strength of the stiffened bottom panel and the stresses actually generated in the panel. This difference is considered to result from the difference of transverse compression stresses generated in the panels. That is to say, the transverse compressive stress of the double bottom local stress of the Ship is generally more than 100 N/mm^2 . Therefore, it is sure that the difference between the Ship and the other target ships described in 4.3.1 of this Report and observed from **Fig. A10-3** to **Fig. A10-9** was adequately evaluated by the buckling collapse analyses in pattern A and B for the condition of initial shape deformation. However, as shown in **Fig. A10-10**, it is necessary to investigate the effect of the condition of initial shape deformation by changing the shape and volume of initial deflection systematically in order to evaluate the buckling collapse strength more quantitatively, and it might be an issue in the future.

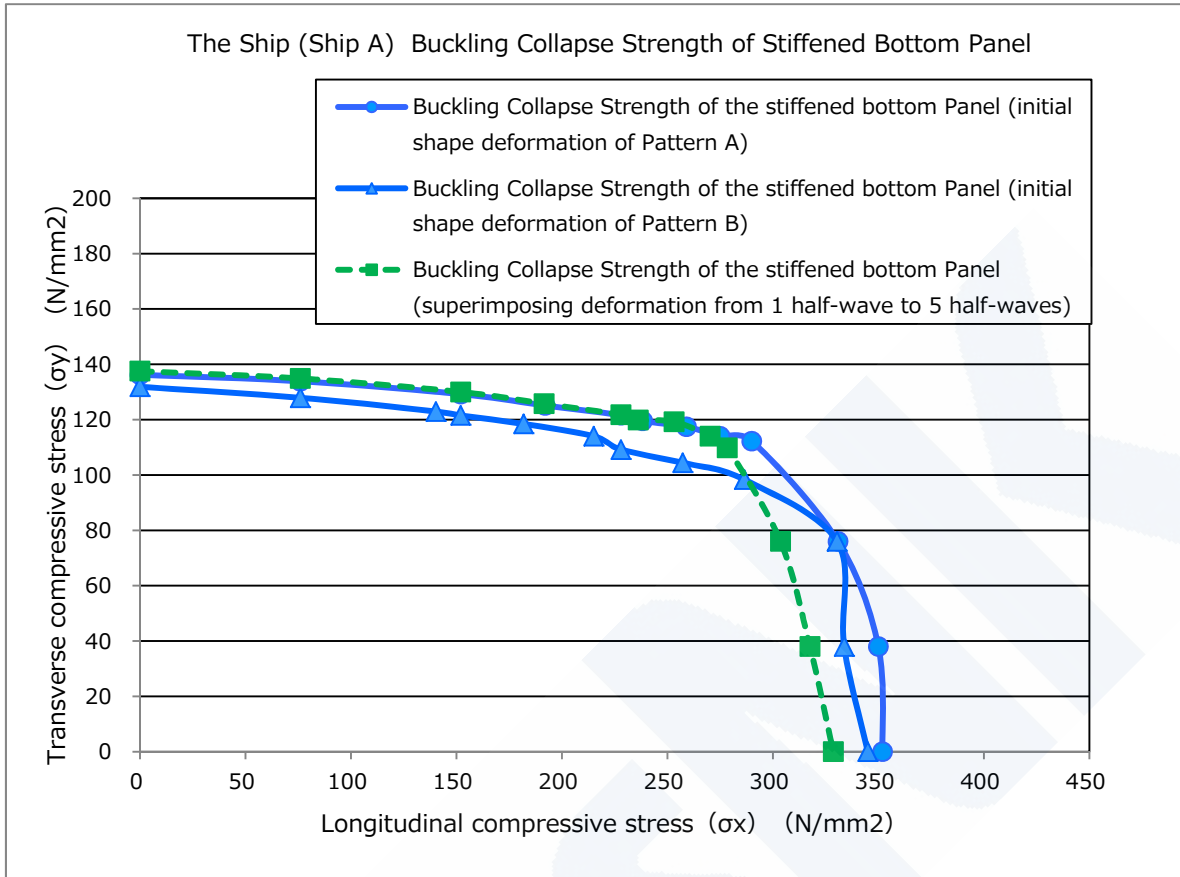


Fig. A10-10 Buckling collapse strength of stiffened bottom panel
(Ship A / No.3 Girder - No.9 Girder / in way of butt joint in midship part)

Comparison of the effect of condition of initial shape deformation on Pattern A, Pattern B and superimposing minute deformation from one half-wave to five half-waves

**Appendix 11 Double Bottom Local Stress generated in Bottom Shell Plate
(related to 4.3.1 of this Report)**

For each target ship on which 3-hold model elasto-plastic analysis was conducted, elastic FE analysis was carried out using the 3-hold model and the stress (σ_x , σ_y) generated in the stiffened bottom panel in each load condition was estimated and a comparison was made.

Table A11-1 shows the load conditions. The same load and boundary conditions as those of the 3-hold model elasto-plastic analysis were applied to the FE model. Therefore, One-bay empty condition without ballast in double bottom was considered as the loading condition. (See **Appendix 8** for detailed loads and boundary conditions.)

Table A11-1 Load condition

Load condition	Details of applied load
Case I	Lateral load (hydrostatic pressure of full draught, wave-induced pressure, hull weight, container load)
Case II	Case I + Allowable still water vertical bending moment + Wave-induced vertical bending moment specified in IACS Rules

The results of comparing the transverse distribution of stress generated in the stiffened bottom panel for each ship in the above load conditions are shown from **Fig. A11-1** to **Fig. A11-4**. The horizontal axis represents the transverse direction and the value corresponds to the bottom longitudinal number. In the figure, M_s means allowable still water vertical bending moment and M_w means wave-induced vertical bending moment specified in IACS Rules.

And the stress shown in these figures is the stress of the stiffened bottom panel at the hull girder fracture section in 3-hold model elasto-plastic analysis.

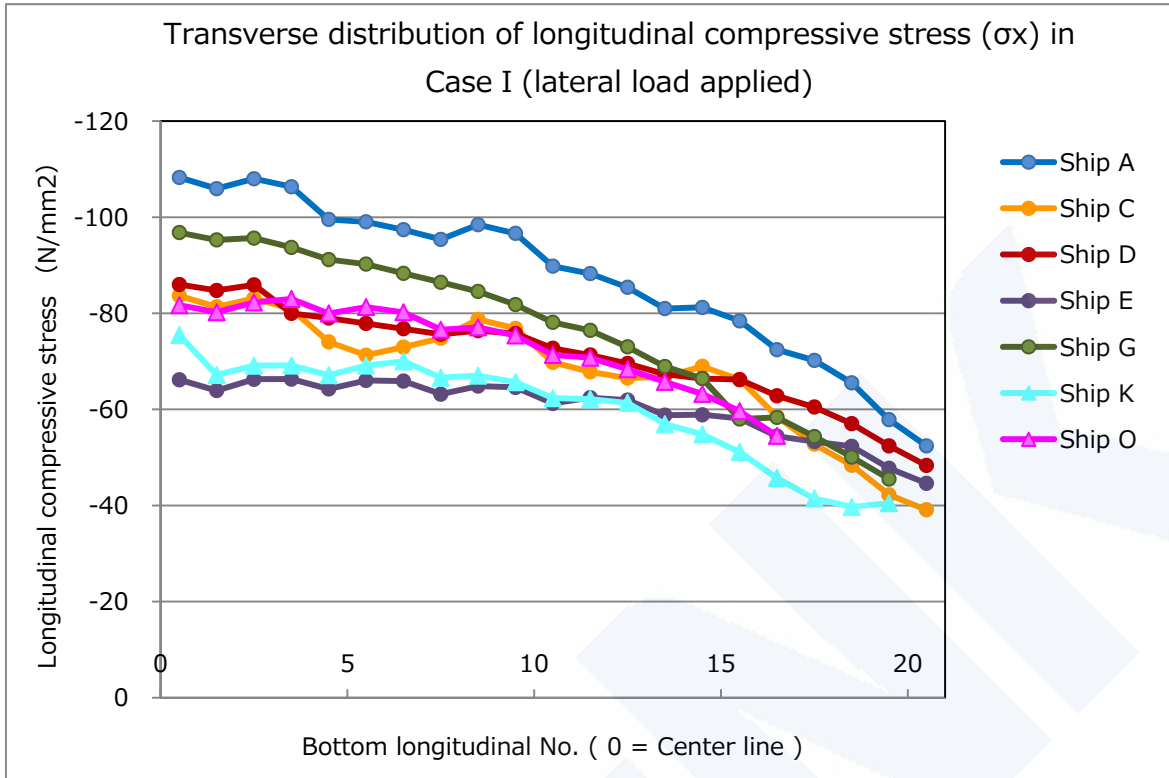


Fig. A11-1 Transverse distribution of longitudinal compressive stress of the bottom shell plate in Case I (at hull girder fracture section)

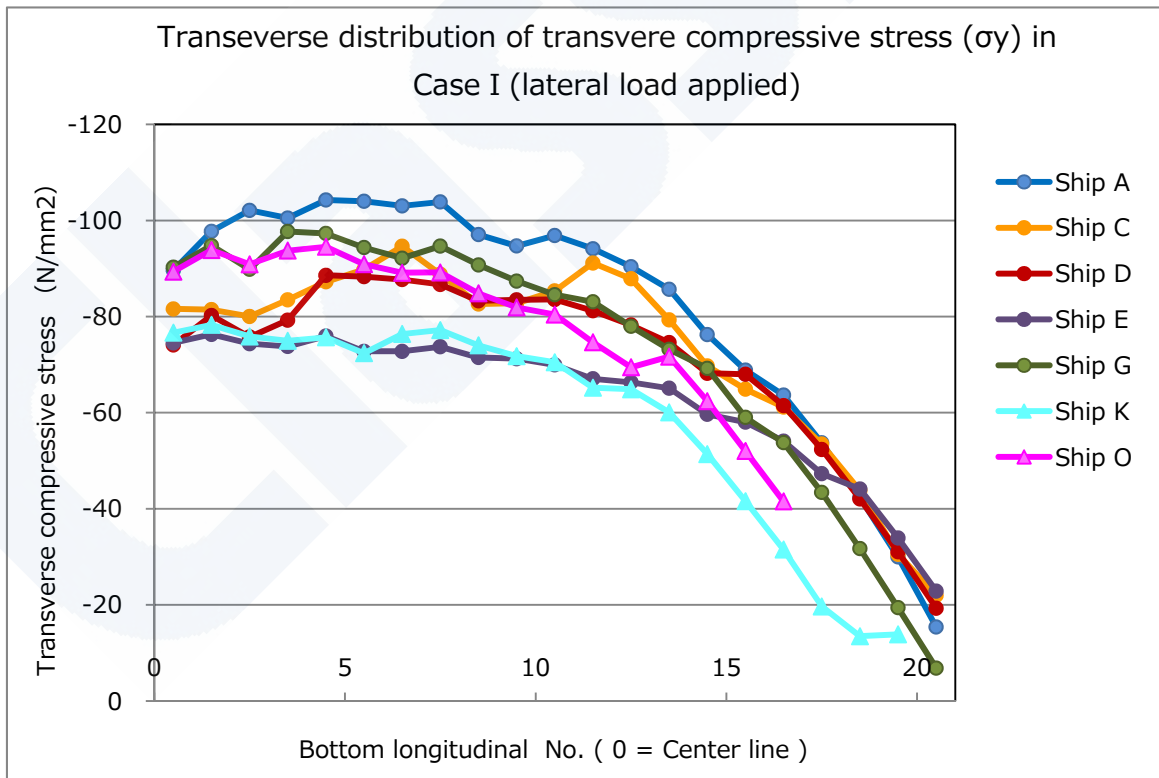


Fig. A11-2 Transverse distribution of transverse compressive stress of the bottom shell plate in Case I (at hull girder fracture section)

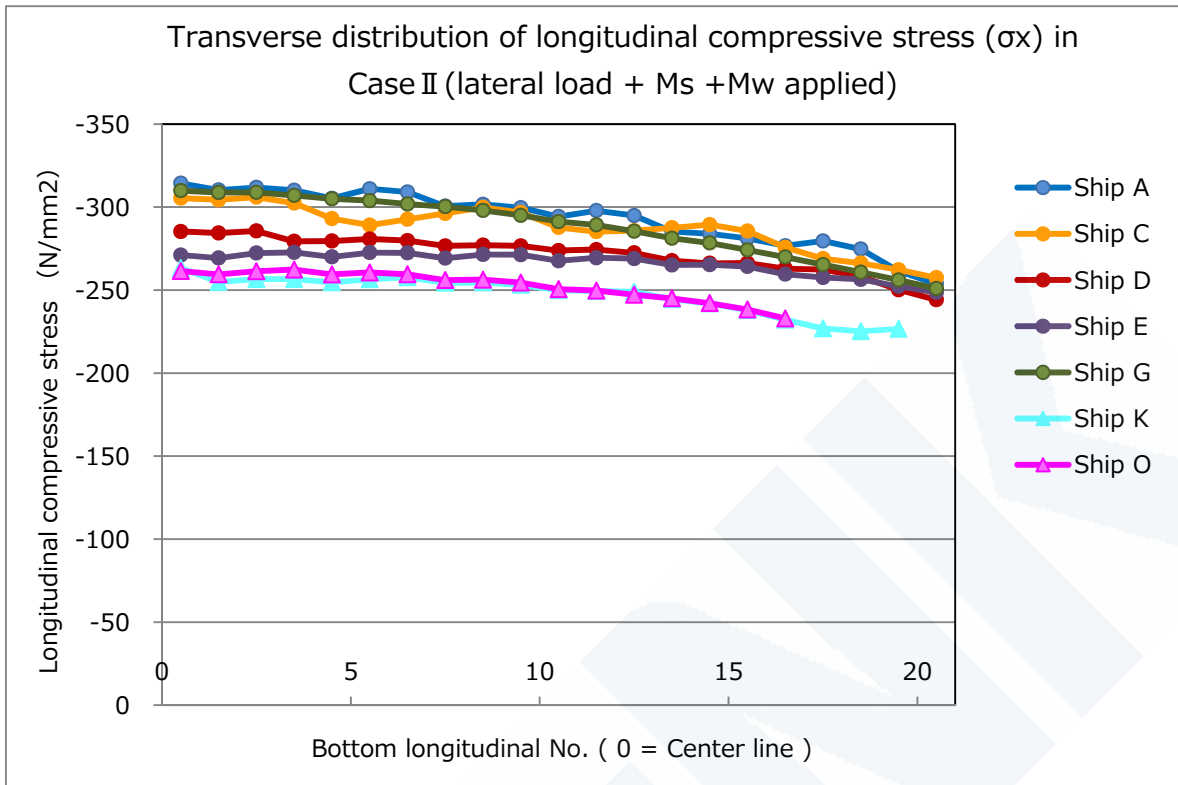


Fig. A11-3 Transverse distribution of longitudinal compressive stress of the bottom shell plate in Case II (at hull girder fracture section)

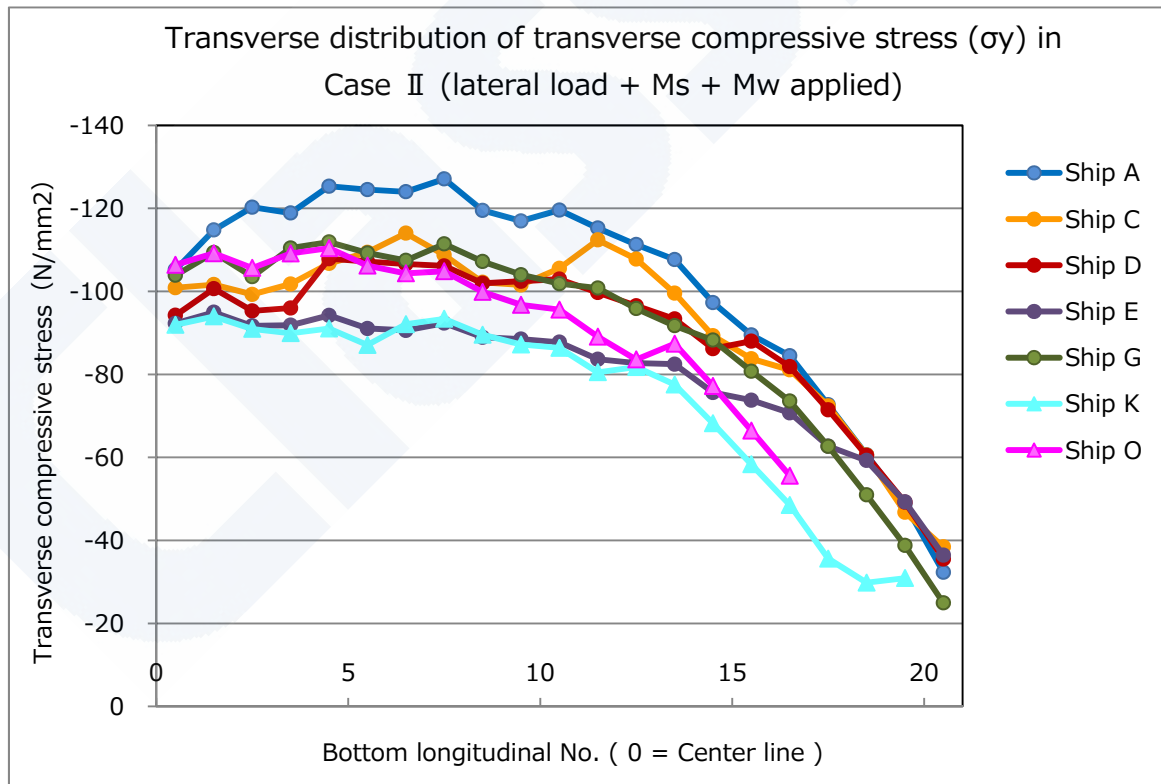


Fig. A11-4 Transverse distribution of transverse compressive stress of the bottom shell plate in Case II (at hull girder fracture section)

**Appendix 12 Characteristics of Post-Panamax Container Ships
(related to 4.4 of this Report)**

With the enlargement of container ships, B/D* of Post-Panamax container ships tends to be increased than those of Panamax container ships which have a restriction of maximum ship-breadth. This feature is particularly noticeable in Post-Panamax container ships of 8,000 TEU Class and over, as shown in Fig. A12-1.

*: B/D : ship-breadth divided by ship-depth

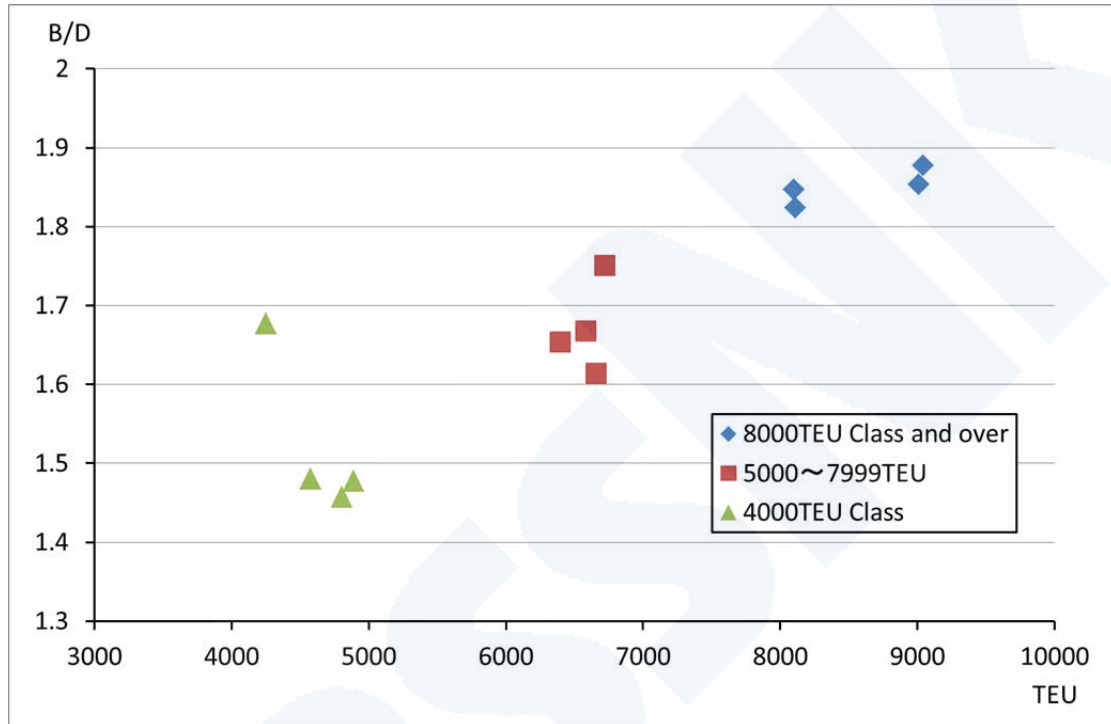


Fig. A12-1 Relationship between B/D and size of container ship

B/D mentioned above is closely related to the stability of a ship. G_0M^{**} , a representative value indicating the amplitude of ship-stability, and also a governing value to comply with the stability requirements, is compared for some container ships in Fig. A12-2. The loading condition used in the comparison is those at which stability is most severe among the standard loading conditions in each Loading Manual. The calculated G_0M values were plotted on Fig. A12-2 in case where ballast water is loaded in double bottom tanks and where ballast water is not loaded in double bottom tanks.

G_0M^{**} : metacentric height considering effect of free surfaces

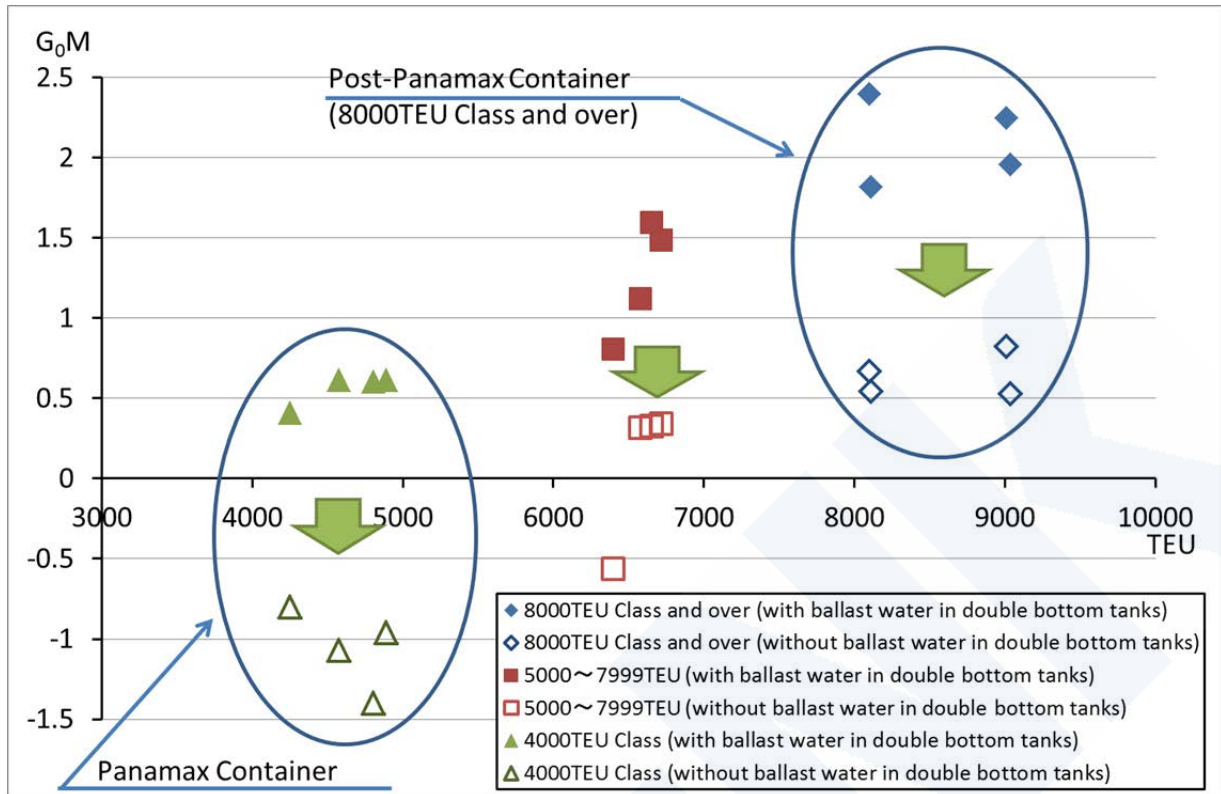


Fig. A12-2 Comparison of G₀M values of various container ships

From **Fig. A12-2**, it is found that Post-Panamax container ships of 8,000 TEU class and over have adequate G₀M values even though ballast water is not loaded in double bottom tanks. In contrast, Panamax container ships are impossible to comply with the minimum G₀M value (0.15 m) of stability requirement in case where ballast water is not loaded in double bottom tanks.

As a conclusion, Post-Panamax container ships have improved their stability and gained more flexibility to comply with the requirements. For instance, the need for ballasting in the double bottom tanks is reduced. Consequently, various loading and ballasting conditions that cannot be carried out in Panamax container ships due to stability restriction are possible in Post-Panamax container ships.

Appendix 13 Analysis of Data of Past On-board Full Scale Measurements of Large Container Ships (related to 4.6 of this Report)

Analysis was conducted on the results of on-board full scale measurements of large container ships carried out in the past with cooperation of the owners and the shipbuilders in order to grasp the feature and the tendency of the actual wave-induced loads acting on container ships.

The measurement data of two container ships, one was an 8,000TEU container ship and the other was a 6,000TEU container ship, were analyzed. **Table A13-1** shows the outline of the on-board full scale measurements of these two ships, the first one of which is hereinafter referred to as Ship X and the second one as Ship Y.

Table A13-1 Outline of On-board full scale measurements used for Analysis

	Ship X	Ship Y
Size	8,000 TEU class	6,000 TEU class
Measurement period	9 months	29 months
Service route at the time of the measurement	between Far East and Europe	between Far East and Europe
Major measurement items	<ul style="list-style-type: none"> • Hull girder stress (Plural transverse sections including midship section) • Ship motions and accelerations • Ship positions (GPS data) 	
Measurement intervals	Continuous	20 minutes every two hours

1. Encountered Sea States

Wave hind-casting (a numerical wave prediction) was conducted using the ship position data (GPS data) and corresponding meteorological data. On the basis of the results and in overall consideration of the log books of the ships and measured response data, the encountered sea states for the ships were estimated.

The estimation indicated that both ships had encountered sea states with the significant wave height of six meters or less at the frequency of 99% or over.

2. Frequency Distribution of Whipping Response Ratio

Whipping response ratio and its frequency distribution were estimated by using the measurement data of the two ships (Ship X and Ship Y), which reflected how the wave-induced vertical bending moment would increase by the effect of the whipping response of the ships.

For the hull structure response subject to the above estimation, the longitudinal stress at the top of the hatch side coaming of Ship X was used. With regard to Ship Y, the longitudinal stress on the upper deck was converted into the value at the top of the hatch side coaming and the result after the conversion was used.

The measurement data on the longitudinal stress at the top of the hatch side coaming was separated at 0.5 Hz as a threshold value and the response data in the lower frequency range was defined as response arising from waves only (wave response component). The raw measurement data without separation contained both the wave response component and the vibration response component arising from the whipping response.

Peak values of the data of the wave response component and the raw measurement data were identified in one period of the wave response component by the zero-up crossing method illustrated in Fig. A13-1.

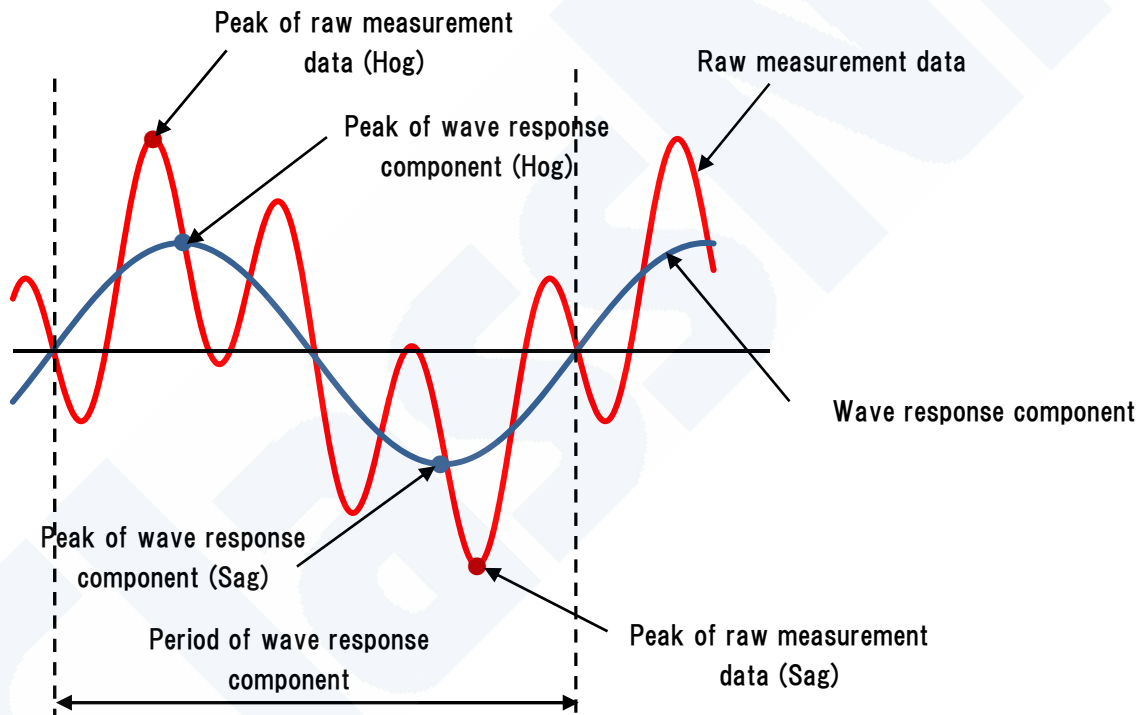


Fig. A13-1 Method of identifying peak response values, i.e. zero-up crossing method

The value calculated by dividing the peak value of the raw measurement data, which contain the wave response component and the whipping response component, by the peak value of the wave response data was defined as the whipping response ratio.

Fig. A13-2 and Fig. A13-3 show the frequency distribution of the whipping response ratio including both results of Ship X and Ship Y. The horizontal axes show the whipping response ratio and the vertical axes show the relative frequency of the occurrence of the whipping response ratio.

In the case where the wave response component (the denominator of the whipping response ratio) is small, the whipping response ratio sometimes becomes very large even though the both of the whipping response component data and the wave response component data are small. **Fig. A13-2** and **Fig. A13-3** indicate the whipping response ratio of 2.0 or over with very small frequency, which are the case mentioned above. Therefore it is important to consider not only the whipping response ratio but also the absolute values of the responses in order to evaluate the effect of the whipping response on the hull structural strength.

Although conclusive outcomes could not be drawn because of small amount of the measurement data and the limited period of the measurement, **Fig. A13-2** and **Fig. A13-3** show that the occurrence frequency of the whipping response ratio has some resemblance to the Gumbel distribution with the mode of around 1.1.

Further on-board full scale measurements on container ships are being carried out and in planning in order to obtain more measurement data. By using the measured data it is planned to investigate the relationship between the wave-induced vertical bending moment specified in the Rules and the measurement results, and investigate method to estimate the whipping response in severe sea states taking account of the occurrence probability of the whipping response ratio and so on.

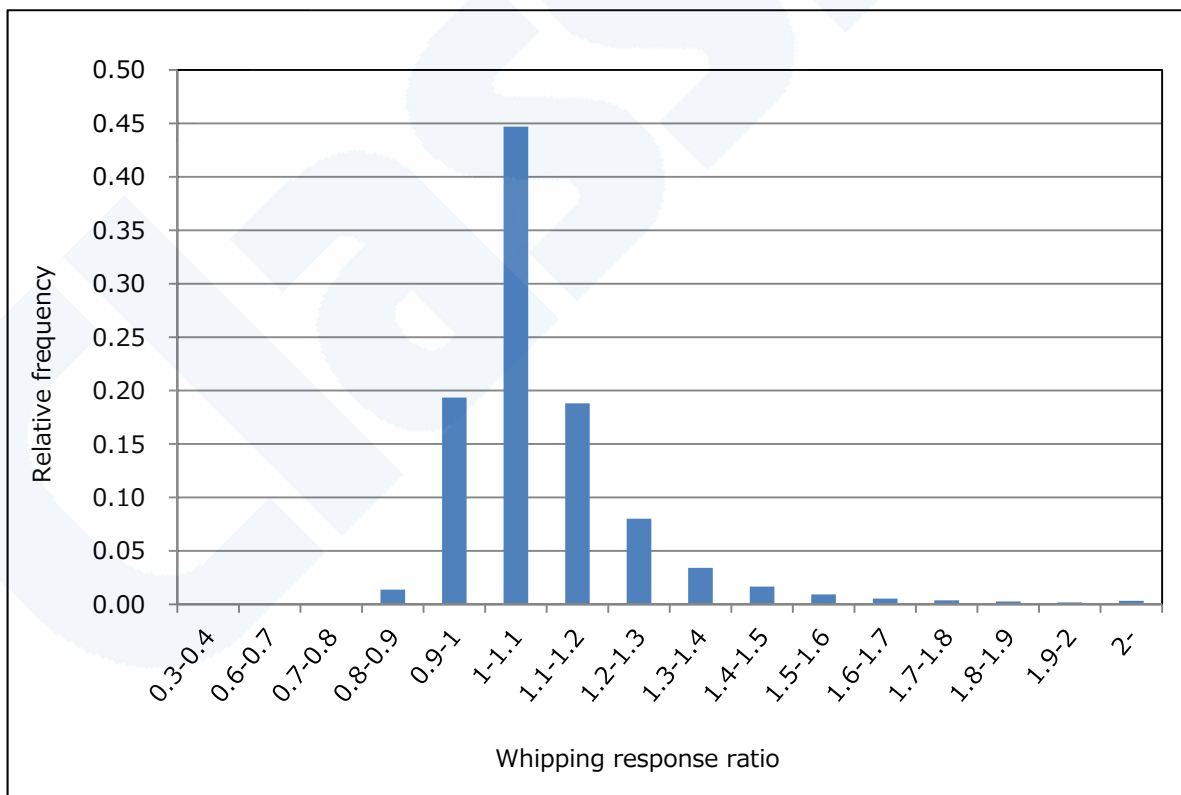


Fig. A13-2 Frequency distribution of whipping response ratio (Hog)
(Analysis of on-board full scale measurements data of Ships X and Y)

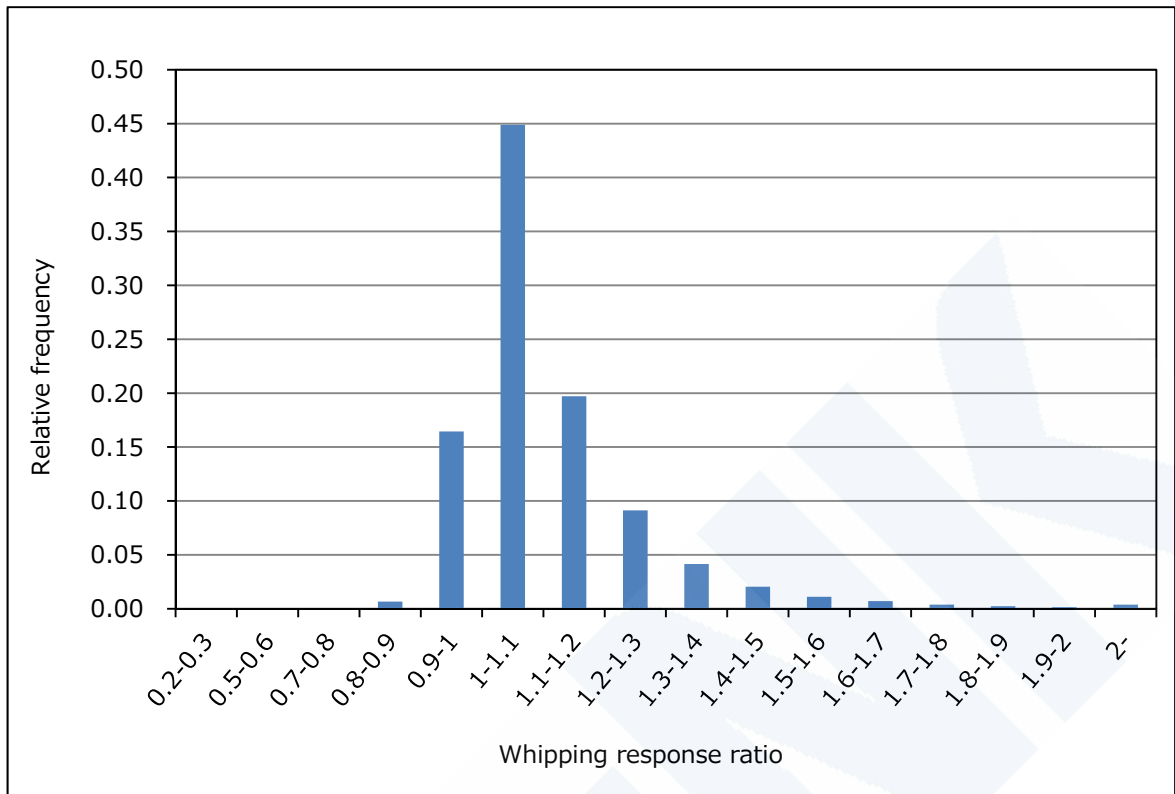


Fig. A13-3 Frequency distribution of whipping response ratio (Sag)
(Analysis of on-board full scale measurements data of Ships X and Y)